THE CHRONOLOGY AND FUNCTION OF UPR ACTIVATION IN SKELETAL MUSCLE ADAPTATIONS TO CHRONIC CONTRACTILE ACTIVITY

JONATHAN M. MEMME

A THESIS SUBMITTED TO THE FACULTY OF GRADUATE STUDIES IN PARTIAL FULFILLMENT OF THE REQUIREMENTS FOR THE DEGREE OF

MASTER OF SCIENCE

GRADUATE PROGRAM IN KINESIOLOGY AND HEALTH SCIENCE

YORK UNIVERSITY
TORONTO, ONTARIO

DECEMBER 2015

ABSTRACT

During exercise-induced mitochondrial biogenesis, a rapid increase in the transcription and translation of nuclear-encoded mitochondrial proteins, under the influence of PGC-1α, require integration with mitochondria-derived proteins. This has the potential to perturb cellular proteostasis and thus induce an unfolded protein response from the mitochondria (UPR^{mt}) and/or endoplasmic reticulum (UPR^{ER}). The role of the UPR in skeletal muscle, particularly with respect to exercise is not well established. We used a chronic contractile activity model over 7 days to examine the chronology of mitochondrial biogenesis, autophagy, UPR^{ER}, and UPR^{mt} activation, and used a drug (TUDCA) to block the ER stress-induced UPR to test its role in adaptations to CCA. Our data reveal that the UPRs are involved in acute and chronic muscle adaptations, independent of CHOP signaling, to augment protein quality control. However the specific mechanism by which the UPR influences these adaptations is an important avenue of future work.

ACKNOWLEDGEMENTS

My deepest gratitude goes out to my supervisor Dr. David Hood, for all the patience and faith he placed in me, and for all the opportunity he provided for me to develop and succeed, I am forever thankful. I also cannot overlook the assistance and positivity that Ashley and Avi provided in making the lab one of the more enjoyable places to be, and especially to Matt who shared my journey every single day, I truly could not have wished for a better partner to have had with me to face the trials and triumphs that come with the daily grind of research and graduate school – its been a heck-of-a-wave of mosting. To Robyn who has been unwavering in her support, encouragement, and love throughout my studies, I consider myself the most fortunate to have you by my side. Finally to my family, Amanda for always providing me the inspiration to think creatively and openly, you are my greatest role model. And to Mom and Dad, I truly could not have asked for more loving, and supportive parents, you have always provided me every opportunity to grow and prosper and provided me encouragement every day. I could never repay the love and devotion you have shown me except to try to carry it forward throughout my endeavors.

TABLE OF CONTENTS

LIST OF TABLES

CHAPTER 2: MANUSCRIPT

APPENDIX A: DATA AND STATISTICAL ANALYSIS

LIST OF FIGURES

CHAPTER 1: REVIEW OF LITERATURE

CHAPTER 2: MANUSCRIPT

APPENDIX B: ADDITIONAL DATA

LIST OF ABBREVIATIONS

Ach	Acetylcholine
AchR	Acetylcholine Receptor
ADP	Adenosine diphosphate
Akt	Serine/threonine protein kinase Akt
AMP	Adenosine monophosphate
AMPK	AMP-activated protein kinase
ANOVA	Analysis of variance
ATF	Activating transcription factor
ATFS-1	Activating transcription factor associated with stress-1
ATG	Autophagy-related protein
ATP	Adenosine triphosphate
Bak	Bcl-2 homologous antagonist killer
Bax	Bcl-2 associated X protein
Bcl-2	B-cell lymphoma 2
BH3	Bcl-2 homology domain 3
Bim	Bcl-2 like protein 11
BiP	Binding immunoglobulin protein (aka GRP78)
bZIP	Basic leucine zipper
C/EBP	CCAAT-enhancer binding protein
Ca^{2+}	Calcium ion
CaMK	Ca^{2+}/calmodulin-dependent protein kinase
cAMP	Cyclic AMP
CCA	Chronic contractile activity
cDNA	Complimentary DNA
CHOP	C/EBP homologous protein
COX	Cytochrome c oxidase
CPN10	10 kDA chaperonin
CRE	cAMP response element
CREB	cAMP response element-binding protein
DNA	Deoxyribonucleic acid
EDL	Extensor digitorum longus
eIF2α	Eukaryotic translation-initiation factor-2 alpha
ER	Endoplasmic reticulum
ERAD	ER-associated degradation machinery
Erg-1	Early growth-response gene-1
ERK	Extracellular signal-regulated kinase
ERO1α	ER oxidase-1 alpha
ERR	Estrogen related receptor
ERSE-I/-II	ER stress response elements –I and -II
ERα	Estrogen receptor alpha

ETC	Electron transport chain
FA	Fatty acids
Foxo	Forkhead box O
FTR	Fast-twitch red
FTW	Fast-twitch white
GADD34	Growth arrest and DNA damage-inducible 34
GRP78	78 kDa Glucose-related protein (aka BiP)
GRP94	94 kDa Glucose related protein
HAF-1	ABC (ATP Binding Cassette) transporter
HRP	Horseradish peroxidase
HSF-1	Heat shock factor-1
HSP	Heat shock protein
IMF	Intermyofibrillar
IMM	Inner mitochondrial membrane
IMS	Intermembrane space
IP	Intraperitoneal
IP3R1	Inositol triphosphate receptor-1
IRE1	Inositol-requiring enzyme-1
JNK	c-jun N-terminal kinase
K^+	Potassium ion
LC3	Microtubule-associated proteins 1A/1B light chain 3A
LDH-H	Heart-specific lactate dehydrogenase
LDH-M	Muscle-specific lactate dehydrogenase
MAM	Mitochondrial-associated membrane
MAPK	Mitogen-activated protein kinase
Mfn2	Mitofusin-1
MHC	Myosin heavy chain
mRNA	Messenger RNA
mtDNA	Mitochondrial DNA
mtHSP70	75 kDA mitochondrial heat shock protein
mTORC1	Mammalian/mechanistic target of rapamycin complex 1
mtPTP	Mitochondrial permeability transition pore
MTS	Mitochondrial targeting sequence
MURE	UPR^{mt} response element
Na^+	Sodium ion
NAD	Nicotinamide adenine dinucleotide
NF-κB	Nuclear factor kappa-light-chain-enhancer of activated B cells
NLS	Nuclear localization sequence
NRF-1/-2	Nuclear respiratory factor-1 and -2
Nrf2	Nuclear factor (erythroid-derived 2)-like 2
OMM	Outer mitochondrial membrane
PCR	Polymerase chain reaction
PE	Phosphatidylethanolamine

PERK	PKR-like ER kinase
PGC-1α	Peroxisome proliferator activator receptor (PPAR) γ coactivator 1 alpha
PIM	Protein import machinery
PINK1	PTEN-induced putative kinase 1
PKR	Protein kinase RNA-activated
PQC	Protein quality control genes
PUMA	p53 upregulate modulator of apoptosis
RIDD	Regulated IRE1-dependent decay
RNA	Ribonucleic acid
RNase	Endoribonuclease
ROS	Reactive oxygen species
rRNA	Ribosomal RNA
S1P	Site-1 protease
S2P	Site-2 protease
SAM	Sorting and assembly complex
SDS-PAGE	Sodium dodecyl sulfate polyacrylamide gel electrophoresis
SirT3	Sirtuin-3
SirtT1	Sirtuin-1
Sp-1	Specificity protein-1
SR	Sarcoplasmic reticulum
SS	Subsarcolemmal
STR	Slow-twitch red
TA	Tibialis anterior
TCA	Tricarboxylic acid cycle
Tfam	Mitochondrial transcription factor A
TFB1M	Transcription factor B1, mitochondrial
TFB2M	Transcription factor B2, mitochondrial
TIM	Translocase of the inner mitochondrial membrane
TNF	Tumor necrosis factor
TOM	Translocase of the outer mitochondrial membrane
TRAF-2	TNF receptor-associated factor 2
tRNA	Transfer RNA
TSC-1	Tuberis sclerosis protein 1
TUDCA	Tauroursodeoxycholic acid
UDCA	Ursodeoxycholic acid
ULK1	Serine/threonine protein kinase ULK1
UPR	Unfolded protein response
UPR^{ER}	Endoplasmic reticulum UPR
UPR^{mt}	Mitochondrial UPR
USF-1	Upstream stimulatory factor 1
XBP1	X-box binding protein 1
XBP1s	Spliced XBP1

CHAPTER 1: REVIEW OF LITERATURE

1.1.0 SKELETAL MUSCLE PHYSIOLOGY

In order to properly understand the factors that govern muscle function and plasticity, it's important to first attempt to understand the constituent components that comprise skeletal muscle and its unique characteristics. Along with muscle fibers, skeletal muscle contains a variety of tissues including neural (motor neurons), vascular (capillaries), as well as various types of connective tissues. Muscle cells, while retaining many of the organelles found within other cell types, are unique in their long cylindrical shape and multinucleated composition, whereby nuclei are arranged along the periphery of the fiber, under the sarcolemma. Furthermore, mitochondria are divided into two subfractions within the myofiber, subsarcolemmal (SS) and intermyofibrillar (IMF) (87). Skeletal muscle gets its contractile ability through the physical interaction of overlapping myofilaments, actin and myosin, which make up the sarcomere. Each muscle cell contains repeating sarcomere subunits that facilitate muscle contraction through the interaction of the myofibrillar proteins in an ATP-dependent manner (193). Overall, muscle exists in a highly organized, yet heterogeneous, arrangement such that differences in myosin isoforms expressed as well as intracellular mitochondrial density within the muscle contribute to differences in performance capability (192). Skeletal muscle is extremely sensitive to its environment, adjusting the internal phenotype of the cell to match the level of activity. Many of the physiological adaptations are well characterized, however the molecular mechanisms that mediate these changes have yet to be fully elucidated.

1.1.1.1. Skeletal Muscle Fiber Types

Skeletal muscle is divided into three sub-classes of fibers, with the designation of

fiber-type dependent on their metabolic and contractile components. Repeated studies have classified muscle fibers based on the immunoprobing of myosin heavy chains (MHC) isoforms within various muscle groups (190, 193). The standard classifications of skeletal muscle is as follows: 1) slow-twitch red (STR) fibers comprised predominantly of MHC type I isoform, 2) fast-twitch red (FTR) fibers containing mainly MHC type IIa isoform, and 3) fast-twitch white (FTW) fibers, of which MHC type IIb or IIx isoforms are most abundant, depending on the species. Despite their classification as being either fast or slow muscle, most muscle groups are heterogeneous in their fiber type composition. Rat soleus (slow) muscle is comprised of 83% STR and 17% FTR, whereas tibialis anterior (TA; fast) muscle is 3% STR, 61% FTR, and 36% FTW (117).

Each fiber type maintains a distinct array of contractile and regulatory proteins, as well as enzymes involved in intermediary metabolism that function in conserving a particular fiber phenotype (27, 89, 181). Specifically, slow-twitch type I fibers contain heightened mitochondrial and oxidative enzyme content, along with an elaborate capillary network which dispose these fibers for prolonged sub-maximal muscle activity (60, 200). STR fibers also maintain a slower contraction velocity and reduced total force output when compared to type II fast-twitch fibers. Moreover, fast-twitch fibers are typically recruited during phasic activity, but remain significantly more diverse in overall composition. These fibers generally produce greater force, however are more prone to fatigue, particularly FTW fibers (20, 51). This reduced fatigue resistance is largely a result of a higher glycolytic enzyme expression relative to mitochondrial oxidative enzymes, and thus enhanced reliance on glycolytic metabolism leading to acidification of the muscle bed. Interestingly, mitochondrial distribution within human skeletal muscle

fiber-types may differ from other animal models (92). For instance, rodent FTR muscle fibers exhibit a higher mitochondrial content and are therefore more oxidative than STR fibers (51, 111). Additionally, other fiber-type specific cellular structures contribute to the contractile differences in muscle fibers. Fast fibers have been shown to have greater density of acetylcholine receptors (AchR) and release of Ach, along with a higher abundance of Na^+ channels on the post-synaptic membrane. Furthermore, these fibers have a more developed sarcoplasmic reticulum (SR) for greater release and uptake of calcium (138, 179, 191). Therefore, overall muscle fiber composition such as contractile characteristics of myosin isoform, along with density of mitochondria and additional subcellular structures govern the differences observed between fiber-types.

1.1.2.1. Mitochondrial Structure

Cellular ATP, required for the function and maintenance of the cell, is primarily derived from mitochondrial respiration. Mitochondria are structurally unique in that they maintain two intra-organelle subdivisions separated by phospholipid membranes, these are: 1) the inner mitochondrial matrix bound by the innermembrane; and 2) the intermembrane space, designated between the outer and innermembrane. The mitochondrial matrix is biochemically dissimilar from the cytosol of the cell, maintained by specialized protein import machinery that lies within the innermembrane in which proteins must pass through to enter the matrix (104, 173). This regulation of the matrix milieu is of critical importance since it houses multiple copies of mitochondrial DNA (mtDNA), a 16kb circular genome that encodes 13 essential respiratory proteins as well as 22 tRNAs and 2 rRNAs (87). Conversely, the outermembrane is porous and allows small molecules (<10kDa) to enter the intermembrane space, independent of import

machineries, and therefore is chemically equivalent to the cytosol (235). Measurement of mitochondrial content within muscle can be made using morphometric techniques such as electron microscopy. More commonly, estimates can be made based on changes in maximal activity under optimal conditions of a typical marker enzyme such as citrate synthase or cytochrome c oxidase, or change in expression of a protein such as cytochrome c (89).

Mitochondria in muscle exist as interconnected networks often referred to as a reticulum. The oxidative capacity of the muscle, along with the region of the fiber in which the mitochondria are located, govern the extensiveness of the reticulum (158). The maintenance of such a network is regulated by dynamic fission and fusion events in order to add new, or remove damaged, mitochondria (213). From a functional standpoint these processes are vital to allow passage of proteins, lipids and mtDNA along the network and maintains a healthy, viable mitochondrial pool (81).

1.1.2.2. Mitochondrial Subfractions

Mitochondria within skeletal muscle are divided into two subcellular localizations with similar, but distinct functional and biochemical properties. SS mitochondria reside along the surface of the muscle fiber below the sarcolemmal membrane, and lye proximal to the myonuclei (90). As this locale may imply, these mitochondria serve to supply ATP for membrane functions, such as NA^{+}/K^{+} ATPase. Conversely, the IMF fraction of mitochondria is primarily responsible for the provision of ATP for actin/myosin interaction and contraction, as this pool of mitochondria are interspersed amongst the skeletal muscle myofibrils (42). SS and IMF mitochondria have been isolated into their respective subfractions in order to experimentally define the exact biochemical profile of

either population. IMF mitochondria make up the majority (80-85%) of the total mitochondrial volume, and they exhibit a markedly elevated level of oxidative enzymes and protein synthesis rate, contributing to a 2-3-fold greater rate of oxygen consumption and higher state 3 and state 4 respiration rates (42, 44, 124, 126, 164, 210). Moreover, IMF mitochondria also display a significantly higher rate of protein import (210). Conversely, SS mitochondria retain a significantly greater membrane potential while producing nearly 3-fold more reactive oxygen species (ROS) (4). Finally, variations in both muscle and activity level can promote changes in electron transport chain and mitochondrial matrix protein stoichiometry, resulting in a change in the respiratory capacity within SS and IMF mitochondria (3, 90, 114, 155). Furthermore, the distinctive localizations as well as biochemical make-up render the subpopulations differentially sensitive to changes in the environment, as SS mitochondria repeatedly exhibit an enhanced lability possibly due to proximity to peripheral myonuclei, or an altered capacity for protein synthesis and import (44, 210).

1.2.0. ADAPTATIONS TO EXERCISE

Skeletal muscle, malleable as it is, responds to stressful conditions in order to match the new demands being placed upon it. Such is the case with exercise in eliciting various changes to the cellular environment in order to sustain optimal function. In the context of muscle performance, repetitive contractile episodes create an augmented energy deficit in the form of ATP, which in turn elicits a reprogramming of the cellular mitochondrial network in order to match the newly imposed demand. Mitochondria, as the cellular powerhouse, undergo remodeling through both synthesis (mitochondrial biogenesis) and turnover (mitophagy) in order to match ATP demand and provide an

optimal cellular network in which to do so, thus shifting to a more oxidative, less glycolytic phenotype (13, 89). The coordinated remodeling of the organelle reticulum has been well studied, as it is important not only to muscle performance but also overall metabolic health. This chapter will provide a description of the processes involved in mitochondrial adaptations with exercise.

1.2.1.1. Mitochondrial Biogenesis with Exercise

While mitochondria contain its own circular DNA, it contributes less than 1% of total mitochondrial proteins with the remainder provided by the nucleus (Fig. 1A). Nevertheless, 13 essential respiratory chain components are derived from mtDNA along with 22 tRNAs and 2 rRNAs which are integral to mitochondrial biogenesis and health (12, 82, 188). Therefore, there exists a complex cascade of events that allow the products of either genome to shuttle to, and integrate within the mitochondrion to facilitate in reticular expansion of the organelle.

Early signaling events involved in mitochondrial biogenesis are initiated during the onset of contractile activity within skeletal muscle and converge largely on the activation of the transcriptional coactivator PGC-1α, regarded as the master regulator of mitochondrial biogenesis (72, 89, 185, 189). The preeminent signaling molecules considered to initiate biogenesis with prolonged exercise include (1) calcium/calmodulin-dependent protein kinase (CaMK; specifically CaMKII), via increased intracellular Ca^{2+} released by the sarcoplasmic reticulum during contraction (160); (2) p38 mitogen-activated protein kinase (MAPK) which is sensitive to a variety of stressors including exercise (6, 172, 174); (3) AMP-activated protein kinase (AMPK), activated by increased ADP:ATP (97, 99, 100, 223); and (4) reactive oxygen species (ROS) generated

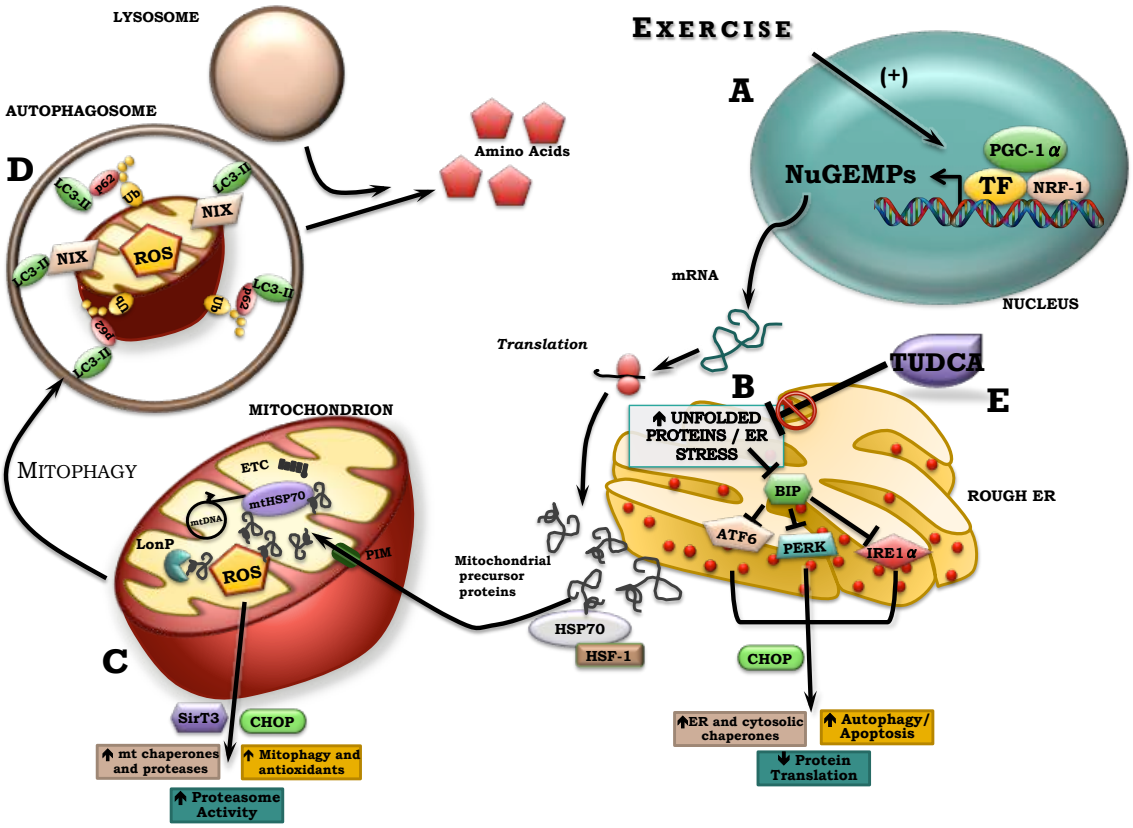

Figure 1. The unfolded protein responses related to mitochondrial biogenesis and autophagy. A) Exercise induces mitochondrial biogenesis through the transcription of Nuclear Genes Encoding Mitochondrial Proteins (NuGEMPs). Transcripts are translated in the cytosol and require appropriate cytosolic and mitochondrial chaperones for trafficking. If the cell is ill-prepared to meet this influx, proteins will accumulate triggering two separate pathways aimed at restoring cellular homeostasis. **B)** The UPR^{ER} contains three independent cascades, stemming from ATF6, PERK and IRE1α, which remain inactive under steady state conditions bound with BiP. BiP releases to bind misfolded proteins as they accumulate in the ER lumen, thus activating the three branches of the UPR ultimately resulting in activation of downstream effectors in order to regain homeostasis by increasing overall cellular protein handling. **C)** If the proteotoxic stress within the mitochondria is too great, it can cause oxidative stress leading to activation of kinases such as Akt or JNK2, ultimately signalling for increased proteasome activity and expression of mitochondrial specific chaperones and proteases, respectively. Likewise, activation of SirT3 induces mitophagy and antioxidant machinery. Ultimately, if the UPR^{ER} and UPR^{mt} are insufficient to restore homeostasis then mitophagy will ensue. **D**) Mitochondria are tagged for degradation by NIX or by Ubiquitin (with p62 acting as an anchor between ubiquitin and LC3-II) ultimately leading to full encapsulation and breakdown. **E)** TUDCA is a chaperone mimetic drug capable of alleviating ER stress and UPR activation, thus reducing the proteotoxic burden to the cell.

throughout the muscle cell and mitochondria (63, 86, 99, 180). Thus during exercise conditions PGC-1α expression can be regulated in a multitude of ways. For instance, elevated intramuscular Ca^{2+}-induced CaMK activation, as well as activation of ATF in a p38-dependent manner, upregulate binding of the cAMP response element (CRE) binding protein (CREB) to the PGC-1α promoter (228). Further, ROS, in an AMPK-dependent manner as well as AMPK directly, can enhance NAD-dependent deacetylase Sirt1 resulting in PGC-1α deacetylation and promote DNA binding (11, 70). PGC-1α is known for its importance in mitochondrial biogenesis, such that its expression is highest in highly oxidative tissues such as heart and type I skeletal muscle fibers (54). Likewise, its expression is typically most regulated with endurance-type exercise (16). PGC-1α has a paramount role in regulating the activity of various transcription factors in order to coordinate the expression of mitochondrial genes both emanating from the nucleus and mitochondria.

While PGC-1α is the master regulator of mitochondrial biogenesis, the regulatory region of mitochondrial genes that are nuclear-encoded are heterogeneous, therefore the regulation of organelle synthesis requires multiple regulators of transcription (89, 119). A number of transcription factors associated with exercise-induced mitochondrial biogenesis have been established, such as CREB, the estrogen related receptors (ERRα,β,γ), early growth-response gene-1 (Erg-1), c-fos, c-myc, specificity protein-1 (Sp-1), upstream stimulatory factor-1 (USF-1), as well as nuclear respiratory factors 1 and 2 (NRF1 and NRF2) (84). Each transcription factor when bound to target gene promoter sequences can upregulate the expression of mitochondrial proteins. Both acute and prolonged contractile activity have been shown to induce transcription of Sp-1, and

Erg-1, regulators of mitochondrial proteins such as cytochrome c (98, 137, 147, 226). Similarly, exercise upregulates NRF-1, which is important in the regulation of proteins which mediate mtDNA expression such as mitochondrial transcription factor B-1M (TFB1M), and -2M (TFB2M) and the mitochondrial transcription factor A (Tfam) which is integral for cytochrome c oxidase complex formation (52, 62, 186, 187). Following an acute exercise bout, PGC-1α promoter activity increases along with mRNA levels, while NRF-1 and -2 increase their DNA binding during the recovery (5, 16). Further regulation of the process is accomplished by an auto-regulatory feedback loop, whereby transcription factors such as USF-1 and CREB can enhance PGC-1α expression (100). Altogether, the coordinated expression and function of these transcription factors along with PGC-1α regulate, and facilitate, overall nuclear-mitochondrial gene expression leading to organelle biogenesis.

1.2.1.2. Protein Handling Machinery and Import

As previously described, the mechanism by which mitochondrial proteins are transcribed and translated is regulated through the collaboration of the mitochondrial and nuclear genomes, with the vast majority of proteins originating outside of the mitochondrion. Thus, handling of these precursor proteins is integral to the expansion of the mitochondrial pool. Newly translated nuclear-encoded proteins are initially synthesized as precursor proteins with a positively charged N-terminal presequence that dictates the protein's destination within the organelle (18). These precursor proteins remain in an unfolded state in order to allow easier passage, however this confirmation leaves them more susceptible to aggregation through unwanted protein-protein interactions (19, 113, 167, 178). Heat shock proteins such as HSP70 and HSP90 exist to

overcome such maladaptive outcomes, and are involved in shuttling of mitochondrial precursor proteins to the mitochondria where they may be imported through the mitochondrial protein import machinery (PIM) (53, 232).

The mitochondrial PIM is composed of the translocase of the outer- and inner-mitochondrial membrane (TOM and TIM). Precursor proteins are translocated to the TOM complex receptors Tom20, and Tom70, where they will continue through the pore, which is comprised predominately of Tom22 and Tom40, as well as Tom6, Tom7, and Tom5 (7, 33, 50, 83, 106). On the outer membrane there exists, along with the TOM complex, a sorting and assembly (SAM) complex responsible for insertion of outer membrane proteins (116). Once proteins have passed through the TOM complex, they are subsequently delivered through the TIM complex forming the TOM-TIM supercomplex (38). The TIM machinery consists of the Tim23 complex, in which Tim17 and Tim23 form a pore that a majority of precursor proteins pass through to reach the matrix. As well, the Tim22 complex facilitates proteins targeted to the innermembrane. Once through the TIM complex mtHSP70 helps pull the preprotein into the matrix in an ATP-dependent manner where the positively charged presequence can be cleaved by matrix proteases. Mitochondrial-specific chaperones HSP10 and HSP60 can then facilitate proper protein conformation and translocation to the final destination within the mitochondrion (19, 24, 25). In the context of exercise-induced mitochondrial adaptations, there is evidence of consensus binding sites for NRF-1 and NRF-2 in the promoter region of various import genes (23, 80). Likewise, import rates of important matrix destined proteins such as Tfam have been found to increase with chronic contractile activity via augmented expression of PIM components as well as an enhanced expression of import

chaperones (66, 161, 208).

1.2.2.1. Autophagy with Exercise

Another important regulator of skeletal muscle health and adaptation to exercise is autophagy, or mitophagy in the context of mitochondria. The process is characterized as the selective degradation of protein aggregates and worn-out organelles through the encapsulation by a double-membrane autophagosome (Fig. 1D). Once fully engulfed, the autophagosome undergoes fusion with a lysosome in order to degrade the selected cargo and allow amino acid recycling (120, 141, 142). Given that the primary role of autophagy is to degrade cellular components, it seems counter-intuitive that it would be of critical importance to muscle health and function (35). Research has discovered that lack of autophagy results in muscle degeneration, wasting, and reduced strength, as well as accumulated protein aggregates, and dysfunctional organelles (such as the sarcoplasmic reticulum and mitochondria) contributing to excessive oxidative stress (35, 67, 133, 134).

Autophagosome formation is dependent on three key molecular events: 1) conjugation of LC3, as well as upstream regulation provided by 2) ULK1, and 3) Beclin1 complexes. Inactive LC3-I requires conjugation to the phospholipid phosphatidylethanolamine to become the active form LC3-II through a series of events regulated by a number of autophagy proteins (Atgs), particularly Atg6-Atg12-Atg16L1 and Atg7. Once activated LC3-II can integrate within the double-membrane phagophore allowing for elongation and interaction with tagged cargo. Generally, LC3 interacts with p62 which provides a bridge between ubiquitin-flagged organelles and LC3-II (120, 140). Activation of this process is under the regulation of ULK1 and Beclin1 complexes, which facilitate phagosome expansion and are integral in sensing the energy status of the cell

under inhibition by the mTORC1 complex (140). mTORC1 acts downstream of the insulin/Akt pathway and can be negatively regulated by AMPK phosphorylation of tuberous sclerosis complex (TSC)-2 tumor suppressor, an upstream regulator, and raptor, a component of mTORC1 (96, 101, 139). Furthermore, AMPK can act directly on both ULK1 and Beclin1 complexes to directly induce complex formation, providing a similar mode of energy-sensing activation to that of mitochondrial biogenesis (108).

Autophagy activation has been of focus in recently published works for its role as a cellular homeostatic response, and not solely degradation, as its absence leads to muscle myopathies (68, 133). Exercise has been shown to be a potent activator of autophagy, contributing to beneficial skeletal muscle remodeling (78, 122). Exercise-induced increases in AMPK, as mentioned, are capable of relieving mTORC1 suppression of ULK1 and Beclin1 complexes. Likewise, a link between p38 MAPK and autophagy in an oxidative stress-induced manner has been reported, similar to the hallmark signaling events that occur with exercise in mediating mitochondrial biogenesis (135). Work investigating basal autophagy in various fiber types discovered enhanced autophagy flux, as well as autophagy and mitophagy protein expression in muscles with the highest oxidative capacity compared to mixed or glycolytic muscle. Moreover, long-term voluntary wheel running resulted in increased autophagy flux, and mitophagy proteins concomitant with mitochondrial biogenesis (122). Recently, PGC-1α has been implicated in mediating autophagy in denervation-induced mitophagy activation, thus providing an overall link between muscle health and metabolic profile, to autophagy (218).

1.2.3.1. CCA as a Model of Exercise

Given that PGC-1α and mitochondrial biogenesis respond most significantly to

endurance exercise in skeletal muscle, it becomes important to utilize practical physiological models capable of eliciting mitochondrial adaptations in a similar manner. The chronic contractile activity (CCA) model of exercise is one such example, which replicates the continuous muscle contractions of skeletal muscle, specifically slow-twitch motor units, during endurance exercise, and can be accomplished both *in vivo* and *in vitro* (45, 184, 209). Both models provide an advantage in their ability to regulate the stimulus, while the animal model further affords the ability to have intra-animal control (non-exercised) muscle matched to the stimulated muscle of the contralateral limb. *In vivo* stimulation involves the implantation of two wire electrodes spanning the common peroneal nerve delivering electrical impulses at a fixed setting (6 volts; 10Hz, 0.1ms) causing muscle contraction of the innervated leg, particularly the tibialis anterior and extensor digitorum longus (125, 209). The same concept of electrical stimulation can be applied in a cell culture model using skeletal muscle cells. With this *in vitro* procedure, platinum wire electrodes are placed on either side of the cell dish, which are attached to an external stimulator to elicit contraction of the muscle cells (45, 214, 222). Similar levels of adaptation can be achieved between both animal and cell models with the only added disadvantage *in vitro* being that isolated cells lack the whole-body effects of contracting within the organism (209, 214).

Some key considerations are to be made with respect to the use of CCA; the stimulator unit must be able to provide a consistent and sufficient current intensity without prolonged disruption, and the integrity of the electrodes must remain intact. As well, differences in the recruitment of muscle fibers exist between CCA and regular exercise in that the asynchronous-hierarchical order of recruitment involved in normal

contractions is abolished, as all motor units are recruited with electrical stimulation. However, these differences can also provide further advantages. In engaging all motor units we are able to elicit a response in fibers normally not recruited with exercise in a target muscle in a reproducible pattern of activation between subject animals (125).

Regular endurance exercise, with incrementally increasing intensity, results in mitochondrial biogenesis within 6-8 weeks (2, 87, 89). A similar level of adaptation can be elicited in a single week of CCA thus providing another distinct advantage of time efficiency (209). Increases in expression and stability of mitochondrial ETC constituent transcripts, and increase protein synthesis and turnover rates were observed with CCA in line with adaptations to regular exercise (44, 55, 85). Additionally, increases in the overall protein handling ability of the muscle was upregulated with prolonged CCA indicating a newly adapted phenotype (161). This increase in mitochondrial content is likely through similar mechanisms of activation as seen with traditional exercise. CCA has been shown to enhance intracellular Ca^{2+}, thus likely contributing to the activation of upstream regulatory kinases such as CaMK (34, 125, 201). Further, a close correlation has been established between CCA-induced increases in PGC-1α and COX activity, as well as nuclear-encoded protein import into the mitochondria such as Tfam (64, 97). Finally, CCA produces a metabolic switch from muscle-specific lactate dehydrogenase (M-LDH) to heart-specific (H-LDH), which coincides with an increase in fatty acid (FA) oxidation (88, 94, 125). Therefore CCA is an important and powerful model in eliciting skeletal muscle adaptations such as mitochondrial biogenesis similar to normal endurance exercise.

1.3.0. THE UNFOLDED PROTEIN RESPONSE

Along with mitochondria, the endoplasmic reticulum (ER) is a vital organelle that plays an important role in protein translation and processing, principally in highly secretory cells such as those found in pancreatic islets, liver and adipose tissue. Of considerable interest to researchers has been the impact of ER stress on cell function and viability, as perturbations within the ER can have considerable consequences on cellular proteostasis and can contribute to various pathologies. In particular, work has focused on a primary response to ER stress, termed the unfolded protein response (UPR). Overall, the UPR serves to balance protein translation with processing in order to maintain, or regain, cellular homeostasis during normal, and stressful conditions, respectively. Generally, this is accomplished through two mechanisms of action: 1) upregulation of folding capacity, through increased chaperones, foldases, and ER enlargement; and 2) down-regulation of protein biosynthetic load by decreasing transcription and translation as well as increasing clearance of misfolded proteins (195).

Skeletal muscle, while not especially secretory in nature, is an intriguing tissue in that it has an expansive network of specialized ER termed the sarcoplasmic reticulum (SR). As mitochondria are critical in skeletal muscle function, their relationship to the ER is of considerable interest as the two exist as tightly connected organelles both functionally and physically, which synchronously regulate, and communicate via intracellular Ca^{2+} (205). Furthermore, interest in a second UPR emanating from the mitochondria (UPR^{mt}) is gaining momentum, although the majority of research has been conducted in lower organisms. Nonetheless, the ability of mitochondria to monitor protein status within the organelle in a similar manner to the ER is of particular interest in

the context of skeletal muscle health and adaptation, especially considering that mitochondria rely on the integration of mtDNA and nDNA-derived proteins.

1.3.1.1. The ER Stress Response – the UPR^{ER}

Stress to the ER can result from various conditions such as elevated intracellular lipids, glucose deprivation, calcium imbalances, as well as marked increases in protein synthesis (Fig.1B). Given the importance of the ER in protein maturation into active cellular components, this stress can be highly damaging, therefore the UPR plays an integral role in maintaining proper function (236). In mammals the UPR has three independent, yet interrelated, branches mediated by the activation of transmembrane proteins imbedded in the ER membrane, those being activating transcription factor-6 (ATF6), protein kinase RNA (PKR)-like ER kinase (PERK), and inositol-requiring enzyme-1 (IRE1), which is a conserved branch across all eukaryotes, indicating the importance of this adaptive response in general cellular function (195). Together, these ER signal transducers carry out three phases of the UPR: 1) an acute response reduces ER protein load; 2) the ER adapts to increase in its protein handling capability; and 3) cell death is invoked if the stress proves to be too great and homeostasis can not be achieved (182).

Proteins are considered unfolded based on their thermodynamic and kinetic conformation. Free energy of each configuration is determined by contacts of its nonpolar groups. Thus, proteins will continuously fold to bury the polar groups at their core, reduce the free energy to the lowest possible, and in this way prevent hydrophobic side chains from being exposed. When these parameters are not met, the protein is deemed unfolded and are sensed by binding immunoglobulin protein (BiP), also referred to as 78

kDa glucose-related protein (GRP78) (203). Under normal conditions, BiP remains bound to the ER luminal domains of the three UPR signaling transducers. As unfolded proteins accumulate, BiP releases and preferentially binds to the hydrophobic peptides exposed on the surface of misfolded proteins in order maintain the protein conformation and prevent further misfolding (61). This release of BiP allows activation of the distinct UPR branches, which will be discussed further below. A similar mode of unfolded protein recognition exists in the cytosol through the cytosolic heat-shock response and is related to the UPR in general function. In a manner reminiscent to BiP, cytosolic chaperones such as HSP70 bind the transactivating domain of heat shock factor-1 (HSF1) thereby repressing its transcriptional activity. As protein folding within the cytosol is perturbed, HSP70 releases to preferentially bind the unfolded proteins, thus allowing HSF1 to translocate to the nucleus and upregulate transcription of chaperones and proteasomal subunits (169, 199).

While IRE1 is the conserved UPR branch, PERK shares many similarities both structurally and functionally (123). Both proteins are type I transmembrane protein kinases, which become active upon BiP release leading to di- or oligomerization and transautophosphorylation of the cytosolic kinase domain (22, 123). IRE1, within its cytosolic region, carries out two enzymatic functions: the first, an endoribonuclease (RNase) which splices a 26 nucleotide intron from the mRNA transcript encoding X-box binding protein 1 (XBP1) (32, 118, 231); and second, a serine/threonine kinase (46). Spliced XBP1 mRNA encodes a potent transcription factor (XBP1s) to modulate the expression of multiple UPR target genes including ER chaperones, phospholipid processing proteins, ER tanslocon components, and ER-associated degradation (ERAD)

factors (118, 182). Additionally, IRE1 can modulate signaling events that crosstalk with other stress pathways, such as apoptosis, autophagy, proliferation, metabolism, and inflammation. In particular, IRE1 binds to TNF-receptor-associated factor 2 (TRAF2), promoting activation of the c-Jun NH_2-terminal kinase (JNK) pathway, and can modulate other pathways including p38, ERK and NF-kB (93, 152, 153, 216). PERK conversely, contains a cytosolic kinase domain, which plays an important role in the acute response of the UPR. Activated PERK phosphorylates eukaryotic translation initiation factor 2 (eIF2α) at serine-51, thus deactivating it and reducing protein synthesis in order to alleviate the misfolded protein burden (74, 123). However, despite this decrease in protein translation, some mRNAs are preferentially translated while eIF2α is suppressed. One example is ATF4, a transcription factor that positively regulates UPR genes involved in amino acid metabolism, antioxidant response, protein folding, autophagy and apoptosis (73, 79, 110). Of the more important ATF4 target genes is CCAAT enhancer binding protein (C/EBP) homologous protein (CHOP), widely considered a pro-apoptotic transcription factor (131, 206, 217). Furthermore, PERK activation leads to phosphorylation, and activation, of the pro-survival transcription factor NF-E2 related factor 2 (Nrf2) to promote transcription of the antioxidant machinery (47).

ATF6 is a type II transmembrane domain protein containing a basic leucine zipper (bZIP) transcription factor in its cytosolic domain (77). Upon BiP release, ATF6 translocates from the ER membrane to the Golgi apparatus where site-1 and site-2 proteases (S1P and S2P) process and release the cytosolic bZIP domain (39, 77, 230). Active ATF6 will then shuttle to the nucleus where it binds to the ATF/cAMP response element (CRE) and the ER stress response elements I and II (ERSE-I and -II) to initiate

transcription of quality control chaperones BiP and GRP94, foldases such as protein disulfide isomerase (PDI), ER proteins involved in glycosylation and Ca^{2+} handling, ERAD components, as well as transcription factors XBP-1 and CHOP (1, 77, 112, 194, 221, 225). Furthermore, ATF6 along with XBP1 contribute to ER biogenesis through expansion of the tubular networks of the rough ER (26, 198, 202). Altogether this suggests a tightly coordinated regulation of cell fate during acute and chronic ER stress.

1.3.1.2. The UPR^{ER}, CHOP, Autophagy, and Apoptosis

The UPR acts as a cell rheostat monitoring the duration and intensity of stress in order to mount appropriate responses to maintain optimal function. In doing so the UPR is capable of shifting from acute phase protein handling to more adaptive processes such as autophagy or apoptosis, largely through CHOP signaling. In particular, CHOP transcribes growth arrest and DNA damage-inducible 34 (GADD34), which dephosphorylates eIF2α, therefore reversing the action of PERK, and has been shown to upregulate over a dozen autophagy genes (Atgs) during prolonged stress (15, 43, 105, 154). CHOP-induced autophagy signaling is further enhanced by the activation of Beclin1 through the IRE1 branch of the UPR in a TRAF2-JNK-dependent manner (156). Additionally, it has been shown that activation of autophagy associated with ER stress can be induced independently of common autophagic activators such as Akt and Foxo, indicating the direct effect the UPR^{ER} has in moderating cell fate (128). Furthermore, while studies have shown that CHOP supports cell-survival signaling, it is typically depicted as pro-apoptotic in function and can facilitate the switch from autophagy in favor of cell-death (14). Primarily, CHOP exerts its influence on apoptosis through inhibition of the anti-apoptotic factor Bcl-2, which otherwise promotes cell survival

through sequestration of BH3-only proteins, such as Bim and PUMA – factors involved in Bax-Bak-mediated mitochondrial permeablization (40, 41, 56, 136). Moreover, research has shown that CHOP, through its transcriptional target ER oxidase 1α (ERO1α), activates the ER calcium release channel inositol triphosphate receptor-1 (IP3R1), important in a variety of mitochondrial processes and can also initiate apoptosis as a consequence of organelle dysfunction (121, 162). Likewise, IRE1 contributes to the apoptotic signaling through a few proposed mechanisms: 1) the activation of JNK via TRAF2 and consequent activation of pro-apoptotic factors such as Bax/Bak (216); 2) regulated IRE1-dependent decay (RIDD), a process that becomes pro-apoptotic with prolonged stress by degrading mRNAs encoding ER chaperones (71, 215); and 3) the activation of murine caspases-12 (or human caspase 4) (143). In part, these events converge on the mitochondrial intrinsic apoptotic-signaling pathway, and reinforce the integrated function of the two organelles as they pertain to cellular viability and adaptation.

1.3.1.3. The UPR^{ER} and Mitochondria

As mentioned, the ER and mitochondria are closely linked organelles both physically and functionally. Specifically, the close-contact communication sites between the ER and mitochondria are termed mitochondria-associated membrane (MAM), with the functional implication of this interaction being a collaborative handling of lipids and calcium homeostasis (21, 205). As well, this physical association between these organelles is reinforced by dimeric bridges formed between the mitochondrial morphology protein mitofusin-2 (Mfn2) localized to both the mitochondria and at the MAM, on the ER (30). The regulated interaction by Mfn2 plays a critical role in

mitochondrial calcium uptake from the ER, and regulates mitochondrial morphology through interaction with PERK (30, 31, 146). As described in the previous section, chronic ER stress is capable of eliciting an apoptotic response through UPR activation, partly dependent on the mitochondrial intrinsic apoptotic pathway, which results in the mtPTP opening and cytochrome c release (207, 219). Moreover, recent work has found that at early stages of ER stress, the ER and mitochondria become more physically connected in order to initially increase mitochondrial metabolism through enhanced calcium transfer and provision of energy substrates, or lead to apoptotic activation following prolonged stress (29). Conversely, while ER stress and UPR activation can affect mitochondrial function, a similar effect can occur through mitochondrial stress on the ER. Recent studies have shown a link between mtDNA damage contributing to oxidative stress and the induction of a number of UPR target genes, ultimately leading to autophagy and apoptosis (233, 234). This indicates a considerable co-reliance and crosstalk between the two cellular networks during perturbations in the organelle milieu.

1.3.2.1. The UPR^{mt}

The coreliance on nuclear and mitochondrial transcribed proteins that require various factors to facilitate the import and assembly into stoichiometric complexes leaves mitochondria susceptible to perturbations in homeostasis. Such events as mitochondrial biogenesis and protein import, mutations in constituent proteins, the presence of damaging reactive oxygen species (ROS), or harsh environmental conditions can negatively impact mitochondrial protein folding and overall function (75). Fortunately, mitochondria launch an organelle-specific unfolded protein response comparable to the ER, to initiate a retrograde signaling cascade to the nucleus and increase transcription of

mitochondrial protein quality control (PQC) genes (Fig. 1C). The UPR^{mt} was first documented in mammalian cells when mtDNA mutations and the accumulation of terminally misfolded proteins resulted in an increase in mitochondrial chaperones and proteases (132, 183, 237). However despite these findings, an understanding of the UPR^{mt} signaling cascade has not been well characterized in mammalian cells, and only recently has a more in-depth clarification of the specific events been resolved in *Caenorhabditis elegans*.

1.3.2.2. The UPR^{mt} in *C. elegans*

Discovery of a novel master transcription factor capable of integrating a complex web of UPR^{mt} pathways has been observed in worms (76). Unfortunately, no mammalian homolog has been identified, however the possibility remains that such a factor does exist (196). Nevertheless, this transcription factor, termed activating transcription factor associated with stress-1 (ATFS-1), provides a unique and novel understanding of the potential integration of the UPR^{mt}. ATFS-1 contains both a nuclear loacalization signal (NLS) as well as a mitochondrial targeting sequence (MTS) and it is degraded under basal conditions in the mitochondrial matrix by LonP (151). However under stressful conditions, accumulated protein aggregates are degraded by proteases, releasing peptide fragments through the mitochondrial HAF-1 transporter into the cytosol (151). These protein fragments in turn reduce ATFS-1 import into the mitochondria allowing it to move to the nucleus where it activates transcription of a host of genes to recover mitochondrial homeostasis. Specifically, it activates mitochondrial chaperones, proteases, and import/transport machineries, detoxification enzymes, as well as autophagy markers, while simultaneously reducing ETC and TCA components but inducing a range of

glycolysis genes (150). This unique mechanism of signaling provides an initial switch in energy supply away from mitochondria during initial repair thus matching biogenesis to mitochondrial proteostatic capacity, and equips the organelle with a greater protein handling for the future.

1.3.2.3. The Mammalian UPR^{mt}

While UPR^{mt} in *C. elegans* has been studied to a greater degree, there are a variety of signaling events that have been observed in mammalian cell models. Mitochondrial chaperones, and proteases in the matrix, as well as the intermembrane space are the prime sensors of misfolded mitochondrial proteins and are capable of sensing, and eliciting, compartment-specific responses (17, 168, 212). Proteotoxic stress localized to the intermembrane space induces an increase in ROS leading to phosphorylation of estrogen receptor α (ERα) through AKT activation. Activated ERα can then enter the nucleus and drive expression of the IMS protease OMI/HtrA2 in order to degrade and remove the accumulated proteins (165). Similarly, proteases ClpP and LonP monitor mitochondrial matrix protein status and can help facilitate the activation of a set of pathways in response to misfolded protein aggregates. In particular, this perturbed compartmental proteostasis prevents further protein accumulation through two mechanisms: first, by blocking protein import via degradation of TIM17A by the protease Yme1l (176); and second, through the activation of dsRNA-activated protein kinase (PKR) and subsequent phosphorylation of eIF2α to reduce global translation similar to the UPR^{ER} (177). Furthermore, the transcription factor c-Jun is activated during the UPR^{mt} through JNK2, which increases the expression of CHOP and C/EBPβ (91, 237). In turn, these two transcription factors heterodimerize and bind to CHOP binding regions

flanked on either side by a UPR^{mt} response element (MURE) in promoter regions of various quality control proteins to induce transcription (8). Antioxidant machinery was shown to increase through c-Jun activation of Nrf2, possibly linking this response to CHOP-C/EBPβ activity (102, 175). Similarly, a secondary responder to mitochondrial proteotoxic stress, SirT3 upregulates antioxidants through deacetylation of Foxo3 (175). Our evolving understanding of the UPR^{mt} suggests that these signaling events associated with mitochondrial stress help align the mitochondrial and nuclear genomes at the protein level, thus helping to coordinate mitochondrial adaptations and remodeling.

1.3.2.4. The UPR^{mt} and Mitophagy

Consistent with the putative role in regulating changes in mitochondria subject to stress, a link between the UPR^{mt} and mitophagy has been gaining traction in the literature. While a potential link could be made to mitophagy through activation of ATFS-1 and AMPK, this has only to this point been observed in lower organisms (69, 170). However, in mammals, an activation of mitophagy has been linked to SirT3 activation and action through Foxo3 (166). During parkin-mediated mitophagy PINK1, which is normally degraded in the matrix by LonP, accumulates on the depolarized OMM and recruits the E3 ubiquitin ligase Parkin, thus targeting the mitochondria to the autophagosome for subsequent degradation (115). The UPR^{mt} is purported to play a role in parkin-mediated mitophagy as the inclusion of a terminally misfolded matrix protein caused PINK1 and Parkin to accumulate on the stressed mitochondria, despite no change in membrane potential (103). This may be regulated through LonP, in that as misfolded proteins accumulate, they compete with PINK1 for degradation by LonP and allow PINK1 to stabilize on the outer membrane, unscathed.

1.3.3.1. The UPR in Skeletal Muscle and Exercise

Increasingly, evidence is continuing to mount to support a role of the UPR in skeletal muscle in response to exercise, despite the low secretory output of this tissue. From a developmental perspective, induction of the UPR has been described to facilitate myoblast differentiation. UPR factors CHOP and BiP were upregulated during myogenesis, while ATF6 activation further proved to be critical in myotube formation (149). Conversely, in aging animal studies specific chaperones were decreased relative to young animals, while ER-stress and apoptotic markers were also elevated (37, 127, 148, 157). Together, these results indicate a potential link between ER function and UPR signaling in the maintenance of skeletal muscle throughout the lifespan. As well, growing evidence indicates that the ER senses alterations in the cellular nutritional and metabolic states and appropriately activates the UPR to adjust, and balance metabolic activities (130). Deldique and colleagues found that excessive nutrient feeding, specifically of fats, resulted in heightened UPR signaling in skeletal muscle (49). In the same study, they observed a crosstalk between ER stress and the mammalian target of rapamycin (mTOR) pathway, which they proposed was responsible for ER stress-induced downregulation of protein synthesis in C2C12 cells. Following this up, they found that the presence of ER stress prevented activation of the mTOR complex 1 (mTORC1), contributing to an increased anabolic resistance (48). Thus further providing a link between ER stress and other conditions of anabolic resistance such as aging, immobilization, and disuse.

It has been established that skeletal muscle is a dynamic and malleable tissue responding to the external conditions placed upon it. Resistance and endurance type exercise can adapt the skeletal muscle phenotype to increase, muscle fiber mass or

oxidative output, respectively, whereas disuse can contribute to a reduction in both. As exercise plays a positive role in skeletal muscle health, research has turned its attention to this phenomena and the potential role of the UPR. Recently, UPR activation was observed in skeletal muscle following a single unaccustomed bout of resistance exercise (159). These results corroborated a previous report that found an association between activation of UPR transcripts in muscle subject to a single bout of resistance exercise, which was attenuated with prolonged training (65). As well, endurance exercise has been shown to elicit the UPR following a single bout of treadmill running, with the intensity of the exercise contributing to the magnitude of the response, while training contributed to an attenuated UPR activation (107, 109, 224). The activation of the UPR during acute endurance and resistance exercise indicates a putative role of the UPR in initial onset adaptations, and to provide protection against future stress as a host of cellular chaperones are increased following a prolonged training program (161). Conversely, with prolonged disuse the results seem mixed as neither 7 days, nor 2 weeks of hindlimb unloading in rats resulted in UPR activation or ER stress, however in a human study several UPR genes were upregulated following 9 days of bed rest (9, 95, 157). Moreover, a major regulator of skeletal muscle adaptation and mitochondrial content, PGC-1α, has been shown to be induced by, and regulate, UPR signaling in an ATF6-dependent manner, indicating an integrated link between these responsive pathways (224). Lastly, a link has been drawn between activation of the UPR^{mt} and mitochondrial biogenesis, despite very little studies focused on this response in skeletal muscle or exercise. Nevertheless, it appears that activation of sirtuins, namely SirT1, could mediate this coordinated expression, indicating a potential role of the UPR^{mt} in skeletal muscle

adaptations to exercise (36, 145, 171).

1.3.4.1. Tauroursodeoxycholic Acid (TUDCA)

As described above, the UPR monitors the cellular environment to regulate its fate. Acute stress and UPR signaling can bring about positive adaptations, whereas chronic stress can result in potentially maladaptive outcomes such as cell death contributing to pathogenesis of various diseases. In particular, both the UPR^{ER}, and to lesser extent the UPR^{mt}, have putative roles in metabolic diseases, neurodegenerative disorders, aging/longevity and cancer among others. Therefore, drugs targeting the ER to reduce overall stress have been utilized in a multitude of studies to analyze their effect on maintaining cell homeostasis. One such example is ursodeoxycholic acid (UDCA) and its taurine conjugated from TUDCA (Fig. 1E). These hydrophilic primary bile acids are generated at low levels, produced by the liver (10, 59). TUDCA is an FDA approved drug for treatment of liver cirrhosis, and has also been shown to reduce symptoms of Alzheimer's and Huntington's diseases, ischemia and stroke, as well as decrease insulin resistance in obese mice (59, 163). TUDCA acts primarily through inhibition of apoptosis, particularly by inhibiting Bax translocation to the mitochondria and caspase activation (10). This mode of action is in line with the UPR^{ER} activation of apoptosis through PERK, IRE1α, and CHOP. Not surprisingly then, recent research *in vitro* has observed a reduced activation of PERK, eIF2α, JNK, as well as IRE1α, and in turn XBP1 splicing (57, 129, 163, 197). As well, it is important to note that the opposite effects of TUDCA treatment have been observed, and that further work elucidating the exact mechanism of TUDCA on the UPR and apoptosis is required (229). Nevertheless, TUDCA has been observed to be a negative regulator of the transcription factor CHOP in

various disease models, as well as other UPR related proteins such as capase-12 and BiP (58, 129, 144, 163, 197, 211, 227). Additionally, TUDCA is proposed to ameliorate ER stress by binding to the hydrophobic regions of unfolded proteins preventing aggregate formation and allowing them to be more easily degraded while concurrently modulating cytosolic $Ca2^{+}$ through modulation of SR/ER ATPases (28, 57, 220). Therefore, TUDCA appears to be a potent regulator of ER stress-induced apoptosis, particularly through UPR^{ER} signaling.

RESEARCH OBJECTIVES

Thus, based on my review of literature, the objectives of my thesis were to:

1. Examine the chronology of responses between the UPR pathways in response to contractile activity;
2. Investigate the UPR^{ER} and UPR^{mt} adaptations associated with acute contractile activity, and whether these responses are attenuated after repeated bouts of muscle activity;
3. Study the relationship of these changes to adaptations and remodeling that occur with exercise in muscle, such as autophagy and mitochondrial biogenesis;
4. Determine whether the UPR is required for adaptations associated with exercise, by reducing ER stress-induced UPR^{ER} activation with the chemical chaperone mimetic drug TUDCA.

HYPOTHESES

1. The UPR^{mt} and the UPR^{ER} will be rapidly activated in the early stages of the CCA-induced training period,
2. Early UPR activation will induce protein handling machinery chaperones and proteases which may facilitate the adaptations typically seen with chronic muscle stimulation, namely mitochondrial biogenesis and autophagy;
3. UPR signaling will be attenuated as CCA persists over multiple days;
4. Blocking the UPR with TUDCA will attenuate some of the adaptations in mitochondrial content and autophagy, as translated proteins may not be properly folded and/or transported to their proper confirmation, or destination within the cell.

REFERENCES

1. **Adachi Y**, **Yamamoto K**, **Okada T**, **Yoshida H**, **Harada A**, **Mori K**. ATF6 is a transcription factor specializing in the regulation of quality control proteins in the endoplasmic reticulum. *Cell Struct Funct* 33: 75–89, 2008.

2. **Adhihetty PJ**, **Irrcher I**, **Joseph A-M**, **Ljubicic V**, **Hood DA**. Plasticity of skeletal muscle mitochondria in response to contractile activity. *Exp Physiol* 88: 99–107, 2003.

3. **Adhihetty PJ**, **Ljubicic V**, **Hood DA**. Effect of chronic contractile activity on SS and IMF mitochondrial apoptotic susceptibility in skeletal muscle. *Am J Physiol Endocrinol Metab* 292: E748–55, 2007.

4. **Adhihetty PJ**, **Ljubicic V**, **Menzies KJ**, **Hood DA**. Differential susceptibility of subsarcolemmal and intermyofibrillar mitochondria to apoptotic stimuli. 3: 994–1001, 2005.

5. **Akimoto T**, **Sorg BS**, **Yan Z**. Real-time imaging of peroxisome proliferator-activated receptor-gamma coactivator-1alpha promoter activity in skeletal muscles of living mice. *Am J Physiol Cell Physiol* 287: C790–6, 2004.

6. **Akimoto T**. Exercise Stimulates Pgc-1 Transcription in Skeletal Muscle through Activation of the p38 MAPK Pathway. *J Biol Chem* 280: 19587–19593, 2005.

7. **Alconada A**, **Kübrich M**, **Moczko M**, **Hönlinger A**, **Pfanner N**. The mitochondrial receptor complex: the small subunit Mom8b/Isp6 supports association of receptors with the general insertion pore and transfer of preproteins. *Mol Cell Biol* 15: 6196–6205, 1995.

8. **Aldridge JE**, **Horibe T**, **Hoogenraad NJ**. Discovery of Genes Activated by the Mitochondrial Unfolded Protein Response (mtUPR) and Cognate Promoter Elements. *PLoS One* 2: e874, 2007.

9. **Alibegovic AC**, **Sonne MP**, **Højbjerre L**, **Jacobsen S**, **Nilsson E**, **Færch K**, **Hiscock N**, **Mortensen B**, **Friedrichsen M**, **Stallknecht B**, **Dela F**, **Vaag A**, **Insulin VA**. Insulin resistance induced by physical inactivity is associated with multiple transcriptional changes in skeletal muscle in young men. *Am J Physiol Endocrinol Metab* 299: E752–E763, 2010.

10. **Amaral JD**, **Viana RJS**, **Ramalho RM**, **Steer CJ**, **Rodrigues CMP**. Bile acids: regulation of apoptosis by ursodeoxycholic acid. *J Lipid Res* 50: 1721–1734, 2009.

11. **Amat R**, **Planavila A**, **Chen SL**, **Iglesias R**, **Giralt M**, **Villarroya F**. SIRT1 Controls the Transcription of the Peroxisome Proliferator-activated Receptor- Co-activator-1 (PGC-1) Gene in Skeletal Muscle through the PGC-1 Autoregulatory Loop and Interaction with MyoD. *J Biol Chem* 284: 21872–21880, 2009.

12. **Anderson S**, **Bankier T**, **Barrell BG**, **de Bruijn MH**, **Coulson AR**, **Drouin J**, **Eperon IC**, **Nierlich DP**, **Roe BA**, **Sanger F**, **Schreier PH**, **Smith AJ**, **Staden R**, **Young IG**. Sequence and organization of the human mitochondrial genome. *Nature* 290: 457–465, 1981.

13. **Ashrafi G**, **Schwarz TL**. The pathways of mitophagy for quality control and clearance of mitochondria. *Cell Death Differ* 20: 31–42, 2013.

14. **B'chir W**, **Chaveroux C**, **Carraro V**, **Averous J**, **Maurin AC**, **Jousse C**, **Muranishi Y**, **Parry L**, **Fafournoux P**, **Bruhat A**. Dual role for CHOP in the crosstalk between autophagy and apoptosis to determine cell fate in response to amino acid deprivation. *Cell Signal* 26: 1385–1391, 2014.

15. **B'chir W**, **Maurin A-C**, **Carraro V**, **Averous J**, **Jousse C**, **Muranishi Y**, **Parry L**, **Stepien G**, **Fafournoux P**, **Bruhat A**. The eIF2 /ATF4 pathway is essential for stress-induced autophagy gene expression. *Nucleic Acids Res* 41: 7683–7699, 2013.

16. **Baar K**, **Wende AR**, **Jones TE**, **Marison M**, **Nolte LA, Chen M**, **Kelly DP**, **Holloszy JO**. Adaptations of skeletal muscle to exercise: rapid increase in the transcriptional coactivator PGC-1. *FASEB J* 16: 1879–86, 2002.

17. **Baker BM**, **Haynes CM**. Mitochondrial protein quality control during biogenesis and aging. *Trends Biochem Sci* 36: 254–261, 2011.

18. **Baker MJ**, **Frazier AE**, **Gulbis JM**, **Ryan MT**. Mitochondrial protein-import machinery: correlating structure with function. *Trends Cell Biol* 17: 456–464, 2007.

19. **Baker MJ**, **Tatsuta T**, **Langer T**. Quality Control of Mitochondrial Proteostasis. *Cold Spring Harb Perspect Biol* 3: a007559–a007559, 2011.

20. **Baldwin KM**, **Klinkerfuss GH**, **Terjung RL**, **Molé PA**, **Holloszy JO**. Respiratory capacity of white, red, and intermediate muscle: adaptative response to exercise. *Am J Physiol* 222: 373–378, 1972.

21. **Berridge MJ**. The endoplasmic reticulum: a multifunctional signaling organelle. *Cell Calcium* 32: 235–249, 2002.

22. **Bertolotti A**, **Zhang Y**, **Hendershot LM**, **Harding HP**, **Ron D**. Dynamic interaction of BiP and ER stress transducers in the unfolded-protein response. *Nat Cell Biol* 2: 326–332, 2000.

23. **Blesa JR**, **Prieto-Ruiz JA**, **Hernández JM**, **Hernández-Yago J**. NRF-2 transcription factor is required for human TOMM20 gene expression. *Gene* 391: 198–208, 2007.

24. **Bohnert M**, **Pfanner N**, **van der Laan M**. A dynamic machinery for import of mitochondrial precursor proteins. *FEBS Lett* 581: 2802–2810, 2007.

25. **Bolender N**, **Sickmann A**, **Wagner R**, **Meisinger C**, **Pfanner N**. Multiple pathways for sorting mitochondrial precursor proteins. *EMBO Rep* 9: 42–49, 2008.

26. **Bommiasamy H**, **Back SH**, **Fagone P**, **Lee K**, **Meshinchi S**, **Vink E**, **Sriburi R**, **Frank M**, **Jackowski S**, **Kaufman RJ**, **Brewer JW**. ATF6 induces XBP1-independent expansion of the endoplasmic reticulum. *J Cell Sci* 122: 1626–1636, 2009.

27. **Booth FW**, **Thomason DB**. Molecular and cellular adaptation of muscle in response to exercise: perspectives of various models. *Physiol Rev* 71: 541–585, 1991.

28. **Bouscarel B**, **Fromm H**, **Nussbaum R**. Ursodeoxycholate mobilizes intracellular Ca2+ and activates phosphorylase a in isolated hepatocytes. *Am J Physiol* 264: G243–51, 1993.

29. **Bravo R**, **Vicencio JM**, **Parra V**, **Troncoso R**, **Munoz JP**, **Bui M**, **Quiroga C**, **Rodriguez AE**, **Verdejo HE**, **Ferreira J**, **Iglewski M**, **Chiong M**, **Simmen T**, **Zorzano A**, **Hill JA**, **Rothermel BA**, **Szabadkai G**, **Lavandero S**. Increased ER-mitochondrial coupling promotes mitochondrial respiration and bioenergetics during early phases of ER stress. *J Cell Sci* 124: 2143–2152, 2011.

30. **de Brito OM**, **Scorrano L**. Mitofusin 2 tethers endoplasmic reticulum to mitochondria. *Nature* 456: 605–610, 2008.

31. **de Brito OM**, **Scorrano L**. Mitofusin 2:A Mitochondria-Shaping Protein with Signaling Roles Beyond Fusion. *Antioxid Redox Signal* 10: 621–633, 2008.

32. **Calfon M**, **Zeng H**, **Urano F**, **Till JH**, **Hubbard SR**, **Harding HP**, **Clark SG**, **Ron D**. IRE1 couples endoplasmic reticulum load to secretory capacity by processing the XBP-1 mRNA. *Nature* 415: 92–96, 2002.

33. **Cao W**, **Douglas MG**. Biogenesis of ISP6, a Small Carboxyl-terminal Anchored Protein of the Receptor Complex of the Mitochondrial Outer Membrane. *J Biol Chem* 270: 5674–5679, 1995.

34. **Carroll S**, **Nicotera P**, **Pette D**. Calcium transients in single fibers of low-frequency stimulated fast-twitch muscle of rat. *Am J Physiol* 277: C1122–C1129, 1999.

35. **Cecconi F**, **Levine B**. The Role of Autophagy in Mammalian Development: Cell Makeover Rather than Cell Death. *Dev Cell* 15: 344–357, 2008.

36. **Cerutti R**, **Pirinen E**, **Lamperti C**, **Marchet S**, **Sauve AA**, **Li W**, **Leoni V**, **Schon EA**, **Dantzer F**, **Auwerx J**, **Viscomi C**, **Zeviani M**. NAD+-Dependent Activation of Sirt1 Corrects the Phenotype in a Mouse Model of Mitochondrial Disease. *Cell Metab* 19: 1042–1049, 2014.

37. **Chabi B**, **Ljubicic V**, **Menzies KJ**, **Huang JH**, **Saleem A**, **Hood DA**. Mitochondrial function and apoptotic susceptibility in aging skeletal muscle. *Aging Cell* 7: 2–12, 2008.

38. **Chacinska A**, **van der Laan M**, **Mehnert CS**, **Guiard B**, **Mick DU**, **Hutu DP**, **Truscott KN**, **Wiedemann N**, **Meisinger C**, **Pfanner N**, **Rehling P**. Distinct Forms of Mitochondrial TOM-TIM Supercomplexes Define Signal-Dependent States of Preprotein Sorting. *Mol Cell Biol* 30: 307–318, 2010.

39. **Chen X**, **Shen J**, **Prywes R**. The Luminal Domain of ATF6 Senses Endoplasmic Reticulum (ER) Stress and Causes Translocation of ATF6 from the ER to the Golgi. *J Biol Chem* 277: 13045–13052, 2002.

40. **Cheng EHY**, **Wei MC**, **Weiler S**, **Flavell RA**, **Mak TW**, **Lindsten T**, **Korsmeyer SJ**. BCL-2, BCL-X L sequester BH3 domain-only molecules preventing BAX- and BAK-mediated mitochondrial apoptosis. *Mol Cell* 8: 705–711, 2001.

41. **Chiribau C-B**, **Gaccioli F**, **Huang CC**, **Yuan CL**, **Hatzoglou M**. Molecular symbiosis of CHOP and C/EBP beta isoform LIP contributes to endoplasmic reticulum stress-induced apoptosis. *Mol Cell Biol* 30: 3722–3731, 2010.

42. **Cogswell AM**, **Stevens RJ**, **Hood DA**. Properties of skeletal muscle mitochondria from subsarcolemmal and intermyofibrillar isolated regions. *Am J Physiol Cell Physiol* 264: C383–C389, 1993.

43. **Connor JH**, **Weiser DC**, **Li S**, **John M**, **Li SHI**, **Hallenbeck JM**. Growth Arrest and DNA Damage-Inducible Protein GADD34 Assembles a Novel Signaling Complex Containing Protein Phosphatase 1 and Inhibitor 1 Growth Arrest and DNA Damage-Inducible Protein GADD34 Assembles a Novel Signaling Complex Containing Protein Phospha. *Mol Cell Biol* 21: 6841–6850, 2001.

44. **Connor MK**, **Bezborodova O**, **Escobar CP**, **Hood DA**. Effect of contractile activity on protein turnover in skeletal muscle mitochondrial subfractions. *J Appl Physiol* 88: 601–1606, 2000.

45. **Connor MK**, **Irrcher I**, **Hood DA.** Contractile Activity-induced Transcriptional Activation of Cytochrome c Involves Sp1 and Is Proportional to Mitochondrial ATP Synthesis in C2C12 Muscle Cells. *J Biol Chem* 276: 15898–15904, 2001.

46. **Cox JS**, **Shamu CE**, **Walter P**. Transcriptional induction of genes encoding endoplasmic reticulum resident proteins requires a transmembrane protein kinase. *Cell* 73: 1197–1206, 1993.

47. **Cullinan SB**, **Diehl JA**. PERK-dependent activation of Nrf2 contributes to redox homeostasis and cell survival following endoplasmic reticulum stress. *J Biol Chem* 279: 20108–20117, 2004.

48. **Deldicque L**, **Bertrand L**, **Patton A**, **Francaux M**, **Baar K**. ER stress induces anabolic resistance in muscle cells through PKB-induced blockade of mTORC1. *PLoS One* 6: e20993, 2011.

49. **Deldicque L**, **Cani PD**, **Philp A**, **Raymackers J-M**, **Meakin PJ**, **Ashford MLJ**, **Delzenne NM**, **Francaux M**, **Baar K**. The unfolded protein response is activated in skeletal muscle by high-fat feeding: potential role in the downregulation of protein synthesis. *Am J Physiol Endocrinol Metab* 299: E695–E705, 2010.

50. **Dietmeier K**, **Hönlinger A**, **Bömer U**, **Dekker PJ**, **Eckerskorn C**, **Lottspeich F**, **Kübrich M**, **Pfanner N**. Tom5 functionally links mitochondrial preprotein receptors to the general import pore. *Nature* 388: 195–200, 1997.

51. **Dudley GA**, **Abraham WM**, **Terjung RL**. Influence of exercise intensity and duration on biochemical adaptations in skeletal muscle. *J Appl Physiol* 53: 844–50, 1982.

52. **Evans MJ**, **Scarpulla RC**. NRF-1: a trans-activator of nuclear-encoded respiratory genes in animal cells. *Genes Dev* 4: 1023–34, 1990.

53. **Fan ACY**, **Bhangoo MK**, **Young JC**. Hsp90 Functions in the Targeting and Outer Membrane Translocation Steps of Tom70-mediated Mitochondrial Import. *J Biol Chem* 281: 33313–33324, 2006.

54. **Finck BN**, **Kelly DP**. PGC-1 coactivators: Inducible regulators of energy metabolism in health and disease. *J Clin Invest* 116: 615–622, 2006.

55. **Freyssenet D**, **Connor MK**, **Takahashi M**, **Hood DA**. Cytochrome c transcriptional activation and mRNA stability during contractile activity in skeletal muscle. *Am J Physiol Endocrinol Metab* 277: E26–32, 1999.

56. **Fu HY**, **Okada K**, **Liao Y**, **Tsukamoto O**, **Isomura T**, **Asai M**, **Sawada T**, **Okuda K**, **Asano Y**, **Sanada S**, **Asanuma H**, **Asakura M**, **Takashima S**, **Komuro I**, **Kitakaze M**, **Minamino T**. Ablation of C/EBP homologous protein attenuates endoplasmic reticulum-mediated apoptosis and cardiac dysfunction induced by pressure overload. *Circulation* 122: 361–9, 2010.

57. **Gani AR**, **Uppala JK**, **Ramaiah KVA.** Tauroursodeoxycholic acid prevents stress induced aggregation of proteins in vitro and promotes PERK activation in HepG2 cells. *Arch Biochem Biophys* 568: 8–15, 2015.

58. **Gao X**, **Fu L**, **Xiao M**, **Xu C**, **Sun L**, **Zhang T**, **Zheng F**, **Mei C**. The Nephroprotective Effect of Tauroursodeoxycholic Acid on Ischaemia/Reperfusion-Induced Acute Kidney Injury by Inhibiting Endoplasmic Reticulum Stress. *Basic Clin Pharmacol Toxicol* 111: 14–23, 2012.

59. **Gaspar JM**, **Martins A**, **Cruz R**, **Rodrigues CMP**, **Ambrósio AF**, **Santiago AR**. Tauroursodeoxycholic acid protects retinal neural cells from cell death induced by prolonged exposure to elevated glucose. *Neuroscience* 253: 380–389, 2013.

60. **Gauthier GF**. Ultrastructural identification of muscle fiber types by immunocytochemistry. *J Cell Biol* 82: 391–400, 1979.

61. **Gething MJ**. Role and regulation of the ER chaperone BiP. *Semin Cell Dev Biol* 10: 465–472, 1999.

62. **Gleyzer N**, **Vercauteren K**, **Scarpulla RC**. Control of mitochondrial transcription specificity factors (TFB1M and TFB2M) by nuclear respiratory factors (NRF-1 and NRF-2) and PGC-1 family coactivators. *Mol Cell Biol* 25: 1354–1366, 2005.

63. **Gomez-Cabrera M-C**, **Borrás C**, **Pallardó FV**, **Sastre J**, **Ji LL**, **Viña J**. Decreasing xanthine oxidase-mediated oxidative stress prevents useful cellular adaptations to exercise in rats. *J Physiol* 567: 113–120, 2005.

64. **Gordon JW**, **Rungi AA**, **Inagaki H**, **Hood DA**. Effects of contractile activity on mitochondrial transcription factor A expression in skeletal muscle. *J Appl Physiol* 90: 389–396, 2001.

65. **Gordon PM**, **Liu D**, **Sartor MA**, **IglayReger HB**, **Pistilli EE**, **Gutmann L**, **Nader GA**, **Hoffman EP**. Resistance exercise training influences skeletal muscle immune activation: a microarray analysis. *J Appl Physiol* 112: 443–453, 2012.

66. **Grey JY**, **Connor MK**, **Gordon JW**, **Yano M**, **Mori M**, **Hood DA**. Tom20-mediated mitochondrial protein import in muscle cells during differentiation. *Am J Physiol Cell Physiol* 279: C1393–C1400, 2000.

67. **Grumati P**, **Bonaldo P**. Autophagy in Skeletal Muscle Homeostasis and in Muscular Dystrophies. *Cells* 1: 325–345, 2012.

68. **Grumati P**, **Coletto L**, **Schiavinato A**, **Casragnaro S**, **Bertaggia E**, **Sandri M**, **Bonaldo P**. Physical exercise stimulates autophagy in normal skeletal muscles but is detrimental for collagen VI-deficient muscles. *Autophagy* 7: 1415–1423, 2011.

69. **Guo B**, **Huang X**, **Zhang P**, **Qi L**, **Liang Q**, **Zhang X**, **Huang J**, **Fang B**, **Hou W**, **Han J**, **Zhang H**. Genome-wide screen identifies signaling pathways that regulate autophagy during Caenorhabditis elegans development. *EMBO Rep* 15: 705–13, 2014.

70. **Gurd BJ**, **Yoshida Y**, **Mcfarlan JT**, **Holloway GP**, **Moyes CD**, **Heigenhauser GJF**, **Spriet L**, **Bonen A**. Nuclear SIRT1 activity , but not protein content , regulates mitochondrial biogenesis in rat and human skeletal muscle. *Am J Physiol Regul Integr Comp Physiol* 301: 67–75, 2011.

71. **Han D**, **Lerner AG**, **Walle L Vande**, **Upton J**, **Xu W**, **Hagen A**, **Backes BJ**, **Oakes SA**, **Papa FR**. IRE1alpha Kinase Activation Modes Control Alternate Endoribonuclease Outputs to Determine Divergent Cell Fates. *Cell* 138: 562–575, 2009.

72. **Handschin C**, **Spiegelman BM**. Peroxisome Proliferator-Activated Receptor γ Coactivator 1 Coactivators, Energy Homeostasis, and Metabolism. *Endocr Rev* 27: 728–735, 2006.

73. **Harding HP**, **Novoa I**, **Zhang Y**, **Zeng H**, **Wek R**, **Schapira M**, **Ron D**. Regulated Translation Initiation Controls Stress-Induced Gene Expression in Mammalian Cells. *Mol Cell* 6: 1099–1108, 2000.

74. **Harding HP**, **Zhang Y**, **Bertolotti A**, **Zeng H**, **Ron D**. Perk is essential for translational regulation and cell survival during the unfolded protein response. *Mol Cell* 5: 897–904, 2000.

75. **Haynes CM**, **Ron D**. The mitochondrial UPR - protecting organelle protein homeostasis. *J Cell Sci* 123: 3849–55, 2010.

76. **Haynes CM**, **Yang Y**, **Blais SP**, **Neubert TA**, **Ron D**. The matrix peptide exporter HAF-1 signals a mitochondrial UPR by activating the transcription factor ZC376.7 in C. elegans. *Mol Cell* 37: 529–40, 2010.

77. **Haze K**, **Yoshida H**, **Yanagi H**, **Yura T**, **Mori K**. Mammalian transcription factor ATF6 is synthesized as a transmembrane protein and activated by proteolysis in response to endoplasmic reticulum stress. *Mol Biol Cell* 10: 3787–99, 1999.

78. **He C**, **Bassik MC**, **Moresi V**, **Sun K**, **Wei Y**, **Zou Z**, **An Z**, **Loh J**, **Fisher J**, **Sun Q**, **Korsmeyer S**, **Packer M**, **May HI**, **Hill JA**, **Virgin HW**, **Gilpin C**, **Xiao G**, **Bassel-Duby R**, **Scherer PE**, **Levine B**. Exercise-induced BCL2-regulated autophagy is required for muscle glucose homeostasis. *Nature* 481: 511–515, 2012.

79. **Heijmans J**, **van Lidth de Jeude JF**, **Koo B-K**, **Rosekrans SL**, **Wielenga MCB**, **van de Wetering M**, **Ferrante M**, **Lee AS**, **Onderwater JJM**, **Paton JC**, **Paton AW**, **Mommaas AM**, **Kodach LL**, **Hardwick JC**, **Hommes DW**, **Clevers H**, **Muncan V**, **van den Brink GR**. ER Stress Causes Rapid Loss of Intestinal Epithelial Stemness through Activation of the Unfolded Protein Response. *Cell Rep* 3: 1128–1139, 2013.

80. **Hernandez JM**, **Giner P**, **Hernandez-Yago J**. Gene structure of the human mitochondrial outer membrane receptor Tom20 and evolutionary study of its family of processed pseudogenes. *Gene* 239: 283–291, 1999.

81. **Herzig S**, **Martinou J**. Mitochondrial Dynamics: To be in Good Shape to Survive *Curr Mol Med* 8: 131–137, 2008.

82. **Hock MB**, **Kralli A**. Transcriptional control of mitochondrial biogenesis and function. *Annu Rev Physiol* 71: 177–203, 2009.

83. **Hönlinger A**, **Bömer U**, **Alconada A**, **Eckerskorn C**, **Lottspeich F**, **Dietmeier K**, **Pfanner N**. Tom7 modulates the dynamics of the mitochondrial outer membrane translocase and plays a pathway-related role in protein import. *EMBO J* 15: 2125–37, 1996.

84. **Hood DA**, **Uguccioni G**, **Vainshtein A**, **D'souza D**. Mechanisms of Exercise-Induced Mitochondrial Biogenesis in Skeletal Muscle: Implications for Health and Disease. *Compr Physiol* 1: 1119–1134, 2011.

85. **Hood DA**, **Zak R**, **Pette D**. Chronic stimulation of rat skeletal muscle induces coordinate increases in mitochondrial and nuclear mRNAs of cytochrome-c-oxidase subunits. *Eur J Biochem* 179: 275–280, 1989.

86. **Hood DA.** Mechanisms of exercise-induced mitochondrial biogenesis in skeletal muscleThis paper is one of a selection of papers published in this Special Issue, entitled 14th International Biochemistry of Exercise Conference – Muscles as Molecular and Metabolic Mach. *Appl Physiol Nutr Metab* 34: 465–472, 2009.

87. **Hood DA**, **Irrcher I**, **Ljubicic V**, **Joseph A-M**. Coordination of metabolic plasticity in skeletal muscle. *J Exp Biol* 209: 2265–2275, 2006.

88. **Hood DA**, **Pette D**. Chronic long-term electrostimulation creates a unique metabolic enzyme profile in rabbit fast-twitch muscle. *FEBS Lett* 247: 471–474, 1989.

89. **Hood DA**. Invited Review: Contractile activity-induced mitochondrial biogenesis in skeletal muscle. *J Appl Physiol* 90: 1137–1157, 2001.

90. **Hoppeler H**. Exercise-Induced UItrastructural Changes in Skeletal Muscle. *Integr J Sport Med* 7: 187–204, 1986.

91. **Horibe T**, **Hoogenraad NJ**. The Chop Gene Contains an Element for the Positive Regulation of the Mitochondrial Unfolded Protein Response. *PLoS One* 2: e835, 2007.

92. **Howald H**, **Hoppeler H**, **Claassen H**, **Mathieu O**, **Straub R**. Influences of endurance training on the ultrastructural composition of the different muscle fiber types in humans. *Pflugers Arch Eur J Physiol* 403: 369–376, 1985.

93. **Hu P**, **Han Z**, **Couvillon AD**, **Kaufman RJ**, **Exton JH**. Autocrine Tumor Necrosis Factor Alpha Links Endoplasmic Reticulum Stress to the Membrane Death Receptor Pathway through IRE1␣-Mediated NF-B Activation and Down-Regulation of TRAF2 Expression. *Society* 26: 3071–3084, 2006.

94. **Hudlická O**, **Brown M**, **Cotter M**, **Smith M**, **Vrbová G**. The effect of long-term stimulation of fast muscles on their blood flow, metabolism and ability to withstand fatigue. *Pflugers Arch* 369: 141–9, 1977.

95. **Hunter RB**, **Mitchell-Felton H**, **Essig DA**, **Kandarian SC**. Expression of endoplasmic reticulum stress proteins during skeletal muscle disuse atrophy. *Am J Physiol Cell Physiol* 281: C1285–90, 2001.

96. **Inoki K**, **Kim J**, **Guan K-L**. AMPK and mTOR in Cellular Energy Homeostasis and Drug Targets. *Annu Rev Pharmacol Toxicol* 52: 381–400, 2012.

97. **Irrcher I**, **Adhihetty PJ**, **Sheehan T**, **Joseph A-M**, **Hood DA**. PPARgamma coactivator-1alpha expression during thyroid hormone- and contractile activity-induced mitochondrial adaptations. *Am J Physiol Cell Physiol* 284: C1669–C1677, 2003.

98. **Irrcher I**, **Hood DA**. Regulation of Egr-1, SRF, and Sp1 mRNA expression in contracting skeletal muscle cells. *J Appl Physiol* 97: 2207–13, 2004.

99. **Irrcher I**, **Ljubicic V**, **Hood DA**. Interactions between ROS and AMP kinase activity in the regulation of PGC-1alpha transcription in skeletal muscle cells. *Am J Physiol Cell Physiol* 296: C116–C123, 2009.

100. **Irrcher I**, **Ljubicic V**, **Kirwan AF**, **Hood DA.** AMP-Activated Protein Kinase-Regulated Activation of the PGC-1α Promoter in Skeletal Muscle Cells. *PLoS One* 3: e3614, 2008.

101. **Jacobs BL**, **You J-S**, **Frey JW**, **Goodman CA**, **Gundermann DM**, **Hornberger TA.** Eccentric contractions increase the phosphorylation of tuberous sclerosis complex-2 (TSC2) and alter the targeting of TSC2 and the mechanistic target of rapamycin to the lysosome. *J Physiol* 591: 4611–4620, 2013.

102. **Jeyapaul J**, **Jaiswal AK**. Nrf2 and c-Jun regulation of antioxidant response element (ARE)-mediated expression and induction of γ-glutamylcysteine synthetase heavy subunit gene. *Biochem Pharmacol* 59: 1433–1439, 2000.

103. **Jin SM**, **Youle RJ**. The accumulation of misfolded proteins in the mitochondrial matrix is sensed by PINK1 to induce PARK2/Parkin-mediated mitophagy of polarized mitochondria. *Autophagy* 9: 1750–7, 2013.

104. **Joseph A-M**, **Hood DA**. Plasticity of TOM complex assembly in skeletal muscle mitochondria in response to chronic contractile activity. *Mitochondrion* 12: 305–12, 2012.

105. **Jousse C**, **Oyadomari S**, **Novoa I**, **Lu P**, **Zhang Y**, **Harding HP**, **Ron D**. Inhibition of a constitutive translation initiation factor 2α phosphatase, CReP, promotes survival of stressed cells. *J Cell Biol* 163: 767–775, 2003.

106. **Kassenbrock CK**, **Cao W**, **Douglas MG**. Genetic and biochemical charaterization of ISP6, a mitochondrial outer membrane protein associated with the protein translocation complex. *EMBO J* 12: 3023–3034, 1993.

107. **Kim HJ**, **Jamart C**, **Deldicque L**, **An G**, **Lee YH**, **Kim CK**, **Raymackers J**, **Francaux M**. Endoplasmic reticulum stress markers and ubiquitin–proteasome pathway activity in response to a 200-km run. *Med Sci Sports Exerc* 43: 18–25, 2011.

108. **Kim J**, **Kim YC**, **Fang C**, **Russell RC**, **Kim JH**, **Fan W**, **Liu R**, **Zhong Q**, **Guan K-L**. Differential Regulation of Distinct Vps34 Complexes by AMPK in Nutrient Stress and Autophagy. *Cell* 152: 290–303, 2013.

109. **Kim K**, **Kim Y-H**, **Lee S-H**, **Jeon M-J**, **Park S-Y**, **Doh K-O**. Effect of exercise intensity on unfolded protein response in skeletal muscle of rat. *Korean J Physiol Pharmacol* 18: 211–216, 2014.

110. **Kimball SR**, **Clemens MJ**, **Tilleray VJ**, **Wek RC**, **Horetsky RL**, **Jefferson LS**. The Double-Stranded RNA-Activated Protein Kinase PKR Is Dispensable for Regulation of Translation Initiation in Response to either Calcium Mobilization from the Endoplasmic Reticulum or Essential Amino Acid Starvation. *Biochem Biophys Res Commun* 280: 293–300, 2001.

111. **Kirkwood SP**, **Munn EA**, **Brooks GA**. Mitochondrial reticulum in limb skeletal muscle. *Am J Physiol* 251: C395–402, 1986.

112. **Kokame K**, **Kato H**, **Miyata T**. Identification of ERSE-II, a New cis-Acting Element Responsible for the ATF6-dependent Mammalian Unfolded Protein Response. *J Biol Chem* 276: 9199–9205, 2001.

113. **Kovermann P**, **Truscott KN**, **Guiard B**, **Rehling P**, **Sepuri NB**, **Müller H**, **Jensen RE**, **Wagner R**, **Pfanner N**. Tim22, the essential core of the mitochondrial protein insertion complex, forms a voltage-activated and signal-gated channel. *Mol Cell* 9: 363–373, 2002.

114. **Krieger DA**, **Tate CA**, **McMillin-Wood J**, **Booth FW**. Populations of rat skeletal muscle mitochondria after exercise and immobilization. *J Appl Physiol* 48: 23–28, 1980.

115. **Kroemer G**, **Mariño G**, **Levine B**. Autophagy and the Integrated Stress Response. *Mol Cell* 40: 280–293, 2010.

116. **Kutik S**, **Stojanovski D**, **Becker L**, **Becker T**, **Meinecke M**, **Krüger V**, **Prinz C**, **Meisinger C**, **Guiard B**, **Wagner R**, **Pfanner N**, **Wiedemann N**. Dissecting Membrane Insertion of Mitochondrial β-Barrel Proteins. *Cell* 132: 1011–1024, 2008.

117. **Laughlin MH**, **Armstrong RB**. Rat muscle blood flows as a function of time during prolonged slow treadmill exercise. *Am J Physiol Circ Physiol* 244: H814–H824, 1983.

118. **Lee K**, **Tirasophon W**, **Shen X**, **Michalak M**, **Prywes R**, **Okada T**, **Yoshida H**, **Mori K**, **Kaufman RJ**. IRE1-mediated unconventional mRNA splicing and S2P-mediated ATF6 cleavage merge to regulate XBP1 in signaling the unfolded protein response. *Genes Dev* 16: 452–466, 2002.

119. **Lenka N**, **Vijayasarathy C**, **Mullick J**, **Avadhani NG**. Structural Organization and Transcription Regulation of Nuclear Genes Encoding the Mammalian Cytochrome c Oxidase Complex. *Prog Nucleic Acid Res Mol Biol* 61: 309–344, 1998.

120. **Levine B**, **Kroemer G**. Autophagy in the pathogenesis of disease. *Cell* 132: 27–42, 2008.

121. **Li G**, **Mongillo M**, **Chin KT**, **Harding H**, **Ron D**, **Marks AR**, **Tabas I**. Role of ERO1-α-mediated stimulation of inositol 1,4,5-triphosphate receptor activity in endoplasmic reticulum stress-induced apoptosis. *J Cell Biol* 186: 783–792, 2009.

122. **Lira VA**, **Okutsu M**, **Zhang M**, **Greene NP**, **Laker RC**, **Breen DS**, **Hoehn KL**, **Yan Z**. Autophagy is required for exercise training-induced skeletal muscle adaptation and improvement of physical performance. *FASEB J* 27: 4184–4193, 2013.

123. **Liu CY**, **Schroder M**, **Kaufman RJ**. Ligand-independent dimerization activates the stress response kinases IRE1 and PERK in the lumen of the endoplasmic reticulum. *J Biol Chem* 275: 24881–24885, 2000.

124. **Ljubicic V**, **Adhihetty PJ**, **Hood DA**. Role of UCP3 in state 4 respiration during contractile activity-induced mitochondrial biogenesis. *J Appl Physiol* 97: 976–83, 2004.

125. **Ljubicic V**, **Adhihetty PJ**, **Hood DA**. Application of Animal Models: Chronic Electrical Stimulation-Induced Contractile Activity. *Can J Appl Physiol* 30: 625–643, 2005.

126. **Ljubicic V**, **Hood DA**. Kinase-specific responsiveness to incremental contractile activity in skeletal muscle with low and high mitochondrial content Kinase-specific responsiveness to incremental contractile activity in skeletal muscle with low and high mitochondrial content. *Am J Physiol Endocrinol Metab* : E195–E204, 2008.

127. **Ljubicic V**, **Joseph A-M**, **Adhihetty PJ**, **Huang JH**, **Saleem A**, **Uguccioni G**, **Hood DA**. Molecular basis for an attenuated mitochondrial adaptive plasticity in aged skeletal muscle. *Aging (Albany NY)* 1: 818–30, 2009.

128. **Madaro L**, **Marrocco V**, **Carnio S**, **Sandri M**, **Bouché M**. Intracellular signaling in ER stress-induced autophagy in skeletal muscle cells. *FASEB J* 27: 1990–2000, 2013.

129. **Malo A**, **Krüger B**, **Seyhun E**, **Schäfer C**, **Hoffmann RT**, **Göke B**, **Kubisch CH**. Tauroursodeoxycholic acid reduces endoplasmic reticulum stress , trypsin activation , and acinar cell apoptosis while increasing secretion in rat pancreatic acini. *Am J Physiol - Gastrointest Liver Physiol* 299: G877–G886, 2010.

130. **Mandl J**, **Mészáros T**, **Bánhegyi G**, **Hunyady L**, **Csala M**. Endoplasmic reticulum: nutrient sensor in physiology and pathology. *Trends Endocrinol Metab* 20: 194–201, 2009.

131. **Marciniak SJ**, **Yun CY**, **Oyadomari S**, **Novoa I**, **Zhang Y**, **Jungreis R**, **Nagata K**, **Harding HP**, **Ron D**. CHOP induces death by promoting protein synthesis and oxidation in the stressed endoplasmic reticulum. *Genes Dev* 18: 3066–3077, 2004.

132. **Martinus RD**, **Garth GP**, **Webster TL**, **Cartwright P**, **Naylor DJ**, **Høj PB**, **Hoogenraad NJ**. Selective induction of mitochondrial chaperones in response to loss of the mitochondrial genome. *Eur J Biochem* 240: 98–103, 1996.

133. **Masiero E**, **Agatea L**, **Mammucari C**, **Blaauw B**, **Loro E**, **Komatsu M**, **Metzger D**, **Reggiani C**, **Schiaffino S**, **Sandri M**. Autophagy is required to maintain muscle mass. *Cell Metab* 10: 507–515, 2009.

134. **Masiero E**, **Sandri M**. Autophagy inhibition induces atrophy and myopathy in adult skeletal muscles. *Autophagy* 6: 307–309, 2014.

135. **McClung JM**, **Judge AR**, **Powers SK**, **Yan Z**. p38 MAPK links oxidative stress to autophagy-related gene expression in cachectic muscle wasting. *Am J Physiol Cell Physiol* 298: C542–C549, 2010.

136. **Mccullough KD**, **Martindale JL**, **Aw T**, **Holbrook NJ**. Gadd153 Sensitizes Cells to Endoplasmic Reticulum Stress by Down-Regulating Bcl2 and Perturbing the Cellular Redox State Gadd153 Sensitizes Cells to Endoplasmic Reticulum Stress by Down-Regulating Bcl2 and Perturbing the Cellular Redox State Downloaded fr. *Mol Cell Biol* 21: 1249–1259, 2001.

137. **Michel JB**, **Ordway GA**, **Richardson JA**, **Williams RS**. Biphasic induction of immediate early gene expression accompanies activity-dependent angiogenesis and myofiber remodeling of rabbit skeletal muscle. *J Clin Invest* 94: 277–85, 1994.

138. **Milton RL**, **Lupa MT**, **Caldwell JH**. Fast and slow twitch skeletal muscle fibres differ in their distribution of Na channels near the endplate. *Neurosci Lett* 135: 41–4, 1992.

139. **Miyazaki M**, **McCarthy JJ**, **Fedele MJ**, **Esser KA.** Early activation of mTORC1 signalling in response to mechanical overload is independent of phosphoinositide 3-kinase/Akt signalling. *J Physiol* 589: 1831–1846, 2011.

140. **Mizushima N**, **Komatsu M**. Autophagy: Renovation of Cells and Tissues. *Cell* 147: 728–741, 2011.

141. **Mizushima N**, **Levine B**, **Cuervo AM**, **Klionsky DJ**. Autophagy fights disease through cellular self-digestion. *Nature* 451: 1069–1075, 2008.

142. **Mizushima N**. Autophagy : process and function. *Genes Dev* 21: 2861–2873, 2007.

143. **Moorwood C**, **Barton ER**. Caspase-12 ablation preserves muscle function in the mdx mouse. *Hum. Mol. Genet.* (May 2014). doi: 10.1093/hmg/ddu249.

144. **Mosbah I Ben**, **Alfany-Fernández I**, **Martel C**, **Zaouali MA**, **Bintanel-Morcillo M**, **Rimola A**, **Rodés J**, **Brenner C**, **Roselló-Catafau J**, **Peralta C**. Endoplasmic reticulum stress inhibition protects steatotic and non-steatotic livers in partial hepatectomy under ischemia–reperfusion. *Cell Death Dis* 1: e52, 2010.

145. **Mouchiroud L**, **Houtkooper RH**, **Moullan N**, **Katsyuba E**, **Ryu D**, **Canto C**, **Mottis A**, **Jo YS**, **Viswanathan M**, **Schoonjans K**, **Guarente L**, **Auwerx J**. The NAD(+)/Sirtuin Pathway Modulates Longevity through Activation of Mitochondrial UPR and FOXO Signaling. *Cell* 154: 430–441, 2013.

146. **Muñoz JP**, **Ivanova S**, **Sánchez-Wandelmer J**, **Martínez-Cristóbal P**, **Noguera E**, **Sancho A**, **Díaz-Ramos A**, **Hernández-Alvarez MI**, **Sebastián D**, **Mauvezin C**, **Palacín M**, **Zorzano A**. Mfn2 modulates the UPR and mitochondrial function via repression of PERK. *EMBO J* 32: 2348–61, 2013.

147. **Murakami T**, **Shimomura Y**, **Yoshimura A**, **Sokabe M**, **Fujitsuka N**. Induction of nuclear respiratory factor-1 expression by an acute bout of exercise in rat muscle. *Biochim Biophys Acta* 1381: 113–22, 1998.

148. **Naidoo N**. ER and aging-Protein folding and the ER stress response. *Ageing Res Rev* 8: 150–9, 2009.

149. **Nakanishi K**, **Sudo T**, **Morishima N**. Endoplasmic reticulum stress signaling transmitted by ATF6 mediates apoptosis during muscle development. *J Cell Biol* 169: 555–560, 2005.

150. **Nargund AM**, **Fiorese CJ**, **Pellegrino MW**, **Deng P**, **Haynes CM**. Mitochondrial and Nuclear Accumulation of the Transcription Factor ATFS-1 Promotes OXPHOS Recovery during the UPR(mt). *Mol Cell* 58: 123–133, 2015.

151. **Nargund AM**, **Pellegrino MW**, **Fiorese CJ**, **Baker BM**, **Haynes CM**. Mitochondrial import efficiency of ATFS-1 regulates mitochondrial UPR activation. *Science* 337: 587–90, 2012.

152. **Nguyen DT**, **Kebache S**, **Fazel A**, **Wong HN**, **Jenna S**, **Emadali A**, **Lee E**, **Bergeron JJM**, **Kaufman RJ**, **Larose L**, **Chevet E**. Nck-dependent Activation of Extracellular Signal-Regulated Kinase-1 and Regulation of Cell Survival During Endoplasmic Reticulum Stress. *Mol Biol Cell* 15: 4248–4260, 2004.

153. **Nishitoh H**, **Matsuzawa A**, **Tobiume K**, **Saegusa K**, **Takeda K**, **Inoue K**, **Hori S**, **Kakizuka A**, **Ichijo H**. ASK1 is essential for endoplasmic reticulum stress-induced neuronal cell death triggered by expanded polyglutamine repeats. *Genes Dev* 16: 1345–1355, 2002.

154. **Novoa I**, **Zeng H**, **Harding HP**, **Ron D**. Feedback inhibition of the unfolded protein response by GADD34-mediated dephosphorylation of eIF2alpha. *J Cell Biol* 153: 1011–1022, 2001.

155. **O'Leary MFN**, **Hood DA**. Effect of prior chronic contractile activity on mitochondrial function and apoptotic protein expression in denervated muscle. *J Appl Physiol* 105: 114–20, 2008.

156. **Ogata M**, **Hino S**, **Saito A**, **Morikawa K**, **Kondo S**, **Kanemoto S**, **Murakami T**, **Taniguchi M**, **Tanii I**, **Yoshinaga K**, **Shiosaka S**, **Hammarback JA**, **Urano F**, **Imaizumi K**. Autophagy is activated for cell survival after endoplasmic reticulum stress. *Mol Cell Biol* 26: 9220–31, 2006.

157. **Ogata T**, **Machida S**, **Oishi Y**, **Higuchi M**, **Muraoka I**. Differential cell death regulation between adult-unloaded and aged rat soleus muscle. *Mech Ageing Dev* 130: 328–36, 2009.

158. **Ogata T**, **Yamasaki Y**. Ultra-high-resolution scanning electron microscopy of mitochondria and sarcoplasmic reticulum arrangement in human red, white, and intermediate muscle fibers. *Anat Rec* 248: 214–223, 1997.

159. **Ogborn DI**, **McKay BR**, **Crane JD**, **Parise G**, **Tarnopolsky MA**. The unfolded protein response is triggered following a single, unaccustomed resistance-exercise bout. *Am J Physiol Regul Integr Comp Physiol* 2100, 2014.

160. **Ojuka EO**, **Jones TE**, **Han D-H**, **Chen M**, **Holloszy JO**. Raising Ca2+ in L6 myotubes mimics effects of exercise on mitochondrial biogenesis in muscle. *FASEB J* 17: 675–681, 2003.

161. **Ornatsky OI**, **Connor MK**, **Hood DA**. Expression of stress proteins and mitochondrial chaperonins in chronically stimulated skeletal muscle. *Biochem J* 311: 119–23, 1995.

162. **Orrenius S**, **Zhivotovsky B**, **Nicotera P**. Regulation of cell death: the calcium–apoptosis link. *Nat Rev Mol Cell Biol* 4: 552–565, 2003.

163. **Ozcan U**, **Yilmaz E**, **Ozcan L**, **Furuhashi M**, **Vaillancourt E**, **Smith RO**, **Görgün CZ**, **Hotamisligil GS**. Chemical chaperones reduce ER stress and restore glucose homeostasis in a mouse model of type 2 diabetes. *Science* 313: 1137–1140, 2006.

164. **Palmer JW**, **Tandler B**, **Hoppel C**. Biochemical Properties of Subsarcolemmal and Interfibrillar Mitochondria Isolated from Rat Cardiac Muscle. *J Biol Chem* 252: 8731–8739, 1977.

165. **Papa L**, **Germain D**. Estrogen receptor mediates a distinct mitochondrial unfolded protein response. *J Cell Sci* 124: 1396–1402, 2011.

166. **Papa L**, **Germain D**. SirT3 regulates the mitochondrial unfolded protein response. *Mol Cell Biol* 34: 699–710, 2014.

167. **Paschen SA**, **Waizenegger T**, **Stan T**, **Preuss M**, **Cyrklaff M**, **Hell K**, **Rapaport D**, **Neupert W**. Evolutionary conservation of biogenesis of b -barrel membrane proteins. *Nature* 426: 862–866, 2003.

168. **Pellegrino MW**, **Nargund AM**, **Haynes CM**. Signaling the mitochondrial unfolded protein response. *Biochim Biophys Acta* 1833: 410–6, 2013.

169. **Perisic O**, **Xiao H**, **Lis JT**. Stable binding of Drosophila heat shock factor to head-to-head and tail-to-tail repeats of a conserved 5 bp recognition unit. *Cell* 59: 797–806, 1989.

170. **Pimenta de Castro I**, **Costa AC**, **Lam D**, **Tufi R**, **Fedele V**, **Moisoi N**, **Dinsdale D**, **Deas E**, **Loh SHY**, **Martins LM**. Genetic analysis of mitochondrial protein misfolding in Drosophila melanogaster. *Cell Death Differ* 19: 1308–1316, 2012.

171. **Pirinen E**, **Cantó C**, **Jo YS**, **Morato L**, **Zhang H**, **Menzies KJ**, **Williams EG**, **Mouchiroud L**, **Moullan N**, **Hagberg C**, **Li W**, **Timmers S**, **Imhof R**, **Verbeek J**, **Pujol A**, **Van Loon B**, **Viscomi C**, **Zeviani M**, **Schrauwen P**, **Sauve AA**, **Schoonjans K**, **Auwerx J**. Pharmacological inhibition of poly(ADP-ribose) polymerases improves fitness and mitochondrial function in skeletal muscle. *Cell Metab* 19: 1034–1041, 2014.

172. **Pogozelski AR**, **Geng T**, **Li P**, **Yin X**, **Lira V a.**, **Zhang M**, **Chi J-T**, **Yan Z**. p38γ Mitogen-Activated Protein Kinase Is a Key Regulator in Skeletal Muscle Metabolic Adaptation in Mice. *PLoS One* 4: e7934, 2009.

173. **Primeau AJ**, **Adhihetty PJ**, **Hood DA**. Apoptosis in Heart and Skeletal Muscle. *Can J Appl Physiol* 27: 349–395, 2002.

174. **Puigserver P**, **Rhee J**, **Lin J**, **Wu Z**, **Yoon JC**, **Zhang CY**, **Krauss S**, **Mootha VK**, **Lowell BB**, **Spiegelman BM**. Cytokine Stimulation of Energy Expenditure through p38 MAP Kinase Activation of PPARγ Coactivator-1. *Mol Cell* 8: 971–982, 2001.

175. **Pulliam DA**, **Deepa SS**, **Liu Y**, **Hill S**, **Lin A-L**, **Bhattacharya A**, **Shi Y**, **Sloane L**, **Viscomi C**, **Zeviani M**, **Van Remmen H**. Complex IV Deficient Surf1-/- Mice Initiate Mitochondrial Stress Responses. *Biochem. J.* (June 2014). doi: 10.1042/BJ20140291.

176. **Rainbolt TK**, **Atanassova N**, **Genereux JC**, **Wiseman RL**. Stress-regulated translational attenuation adapts mitochondrial protein import through Tim17A degradation. *Cell Metab* 18: 908–919, 2013.

177. **Rath E**, **Berger E**, **Messlik A**, **Nunes T**, **Liu B**, **Kim SC**, **Hoogenraad NJ**, **Sans M**, **Sartor RB**, **Haller D**. Induction of dsRNA-activated protein kinase links mitochondrial unfolded protein response to the pathogenesis of intestinal inflammation. *Gut* 61: 1269–1278, 2012.

178. **Rehling P**, **Pfanner N**, **Meisinger C**. Insertion of Hydrophobic Membrane Proteins into the Inner Mitochondrial Membrane—A Guided Tour. *J Mol Biol* 326: 639–657, 2003.

179. **Reid B**, **Slater CR**, **Bewick GS**. Synaptic vesicle dynamics in rat fast and slow motor nerve terminals. *J Neurosci* 19: 2511–2521, 1999.

180. **Ristow M**, **Zarse K**, **Oberbach A**, **Klöting N**, **Birringer M**, **Kiehntopf M**, **Stumvoll M**, **Kahn CR**, **Blüher M**. Antioxidants prevent health-promoting effects of physical exercise in humans. *Proc Natl Acad Sci U S A* 106: 8665–8670, 2009.

181. **Rivero JL**, **Talmadge RJ**, **Edgerton VR**. Fibre size and metabolic properties of myosin heavy chain-based fibre types in rat skeletal muscle. *J Muscle Res Cell Motil* 19: 733–42, 1998.

182. **Ron D**, **Walter P**. Signal integration in the endoplasmic reticulum unfolded protein response. *Nat Rev Mol Cell Biol* 8: 519–529, 2007.

183. **Ryan MT**, **Hoogenraad NJ**. Mitochondrial-Nuclear Communications. *Annu Rev Biochem* 76: 701–722, 2007.

184. **Salmons S**, **Vrbová G**. The influence of activity on some contractile characteristics of mammalian fast and slow muscles. *J Physiol* 201: 535–49, 1969.

185. **Scarpulla RC**, **Vega RB**, **Kelly DP**. Transcriptional integration of mitochondrial biogenesis. *Trends Endocrinol Metab* 23: 459–466, 2012.

186. **Scarpulla RC**. Nuclear activators and coactivators in mammalian mitochondrial biogenesis. *Biochim Biophys Acta - Gene Struct Expr* 1576: 1–14, 2002.

187. **Scarpulla RC**. Nuclear control of respiratory gene expression in mammalian cells. *J Cell Biochem* 97: 673–683, 2006.

188. **Scarpulla RC**. Transcriptional Paradigms in Mammalian Mitochondrial Biogenesis and Function. (2008). doi: 10.1152/physrev.00025.2007.

189. **Scarpulla RC**. Metabolic control of mitochondrial biogenesis through the PGC-1 family regulatory network. *Biochim Biophys Acta* 1813: 1269–78, 2011.

190. **Schiaffino S**, **Ausoni S**, **Gorza L**, **Saggin L**, **Gundersen K**, **Lomo T**. Myosin heavy chain isoforms and velocity of shortening of type 2 skeletal muscle fibres. *Acta Physiol Scand* 134: 575–576, 1988.

191. **Schiaffino S**, **Hanzlíková V**, **Pierobon S**. Relations between structure and function in rat skeletal muscle fibers. *J Cell Biol* 47: 107–19, 1970.

192. **Schiaffino S**, **Reggiani C**. Myosin isoforms in mammalian skeletal muscle. *J Appl Physiol* 77: 493–501, 1994.

193. **Schiaffino S**, **Reggiani C**. Fiber Types in Mammalian Skeletal Muscles. *Physiol Rev* 91: 1447–1531, 2011.

194. **Schröder M**, **Kaufman RJ**. the Mammalian Unfolded Protein Response. *Annu Rev Biochem* 74: 739–789, 2005.

195. **Schröder M**, **Kaufman RJ**. ER stress and the unfolded protein response. *Mutat Res* 569: 29–63, 2005.

196. **Schulz AM**, **Haynes CM**. UPR(mt)-mediated cytoprotection and organismal aging. *Biochim Biophys Acta* 1847: 1448–1456, 2015.

197. **Seyhun E**, **Malo A**, **Schäfer C**, **Moskaluk CA, Hoffmann R**, **Göke B**, **Kubisch CH**. Tauroursodeoxycholic acid reduces endoplasmic reticulum stress , acinar cell damage , and systemic inflammation in acute pancreatitis. *Am J Physiol - Gastrointest Liver Physiol* 301: G773–G782, 2011.

198. **Shaffer AL**, **Shapiro-Shelef M**, **Iwakoshi NN**, **Lee A-H**, **Qian S-B**, **Zhao H**, **Yu X**, **Yang L**, **Tan BK**, **Rosenwald A**, **Hurt EM**, **Petroulakis E**, **Sonenberg N**, **Yewdell JW**, **Calame K**, **Glimcher LH**, **Staudt LM**. XBP1, downstream of Blimp-1, expands the secretory apparatus and other organelles, and increases protein synthesis in plasma cell differentiation. *Immunity* 21: 81–93, 2004.

199. **Shi Y**, **Mosser DD**, **Morimoto RI**. Molecular chaperones as HSF1-specific transcriptional repressors. *Genes Dev* 12: 654–666, 1998.

200. **Sieck GC**, **Zhan W-Z**, **Prakash YS**, **Daood MJ**, **Watchko JF**. SDH and actomyosin ATPase activities of different fiber types in rat diaphragm muscle. *J Appl Physiol* 79: 1629–1639, 1995.

201. **Sreter FA**, **Lopez JR**, **Alamo L**, **Mabuchi K**, **Gergely J**. Changes in intracellular ionized Ca concentration associated with muscle fiber type transformation. *Am J Physiol* 253: C296–300, 1987.

202. **Sriburi R**, **Bommiasamy H**, **Buldak GL**, **Robbins GR**, **Frank M**, **Jackowski S**, **Brewer JW**. Coordinate regulation of phospholipid biosynthesis and secretory pathway gene expression in XBP-1(S)-induced endoplasmic reticulum biogenesis. *J Biol Chem* 282: 7024–7034, 2007.

203. **Stevens FJ**, **Argon Y**. Protein folding in the ER. *Semin Cell Dev Biol* 10: 443–54., 1999.

204. **Stone SJ**, **Vance JE**. Phosphatidylserine Synthase-1 and -2 Are Localized to Mitochondria-associated Membranes. *J Biol Chem* 275: 34534–34540, 2000.

205. **Szabadkai G**, **Duchen MR**. Mitochondria : The Hub of Cellular Ca2+ Signaling. *Physiology* 23: 84–94, 2008.

206. **Szegezdi E**, **Logue SE**, **Gorman AM**, **Samali A**. Mediators of endoplasmic reticulum stress-induced apoptosis. *EMBO Rep* 7: 880–885, 2006.

207. **Szegezdi E**, **Macdonald DC**, **Chonghaile TN**, **Gupta S**, **Samali A**. Bcl-2 family on guard at the ER. *Am J Physiol Cell Physiol* 296: C941–C953, 2009.

208. **Takahashi M**, **Chesley A**, **Freyssenet D**, **Hood DA**. Contractile activity-induced adaptations in the mitochondrial protein import system. *Am J Physiol* 274: C1380–7, 1998.

209. **Takahashi M**, **Hood DA**. Chronic stimulation-induced changes in mitochondria and performance in rat skeletal muscle. *J Appl Physiol* 74: 934–941, 1993.

210. **Takahashi M**, **Hood DA**. Protein Import into Subsarcolemmal and Intermyofibrillar Skeletal. *J Biol Chem* 271: 27285–27291, 1996.

211. **Tanaka Y**, **Ishitsuka Y**, **Hayasaka M**, **Yamada Y**, **Miyata K**, **Endo M**, **Kondo Y**, **Moriuchi H**, **Irikura M**, **Tanaka K-I**, **Mizushima T**, **Oike Y**, **Irie T**. The exacerbating roles of CCAAT/enhancer-binding protein homologous protein (CHOP) in the development of bleomycin-induced pulmonary fibrosis and the preventive effects of tauroursodeoxycholic acid (TUDCA) against pulmonary fibrosis in mice. *Pharmacol Res* 99: 52–62, 2015.

212. **Tatsuta T**, **Langer T**. Quality control of mitochondria: protection against neurodegeneration and ageing. *EMBO J* 27: 306–314, 2008.

213. **Twig G**, **Hyde B**, **Shirihai OS**. Mitochondrial fusion, fission and autophagy as a quality control axis: The bioenergetic view. *Biochim Biophys Acta - Bioenerg* 1777: 1092–1097, 2008.

214. **Uguccioni G**, **Hood DA**. The importance of PGC-1α in contractile activity-induced mitochondrial adaptations. *Am J Physiol Endocrinol Metab* 300: E361–71, 2011.

215. **Upton J-P**, **Wang L**, **Han D**, **Wang ES**, **Huskey NE**, **Lim L**, **Truitt M**, **McManus MT**, **Ruggero D**, **Goga A**, **Papa FR**, **Oakes SA**. IRE1α cleaves select microRNAs during ER stress to derepress translation of proapoptotic Caspase-2. *Science* 338: 818–22, 2012.

216. **Urano F**, **Wang X**, **Bertolotti A**, **Zhang Y**, **Chung P**, **Harding HP**, **Ron D**. Coupling of stress in the ER to activation of JNK protein kinases by transmembrane protein kinase IRE1. *Science* 287: 664–666, 2000.

217. **Urra H**, **Dufey E**, **Lisbona F**, **Rojas-Rivera D**, **Hetz C**. When ER stress reaches a dead end. *Biochim Biophys Acta - Mol Cell Res* 1833: 3507–3517, 2013.

218. **Vainshtein A**, **Desjardins EM**, **Armani A**, **Sandri M**, **Hood DA**. PGC-1α modulates denervation-induced mitophagy in skeletal muscle. *Skelet Muscle* 5: 9, 2015.

219. **Vannuvel K**, **Renard P**, **Raes M**, **Arnould T**. Functional and morphological impact of ER stress on mitochondria. *J Cell Physiol* 228: 1802–1818, 2013.

220. **Wang L**, **Piguet A-C**, **Schmidt K**, **Tordjmann T**, **Dufour J-F**. Activation of CREB by tauroursodeoxycholic acid protects cholangiocytes from apoptosis induced by mTOR inhibition. *Hepatology* 41: 1241–51, 2005.

221. **Wang Y**, **Shen J**, **Arenzana N**, **Tirasophon W**, **Kaufman RJ**, **Prywes R**. Activation of ATF6 and an ATF6 Binding Site by the ER Stress Response. *J Biol Chem* 275: 27013–20, 2000.

222. **Wehrle U**, **Düsterhöft S**, **Pette D**. Effects of chronic electrical stimulation on myosin heavy chain expression in satellite cell cultures derived from rat muscles of different fiber-type composition. *Differentiation* 58: 37–46, 1994.

223. **Winder WW**, **Holmes BF**, **Rubink DS**, **Jensen EB**, **Chen M**, **Holloszy JO**. Activation of AMP-activated protein kinase increases mitochondrial enzymes in skeletal muscle. *J Appl Physiol* 88: 2219–2226, 2000.

224. **Wu J**, **Ruas JL**, **Estall JL**, **Rasbach KA**, **Choi JH**, **Ye L**, **Boström P**, **Tyra HM**, **Crawford RW**, **Campbell KP**, **Rutkowski DT**, **Kaufman RJ**, **Spiegelman BM**. The unfolded protein response mediates adaptation to exercise in skeletal muscle through a PGC-1α/ATF6α complex. *Cell Metab* 13: 160–9, 2011.

225. **Wu J**, **Rutkowski DT**, **Dubois M**, **Swathirajan J**, **Saunders T**, **Wang J**, **Song B**, **Yau GD**, **Kaufman RJ**. ATF6alpha Optimizes Long-Term Endoplasmic Reticulum Function to Protect Cells from Chronic Stress. *Dev Cell* 13: 351–364, 2007.

226. **Xia Y**, **Buja LM**, **Scarpulla RC**, **McMillin JB**. Electrical stimulation of neonatal cardiomyocytes results in the sequential activation of nuclear genes governing mitochondrial proliferation and differentiation. *Proc Natl Acad Sci USA* 94: 11399–11404, 1997.

227. **Xie Q**, **Khaoustov VI**, **Chung CC**, **Sohn J**, **Krishnan B**, **Lewis DE**, **Yoffe B**. Effect of tauroursodeoxycholic acid on endoplasmic reticulum stress-induced caspase-12 activation. *Hepatology* 36: 592–601, 2002.

228. **Yan Z**, **Li P**, **Akimoto T**. Transcriptional control of the Pgc-1alpha gene in skeletal muscle in vivo. *Exerc Sport Sci Rev* 35: 97–101, 2007.

229. **Yang J-S**, **Kim JT**, **Jeon J**, **Park HS**, **Kang GH**, **Park KS**, **Lee HK**, **Kim S**, **Cho YM**. Changes in hepatic gene expression upon oral administration of taurine-conjugated ursodeoxycholic acid in ob/ob mice. *PLoS One* 5: e13858, 2010.

230. **Ye J**, **Rawson RB**, **Komuro R**, **Chen X**, **Davé UP**, **Prywes R**, **Brown MS**, **Goldstein JL**. ER Stress Induces Cleavage of Membrane-Bound ATF6 by the Same Proteases that Process SREBPs. *Mol Cell* 6: 1355–1364, 2000.

231. **Yoshida H**, **Matsui T**, **Yamamoto A**, **Okada T**, **Mori K**. XBP1 mRNA is induced by ATF6 and spliced by IRE1 in response to ER stress to produce a highly active transcription factor. *Cell* 107: 881–91, 2001.

232. **Young JC**, **Hoogenraad NJ**, **Hartl FU**. Molecular Chaperones Hsp90 and Hsp70 Deliver Preproteins to the Mitochondrial Import Receptor Tom70. *Cell* 112: 41–50, 2003.

233. **Yuzefovych LV**, **Musiyenko SI**, **Wilson GL**, **Rachek LI**. Mitochondrial DNA damage and dysfunction, and oxidative stress are associated with endoplasmic reticulum stress, protein degradation and apoptosis in high fat diet-induced insulin resistance mice. *PLoS One* 8: e54059, 2013.

234. **Yuzefovych LV**, **LeDoux SP**, **Wilson GL**, **Rachek LI**. Mitochondrial DNA damage via augmented oxidative stress regulates endoplasmic reticulum stress and autophagy: Crosstalk, links and signaling. *PLoS One* 8: 6–10, 2013.

235. **Zalman LS**, **Nikaido H**, **Kagawa Y**. Mitochondrial Outer Membrane Contains a Protein Producing Nonspecific Diffusion Channels. *J Biol Chem* 255: 1771–1774, 1980.

236. **Zhang K**, **Kaufman RJ**. protein folding in the endoplasmic reticulum and the unfolded protein response. *Hanb Exp Pharmacol* 172: 69–91, 2006.

237. **Zhao Q**, **Wang J**, **Levichkin I V.**, **Stasinopoulos S**, **Ryan MT**, **Hoogenraad NJ**. A mitochondrial specific stress response in mammalian cells. *EMBO J* 21: 4411–4419, 2002.

CHAPTER 2: MANUSCRIPT
(SUBMITTED FOR PUBLICATION)

MANUSCRIPT AUTHOR CONTRIBUTIONS

Jonathan M. Memme: Performed all chronic contractile activity surgeries for both time-course and TUDCA/vehicle treated animals; qPCR, cytochrome c oxidase, and western blotting experiments; data analysis and interpretation; and wrote the manuscript.

Ashley N. Oliveira: Assisted in western blotting and experiment preparation, as well as animal TUDCA/vehicle injections.

Dr. David A. Hood: Supervised this project and he is the principal investigator.

THE CHRONOLOGY AND FUNCTION OF UPR ACTIVATION IN SKELETAL MUSCLE ADAPTATIONS TO CHRONIC CONTRACTILE ACTIVITY

Jonathan M. Memme, Ashley N. Oliveira and David A. Hood

Muscle Health Research Centre, School of Kinesiology and Health Science, York University, Toronto, Ontario, M3J 1P3, Canada

To whom correspondence should be addressed: David A. Hood
School of Kinesiology
York University, Toronto, ON
M3J 1P3, Canada

ABSTRACT

The mitochondrial (UPR^{mt}) and the endoplasmic reticulum (UPR^{ER}) unfolded protein responses are important in maintaining cellular homeostasis during stimulus-induced increases in protein synthesis. Exercise is a well-established trigger for the synthesis of mitochondrial proteins via organelle biogenesis, regulated by PGC-1α. To investigate the role of the UPR^{mt} and the UPR^{ER} in exercise-induced adaptations, we subjected rats to 3-hrs of chronic contractile activity (CCA) for 1, 2, 3, 5 or 7 days, followed by 3-hrs recovery. Mitochondrial biogenesis signaling, through PGC-1α mRNA, increased 14-fold after an acute bout of CCA. This was manifest in a 10-32% increase in COX activity, an indicator of mitochondrial content, between days 3-7, as well as a concomitant increase in the autophagic degradation of p62 and LC3-II protein. Preceding these adaptive events, UPR^{ER} transcripts ATF4, XBP1s, and BiP were elevated (1.3-3.8-fold) from 1-3 days while CHOP and chaperones BiP and HSP70 were elevated at both mRNA and protein levels (1.5-3.9-fold) from 1-7 days of CCA. Mitochondrial chaperones CPN10, HSP60, and mtHSP70, protease ClpP, and regulatory protein SirT3, of the UPR^{mt} were concurrently induced 10-80% between 1-7 days. To test the role of the UPR in CCA-induced remodeling, we treated animals with the ER stress suppressor TUDCA and subjected them to 2 or 7 days of CCA. TUDCA attenuated CHOP and HSP70 protein induction, however this failed to impact mitochondrial and cellular remodeling. Our data indicate that signaling to the UPR is rapidly activated following acute contractile activity, that this is attenuated with repeated bouts, and that the UPR is involved in chronic adaptations to CCA, however this appears to be independent of CHOP signaling.

INTRODUCTION

Skeletal muscle is a highly adaptable tissue, responsive to multiple stressors leading to changes in whole-body metabolism. It has been established that exercise induces many physiological adaptations that are beneficial for muscle performance capabilities, such as remodeling of the mitochondrial reticulum through mitochondrial biogenesis as well as the removal of damaged or dysfunctional organelles through a process termed autophagy (28, 39, 49). Mitochondria are the essential cellular organelles with primary roles in energy production in the form of ATP (27). At the onset of contractile activity, early signaling events involved in mitochondrial biogenesis are initiated within skeletal muscle and converge largely on the activation of the transcriptional coactivator PGC-1α (20, 27, 50, 52). The vast majority of component proteins are transcribed in the nucleus and require transport to the mitochondria via chaperone and import machineries to facilitate protein shuttling and organelle assembly (12, 25, 30, 63). Less than 1% of total mitochondrial proteins are derived from mitochondrial DNA (mtDNA) with the remainder provided by the nucleus (3, 24, 51). Therefore, to produce a functional organelle capable of adequate ATP supply, contractile-activity-induced mitochondrial biogenesis requires the integration, coordination, and timely expression of the nuclear and mitochondrial genomes.

Under conditions of cellular stress, such as unaccustomed exercise, proteins may become misfolded and unable to reach their appropriate destination within the mitochondrion, leading to a proteotoxic cellular environment (21, 46). However, the unfolded protein response (UPR) is gaining attention as a protective mechanism that helps to maintain homeostasis under cell stress. To date, two such UPR pathways have

been observed. The first, an endoplasmic reticulum-mediated UPR (UPR^{ER}) senses misfolded proteins within the ER lumen through the resident chaperone BiP (48). BiP preferentially binds unfolded proteins thus disassociating, and thereby activating, ER membrane-bound kinases IRE1α and PERK, as well as releasing a potent transcription factor ATF6 to increase a host of chaperones and proteases while simultaneously reducing global translation (53). The second is a mitochondrial UPR (UPR^{mt}), which senses proteotoxic stress in the matrix and intermembrane space to independently activate a variety of mitochondria-specific chaperones and proteases and regain homeostasis (6, 46, 58). Together, the UPR^{ER} and the UPR^{mt} initiate an acute response to reduce protein load, and an adaptive response to increase protein-handling ability. Ultimately if homeostasis is not reached, autophagy will be induced (29, 46).

The molecular mechanisms involved in the metabolic adaptations observed with exercise have yet to be fully elucidated. It has recently been found that exercise is capable of eliciting an unfolded protein response in untrained muscle, and in an intensity-dependent manner (32, 42, 55, 61). However, despite these recent findings, no work has focused on the role of the UPR^{ER}, or the UPR^{mt}, with exercise in relation to mitochondrial biogenesis and the induction of autophagy in skeletal muscle. Therefore, our objectives were to examine: 1) the chronology of the UPR^{ER} and UPR^{mt} activation with contractile activity in relation to mitochondrial biogenesis and autophagy; and 2) whether the UPR is required for these exercise-associated adaptations by administering the chemical chaperone mimetic Tauroursodeoxycholic acid, a naturally occurring bile acid capable of blocking ER stress-induced UPR activation (44, 62).

METHODS

Animals and chronic contractile activity. The chronic contractile activity (CCA) model has been described previously as a useful model of chronic exercise (33, 56). Briefly, male Sprague-Dawley rats (SD; Charles River, St. Constant, QC, Canada), weighing 350-550 g were anaesthetized with isofluorane. Wire electrodes (Medwire, Leico Industries, New York, NY) were passed unilaterally and subcutaneously from the left hindlimb to the top of the back to connect to an external stimulation unit secured with surgical tape. Animals were allowed 5-7 days of recovery following surgery before TA and EDL muscles were subjected to stimulation (6V, 10Hz, 0.1ms duration). For all animals, contractions were induced for 3 hrs/ day. Animals in the time-course study were for subjected to 1, 2, 3, 5, or 7 days of contractile activity, whereas vehicle/TUDCA treated animals were subjected to either 2 or 7 days of stimulation. Three hours following the final bout of contractile activity, animals were sacrificed and the TA and EDL of both control and stimulated hindlimbs were extracted and flash frozen in liquid nitrogen, and then pulverized into fine powder for subsequent experimental analysis. Immediately following tissue removal, animals were euthanized via cardiac excision. Animal protocols have been approved by the York University Animal Care Committee.

TUDCA and vehicle treatment. Animals as described above, were randomly divided into TUDCA or vehicle-treated groups. TUDCA (EMD Millipore, Billerica, MA) was dissolved in phosphate buffered saline (PBS; Wisent Bio Products, Saint-Jean-Baptiste, QC) at 200 mg/ml and pH of 7.5. Animals were administered 400 mg/kg of either TUDCA or equal volume of sterile PBS (vehicle) daily via intraperitoneal (IP) injection beginning 3 days prior to surgery. Injections continued throughout the recovery

and stimulation period and terminated one day prior to tissue extraction in order to avoid the acute effects of drug treatment.

Cytochrome c oxidase activity. Cytochrome *c* oxidase (COX) activity was used as a marker of mitochondrial content. Pulverized whole muscle homogenates were prepared and sonicated for 10 s on ice at a power output of 20–30%. A buffered test solution was prepared containing fully reduced horse heart cytochrome *c* (C-2506; Sigma, Oakville, ON, Canada). With the use of a multipipette, 240 µl of test solution were added to 50 µl of whole muscle homogenate in a 96-well plate. COX enzyme activity was determined spectrophotometrically as the maximal rate of oxidation of fully reduced cytochrome c (C-2506, Sigma, Oakville, ON, Canada), measured by the change in absorbance at 550 nm and temperature of 30°C in a Synergy HT (Bio-tek Instruments, Winooski, VT) microplate reader. For each sample, the COX activity measurement was calculated as an average of three trials.

In vitro RNA isolation and reverse transcription. Total RNA was isolated from frozen, whole muscle TA powders as described previously (43). Briefly, Tissue powder (~70 mg) was added to TRIzol® reagent, homogenized, then mixed with chloroform. Samples were centrifuged at 4°C at 16,000 *g* for 15 min and the upper aqueous phase of the sample was transferred into a new tube along with isopropanol and left overnight at −20°C to precipitate. Samples were once again centrifuged at 4°C at 16,000 *g* for 10 min. The resultant supernate was discarded and pellet resuspended in 30 µl of molecular grade sterile H_2O (Wisent Bio Products, Saint-Jean-Baptiste, QC). The concentration and purity of the RNA was measured using a Nano Drop 2000 Spectrophotometer. SuperScript® III reverse transcriptase (Invitrogen, Carlsbad, CA, USA) was used to reverse transcribe 1.5

µg of total RNA into cDNA.

Real-time PCR. Using sequences from GenBank, primers were designed with Primer 3 v. 0.4.0 software (Massachusetts Institute of Technology, Cambridge, MA) for genes of interest (Table 1). Primer specificity was confirmed by OligoAnalyzer 3.1 (Integrated DNA Technologies, Toronto, ON, Canada). mRNA expression was measured with SYBR® Green chemistry (PerfeCTa SYBR® Green SuperMix; ROX, Quanta BioSciences, Gaithersburg, MD). Each well contained: SYBR® Green SuperMix, forward and reverse primers (20 µM), sterile water, and 10 ng of cDNA. The detection of all real-time PCR amplification took place in a 96-well plate using a StepOnePlus® Real-Time PCR System (Applied Biosystems, Foster City, CA). The final reaction volume of each well was 25 µl. Samples were run in duplicates to ensure accuracy. The PCR program consisted of an initial holding stage (95°C for 10 min), followed by 40 amplification cycles (60°C for 1 min, 95°C for 15 s), and was completed with a final melting stage (95°C for 15 s, 60°C for 1 min, 95°C for 15 s). Nonspecific amplification and primer dimers were controlled for by the analysis of melt curves generated by the instrument for SYBR® Green analyses. Negative control wells contained water in place of cDNA.

Real-time qPCR quantification. First, the threshold cycle (CT) number of the endogenous reference gene was subtracted from the CT number of the target gene [ΔCT = CT(target) − CT(reference)]. Next, the ΔCT value of the control tissue was subtracted from the ΔCT value of the experimental tissue [ΔΔCT = ΔCT(experimental) − ΔCT(control)]. Results were reported as fold-changes using the ΔΔCT method, calculated as $2^{-\Delta\Delta CT}$. Primers detecting ribosomal protein s12 along with glyceraldehyde-3-

Table 1. List of primer oligonucleotide sequences used in real-time qPCR analysis for *Rattus norvegicus.* Alternative names used in this paper are written in parenthesis.

Gene, Size (bp)	Accession Number	Forward Primer	Reverse Primer
Ppargc1a (PGC-1α), 142	NM_031347.1	5'-CAT CGC AAT TCT CCC TTG TAT-3'	5'-CAG ACT CCC GCT TCT CAT ACT-3'
ATF4, 107	NM_024403.2	5'-CTC TCG CCA AAG AGA TTC AGT A-3'	5'-ACA AGC ACA AAG CAC CTG ACT A-3'
Hspa5 (BiP), 137	NM_013083.2	5'-TTG AAA CTG TGG GAG GTG T-3'	5'-GGG TCG TTC ACC TTC GTA GA-3'
Ddit3 (CHOP), 130	NM_001109986.1	5'-GAG CTG GAA GCC TGG TAT GA-3'	5'-GGG ATG CAG GGT CAA GAG TA-3'
Clpp, 145	XM_217313.8	5'-GAG CGA TAC GTG GGA GAC A-3'	5'-ACG TTG CTT CCT TAC TCA GCA-3'
Hspe1 (CPN10), 124	NM_012966.1	5'-CAC GGA GGC ACC AAA GTA GT-3'	5'-GGA ATG GGC AGC TTC ATG T-3'
Esr1 (Erα), 126	NM_012689.1	5'-CAT GAT GAA AGG CGG GAT A-3'	5'-AGG TTG GCA GCT CTC ATG T-3'
GAPDH, 122	NM_017008.3	5'-CTC TCT GCT CCT CCC TGT TCT-3'	5'-GGT AAC CAG GCG TCC GAT AC-3'
Hspd1 (HSP60), 138	NM_022229.2	5'-AGG CAG GTT CCT CAC CAA TAA-3'	5'-GCA TGG ACA ATG ACA GCA GTA-3'
Hspa4 (HSP70), 101	NM_153629.1	5'-CAT GGT GCT GAC CAA GAT GA-3'	5'-GCT GCG AGT CGT TGA AGT A-3'
Map1lc3 (LC3), 101	NM_199500.2	5'-GCA CAG CAT GGT GAG TGT AT-3'	5'-AGG TTT CTT GGG AGG CAT AGA-3'
Lonp1 (LonP), 117	NM_133404.1	5'-CTT GTG GTT CCC AAG CAT GT-3'	5'-CGT CAG CCA GTC CAG GTA GT-3'
Hspa9 (mtHSP70), 116	NM_001100658.2	5'-CCT TCT GTG GTT GCC TTT ACA-3'	5'-CGT CCA ATA AGA CGC TTT GTA-3'
Bnip3l (NIX), 133	NM_080888.1	5'-CCC TGC ACA ACA ACA ACA AC-3'	5'-CCA TTC TTC CCA TTT CCA TTA C-3'
Nqo1 (NQO1), 148	NM_017000.3	5'-TTC TGT GGC TTC CAG GTC TTA-3'	5'-GCT GCT TGG AGC AAA GTA GA-3'
Sqstm1 (P62), 117	NM_175843.4	5'-GGA ACT GAT GGA GTC GGA TAA C-3'	5'-TCC GAT TCT GGC ATC TGT AG-3'
Rps12 (S12), 127	NM_031709.3	5'-ATG GAC GTC AAC ACT GCT CT-3'	5'-ATG CAA GCA CGC AGA GAT-3'
SirT3, 118	NM_001106313.2	5'-GCC CAA TGT CGC TCA CTA CT-3'	5'-CAG CTT TGA GGC AGG GAT A-3'
Uqcrc1, 135	NM_001004250.2	5'-TCG AGA GGT TTG CTC CAA GTA-3'	5'-CGC AGA CTT CCT GCC TAG A-3'
XBP1s, 86	NM_001271731.1	5'-TGC TGA GTC CGC AGC AGG T-3'	5'-AAT CTG AAG AGG CAA CAG CGT-3'
XBP1t, 114	NM_001271731.1	5'-CCT TCT CCC TTC AGC GAC AT-3'	5'-CAG TGG TGG GTG GCT TTA GA-3'

phosphate dehydrogenase (GAPDH) were chosen as endogenous reference genes.

Immunoblotting. Whole muscle protein extracts were separated by 10–15% SDS-PAGE and transferred to nitrocellulose membranes with a wet electrotransfer apparatus (Mini Trans-Blot electrophoretic transfer cell, Bio-Rad, Mississauga, Canada). Nitrocellulose membranes were blocked in a 5% skim milk solution and subsequently incubated overnight at 4°C with the appropriate concentration of primary antibody (see Table 2 for list of antibodies). Membranes were then washed and incubated with the suitable HRP-conjugated secondary antibody for 1 h at room temperature and visualized with enhanced chemiluminescence. Quantification was performed with Image J Software (NIH, Bethesda, MD, USA), and values were normalized to the appropriate loading control.

Statistical Analysis. To compare control vs. stimulated muscles at a given time point and within vehicle/TUDCA conditions for mRNA, protein and cytochrome c oxidase activity experiments, a repeated-measures two-way analysis of variance (ANOVA) was performed followed by a Bonferroni post hoc test when necessary. mRNA analysis was performed using the ΔCT value. All statistical analyses were performed using Graphpad Prism 6 Software All values represent the mean ± SEM and significance was set at $P<0.05$.

Table 2: List of Antibodies Used

Antibody	Manufacturer	Reference No.
Aciculin	*In house*	See Reference (7)
ATF4	Santa Cruz Biotechnology	SC-200
ATF6	Abcam	ab203119
BiP	Cell Signaling	3183S
CHOP	Cell Signaling	2895
COX IV	Abcam	ab140643
CPN10	Enzo Life Sciences	ADI-SPA-110
eIF2a (p) [Ser 51]	Invitrogen	44728G
GAPDH	Abcam	Ab8245
HSP60	Enzo Life Sciences	ADI-SPA-806
HSP70	Enzo Life Sciences	ADI-SPA-810
JNK (p)	Cell Signaling	4668S
LC3 II (A/B)	Cell Signaling	4108S
mtHSP70	Enzo Life Sciences	ADI-SPA-825
p62	Sigma	P0067
PGC-1a	Millipore	AB3242
SirT3	Cell Signaling	5490S
Uqcrc2	Abcam	ab14745

RESULTS

Chronic contractile activity induces changes in mitochondrial content. We sought to establish a time-course relationship between mitochondrial adaptations in response to the CCA protocol over 1-7 days. To observe the activation of mitochondrial biogenesis signaling, we measured the mRNA expression of the transcriptional coactivator PGC-1α, regarded as the master regulator of this process. A single 3-hour bout of contractile activity was sufficient to elicit a 14-fold increase in the transcript level, which remained markedly elevated throughout 7 days of CCA ($P<0.05$; Fig. 1A). In order to effectively quantify the changes in mitochondrial content we also measured whole muscle cytochrome c oxidase (COX) enzyme activity. COX activity displayed an 11% increase as early as 3 days ($P=0.06$), which progressed to 32% after 7 days of contractile activity ($P<0.05$; Fig. 1B). We corroborated these data with protein expression of PGC-1α, as well as integral nuclear-encoded ETC component proteins, cytochrome c oxidase subunit IV (COX IV) and the cytochrome bc_1 complex III subunit 2 (Uqcrc2) after 7 days of chronic stimulation (Fig. 1C). CCA significantly induced Uqcrc2 by 1.9-fold with trends toward 1.3-1.4-fold increases in PGC-1α and COX IV, in line with previous reports from our laboratory (18, 26).

Chronic contractile activity elicits an autophagy response. To focus on the autophagy response as it pertains to mitochondrial remodeling and removal of dysfunctional organelles (10), we selected the adapter protein p62, and the autophagosomal membrane protein LC3, which together play important roles in facilitating subsequent organelle degradation. The mRNA expression of p62 displayed a 2.3-fold increase at day 2 of CCA ($P<0.05$; Fig. 2A), while LC3 mRNA exhibited no changes over the course of 7 days

Fig. 1

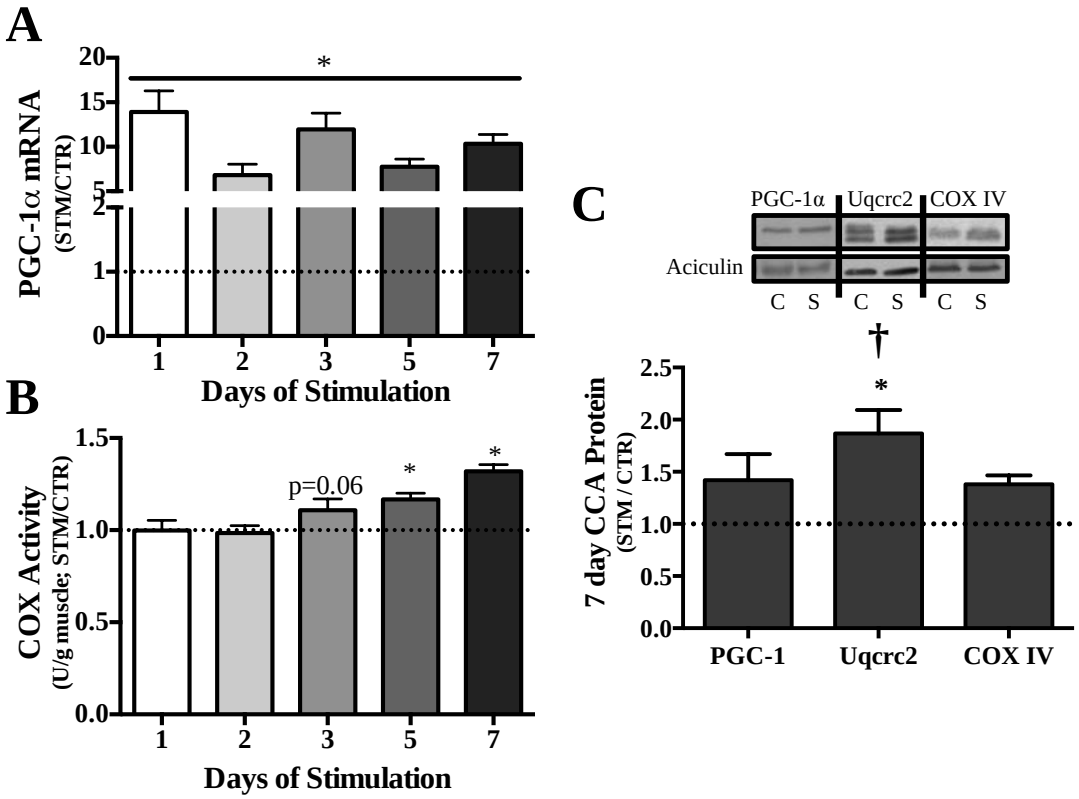

Figure 1: Time-course of CCA-induced mitochondrial biogenesis and adaptations. **(A)** Fold-change in mRNA expression of the mitochondrial biogenesis transcriptional coactivator PGC-1α, and **(B)** indicator of mitochondrial content, cytochrome c oxidase (COX) enzyme activity, throughout 1-7 days of CCA (PGC-1α mRNA, and COX activity, n=6, per day). **(C)** Spliced western blot and associated graph of PGC-1α, and nuclear-encoded ETC components Uqcrc2, and COX IV protein content illustrating mitochondrial adaptation following 7 days of CCA, (PGC-1α, n=5; Uqcrc2, and COX IV, n=6, per day). Bars represent fold-change in stimulated muscle relative to matched controls; means ± SEM. **P<0.05,* stimulated vs. control TA muscle at a given time point. †*P*<0.05, main effect of CCA relative to control across all conditions.

Fig. 2

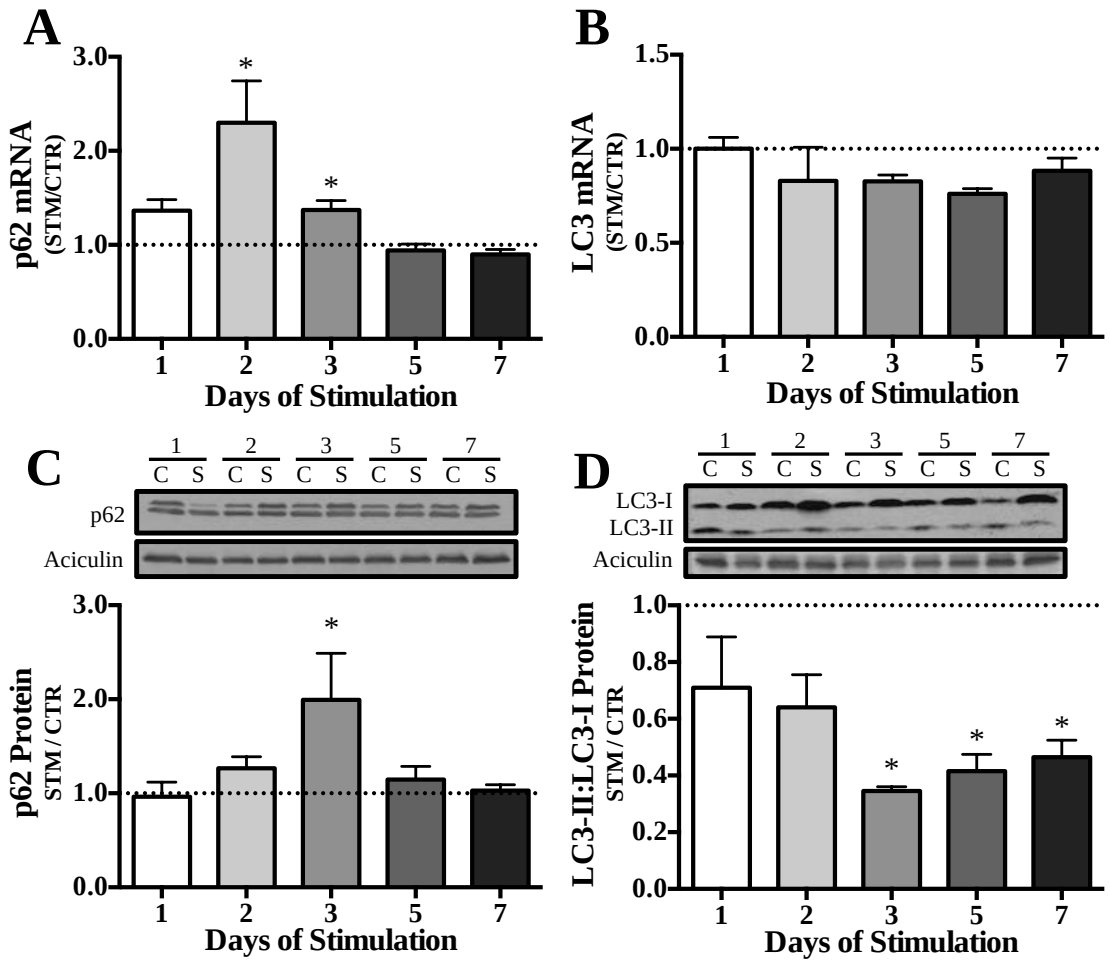

Figure 2: Time-course of CCA-induced autophagy induction. Fold-change in the transcript levels of autophagy markers **(A)** p62, and **(B)** LC3 over 1-7 days of CCA (p62, n=6; LC3, n=7, per day). Corresponding protein expression of **(C)** p62, and **(D)** the ratio of lipidated LC3-II to inactive LC3-I throughout the exercise protocol (LC3-II: LC3-I; n=6; p62, n=7, per time point). Bars represent fold-change in stimulated muscle relative to matched controls; means ± SEM. **P*<0.05, stimulated vs. control TA muscle at a given time point.

(Fig. 2B). Corresponding western blot analysis detected a 2-fold elevation in p62 protein levels following 3 days of CCA that returned back to control levels by day 5 ($P<0.05$; Fig. 2C). We also measured protein expression of LC3, as a ratio of its inactive form, LC3-I, to the active form LC3-II. We found that the LC3-II: LC3-I ratio was significantly reduced by roughly 55-65% from 3-7 days following repeated bouts of contractile activity (Fig. 2D).

Chronic contractile activity induces the UPR^{ER} as acute and adaptive responses. Given that we found an increase in mitochondrial content and autophagy signaling, we also measured selected UPR^{ER} transcripts and proteins as they relate to these adaptive mechanisms over the time-course of contractile activity. The activation of the PERK and IRE1α branches were assessed by the mRNA induction of their respective targets. In general, we detected a significant main effect of CCA ($P<0.05$) on the mRNA expression of all UPR^{ER} factors measured as early as day 1 and throughout our 7-day time-course. Specifically, ATF4, which is activated downstream of PERK, exhibited a 1.5-1.8-fold increase at days 2 and 3 ($P<0.05$), with levels returning back to control values by day 5 (Fig. 3A). We found that XBP1s was similarly enhanced during the first 3 days of contractile activity, reaching a 3.3-fold increase at day 2, and by day 7 was reduced by 45% in the stimulated, relative to the control, muscle ($P<0.05$; Fig. 3B). We also extended our analysis to include downstream targets of the UPR^{ER}. The transcription factor CHOP, and ER chaperone BiP, were significantly enriched at the transcript level by 2.2-3.9-fold throughout 1-7 days of chronic stimulation (Fig. 3C, E). Furthermore, CHOP protein levels displayed a main effect of CCA at all time points leading to a 1.8-fold increase by day 7 ($P<0.05$; Fig. 3D), while BiP protein remained unchanged until

Fig. 3

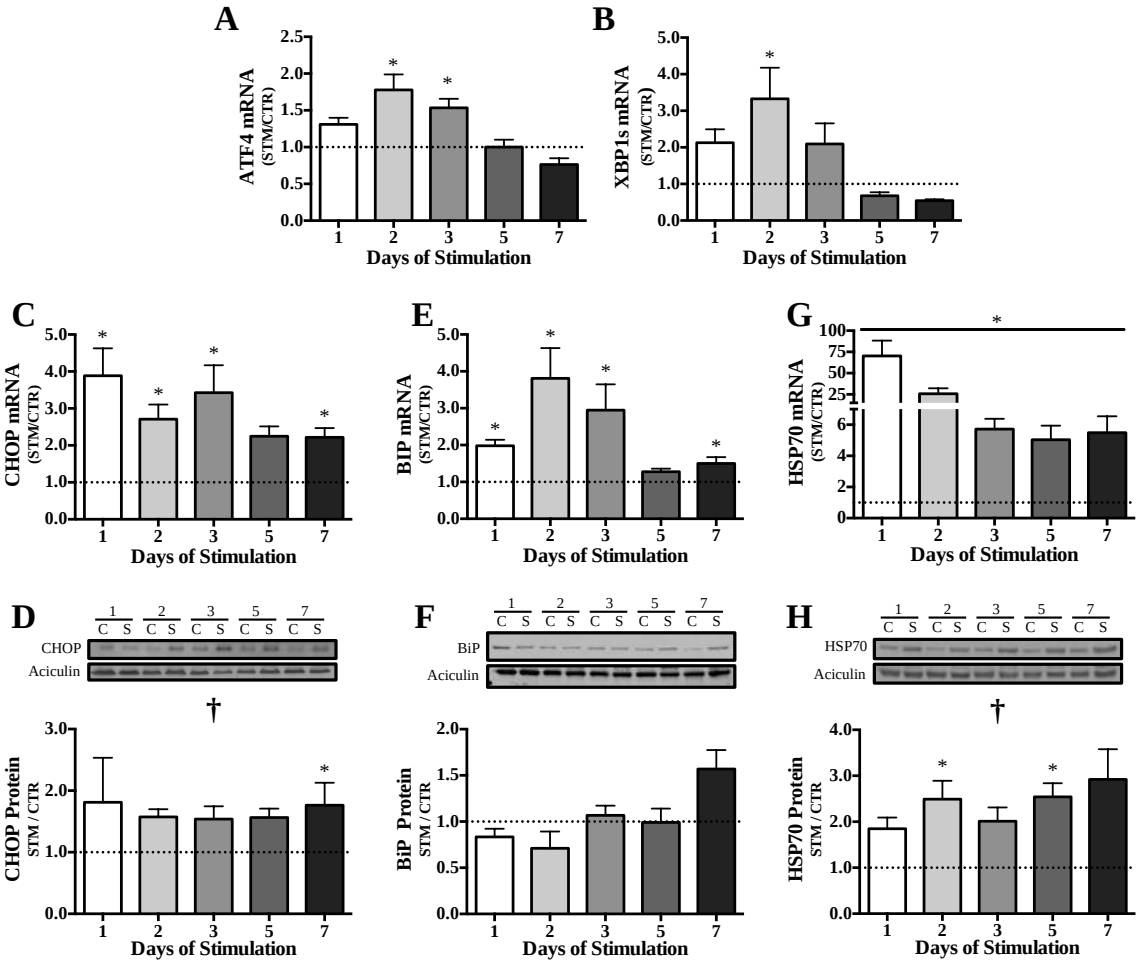

Figure 3: Time-course of the CCA-induced UPR^{ER}. Fold-change in the mRNA levels of UPR^{ER}-associated transcription factors **(A)** ATF4, **(B)** active XBP1s, and **(C)** CHOP, as well as chaperones **(E)** BiP, and **(G)** HSP70 during 1-7 days of CCA (ATF4, XBP1s, CHOP, BiP, and HSP70, n=6, per day). Corresponding protein expression of **(D)** CHOP, **(F)** BiP, and **(H)** HSP70 (CHOP and BiP, n=7, per day; HSP70, n=6, days 1-5, n=5, for day 7). Bars represent fold-change in stimulated muscle relative to matched controls; means ± SEM. **P*<0.05, stimulated vs. control TA muscle at a given time point. †*P*<0.05, main effect of CCA relative to control across all conditions.

day 7, where it trended toward an increase of 47% (P=0.2; Fig. 3F). Lastly, the cytosolic HSP70 chaperone was markedly augmented throughout days 1-7 (P<0.05) at the mRNA level with a similar effect of CCA throughout our time-course, specifically reaching as high as 2.5-fold increases at days 2 and 5 (Fig. 3G & H).

Chronic contractile activity elicits the UPR^{mt} concurrent with the UPR^{ER}. To investigate whether the UPR^{mt} plays a coordinated role in mitochondrial adaptations to exercise, we expanded our mRNA and protein analyses to include mitochondrial-specific factors. First, mRNA levels of the mitochondrial protease ClpP, which both senses and responds to unfolded matrix proteins (1, 6, 58), was significantly upregulated by CCA throughout the time-course, particularly reaching a 70% increase by day 2 and maintained a 45% elevation at days 5 and 7 (P<0.05; Fig. 4A). Likewise the mitochondrial regulatory protein SirT3 (45) displayed enhanced protein expression as a result of CCA following 2-7 days reaching elevations of 46% by day 7 (P<0.05; Fig. 4B). Finally, consistent 25-80% elevations in the mRNA levels of mitochondrial chaperones CPN10, HSP60, and mtHSP70 were observed throughout the 7-day contractile activity protocol (P<0.05; Fig. 4C, E, G). This was further reinforced by their changes in protein expression, which exhibited a main effect of CCA across all time points culminating in a 75% enhancement of CPN10 by day 7 specifically (P<0.05; Fig. 4D, F, H).

TUDCA treatment does not impact CCA-induced activation of the UPR^{ER} or UPR^{mt}. TUDCA has previously been shown to be capable of preventing ER stress-associated UPR activation (16, 35, 44). Therefore we wanted to test the impact of the drug on mitochondrial adaptations, since our data illustrate that UPR activation seems to precede organelle remodeling in response to chronic muscle activity. Despite an approximate 50%

Fig. 4

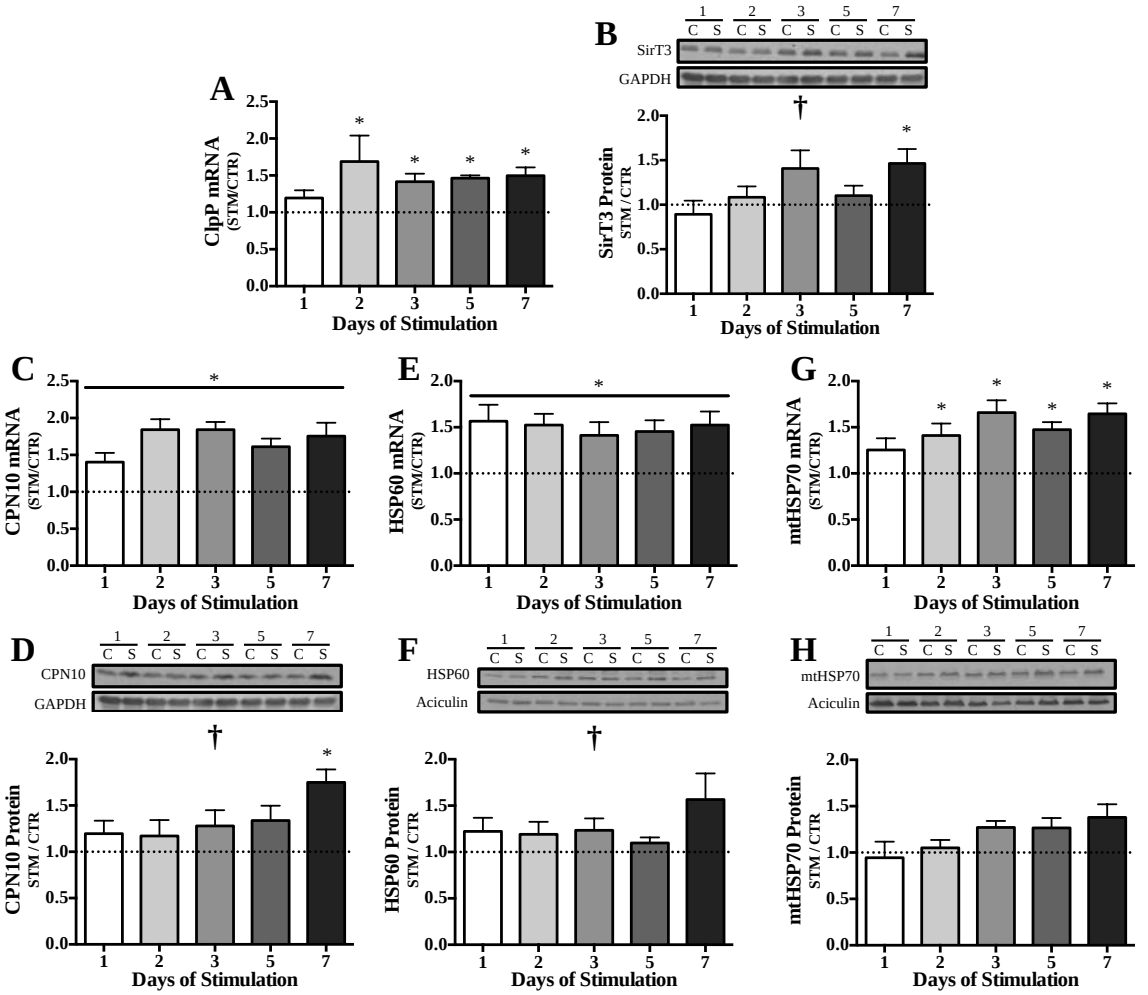

Figure 4: Time-course of the CCA-induced UPR^{mt}. Fold-change in the mRNA levels of **(A)** mitochondrial protease ClpP, and mitochondrial chaperones **(C)** CPN10, **(E)** HSP60, and **(G)** mtHSP70 throughout 7 days of muscle contractile activity (CPN10, n=6; ClpP, HSP60, and mtHSP70,n=8, per day). Coterminous expression of **(B)** the UPR^{mt} regulatory protein SirT3, and chaperone proteins **(D)** CPN10, **(F)** HSP60, and **(H)** mtHSP70 (SirT3, n=8; CPN10, HSP60 and mtHSP70, n=7, per day). Bars represent fold-change in stimulated muscle relative to matched controls; means ± SEM. **P*<0.05, stimulated vs. control TA muscle at a given time point. †*P*<0.05, main effect of CCA relative to control across all conditions.

attenuation ($P<0.05$) in the CCA-induced activation of CHOP protein (Fig. 5A, B), a hallmark of TUDCA activity (44, 57), along with a 31% reduction in the HSP70 adaptation to CCA ($P<0.05$; Fig. 5D, E), we were unable to detect any discernable differences in the expression of other UPR^{ER} targets in vehicle- and TUDCA-treated animals. The principal mechanism of action of TUDCA is in facilitating protein handling and translation (8, 15), therefore it is no surprise that the mRNA expression of both CHOP (Fig. 5C), and HSP70 (Fig. 5F) were significantly enriched following 2 of muscle stimulation in either treatment group. The mRNA of ATF4 (Fig. 5G), XBP1s (Fig. 5H), and BiP (Fig. 5I) was markedly elevated at 2 days in both treatment groups, with levels dropping to equal, or below control following 7 days of CCA ($P<0.05$). In line with our earlier findings, CCA had a significant main effect on the mRNA of mitochondrial chaperones CPN10 (Fig. 6A), and HSP60 (Fig. 6C), and protease ClpP (Fig. 6D) in expression following 2 and 7 days of activity, with no significant difference detected between treatments. Specifically, CPN10 mRNA displayed roughly 60-80% increases ($P<0.05$) across all conditions while HSP60 followed the same trend and displayed a significant increase of 30% in TUDCA-treated animals subjected to 7 days of stimulation ($P<0.05$). Moreover, CPN10 protein increased approximately 20% after 2 days of CCA, and as much as 70% after 7 days, while TUDCA treatment did not have an effect on the level of induction relative to vehicle-treatment ($P<0.05$; Fig. 6B).

TUDCA treatment has no effect on CCA-induced mitochondrial biogenesis or autophagy. We assessed changes in mitochondrial content through COX enzyme activity in animals treated with either vehicle or TUDCA, and subjected to either 2 or 7 days of CCA. Consistent with our earlier results, we observed 22% and 24% increases in

Fig. 5

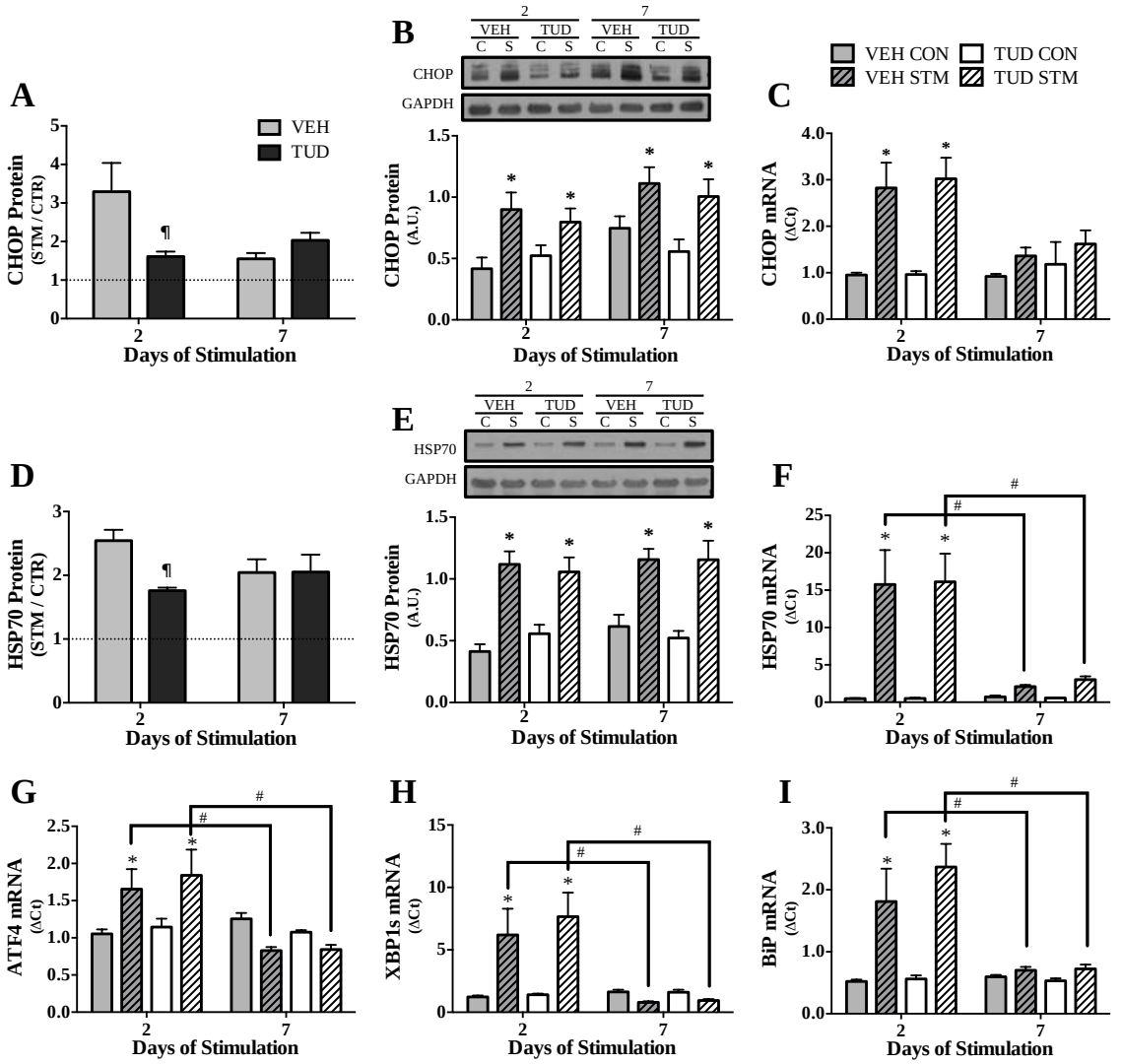

Figure 5. Effect of TUDCA on the CCA-induced UPR^{ER}. (A) CHOP protein expression represented as fold-change, and **(B)** relative control vs stimulated levels, for a given day/treatment. **(D)** HSP70 protein expressed as fold-change, and as **(E)** relative control vs. stimulated levels for a given day/treatment (CHOP, and HSP70, n=7, per day/condition). Relative mRNA levels of UPR^{ER} markers **(C)** CHOP, **(F)** HSP70, **(G)** ATF4, **(H)** XBP1s, and **(I)** BiP, in control and stimulated muscle of vehicle-, and TUDCA-treated animals subject to 2 or 7 days of muscle stimulation (ATF4, XBP1s, BiP, CHOP, and HSP70, n=8, per day/treatment). For mRNA and protein graphs, open grey, and open white bars represent control muscle in vehicle-, and TUDCA-treated animals, respectively; hatched grey, and hatched white bars represent stimulated muscle in vehicle-, and TUDCA-treated animals, respectively. For fold-change graphs of CHOP and HSP70 protein expression, grey, and black, bars represent vehicle-, and TUDCA-treated animals, respectively, expressed as fold-change in stimulated muscle relative to matched control. Values represent means ± SEM. **P*<0.05, stimulated vs. control TA muscle at a given time point and treatment. *#P*<0.05, 2 days stimulated vs. 7 days stimulated for the same drug treatment. ¶*P*<0.05, TUDCA vs. vehicle for a given time point.

Fig. 6

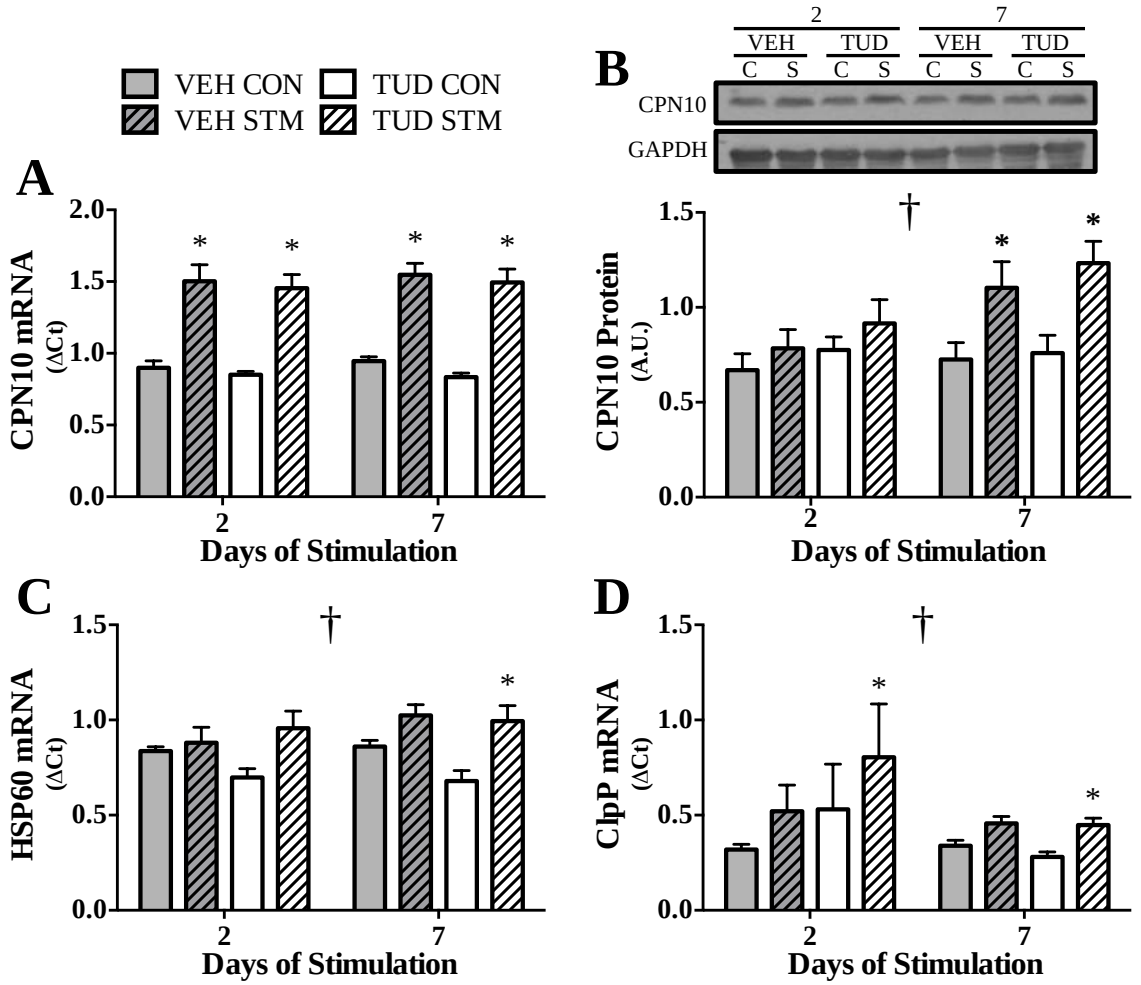

Figure 6. Effect of TUDCA on the CCA-induced UPR^{mt}. Relative transcript levels of mitochondrial chaperones **(A)** CPN10 and **(C)** HSP60, as well as the protease **(D)** ClpP in control and stimulated muscle of vehicle-, and TUDCA-treated animals following 2 or 7 days of contractile activity (CPN10, and ClpP, n=8; HSP60, n=6 per day/treatment). **(B)** Corresponding protein expression of CPN10 (CPN10, n=8, per day/treatment). Open grey, and open white bars represent control muscle in vehicle-, and TUDCA-treated animals, respectively; hatched grey, and hatched white bars represent stimulated muscle in vehicle-, and TUDCA-treated animals, respectively. Values represent means ± SEM. *P<0.05, stimulated vs. control TA muscle at a given time point and treatment. †P<0.05, main effect of CCA relative to control across all conditions.

mitochondria with 7 days of contractile activity in vehicle-, and TUDCA-treated animals, respectively ($P<0.05$; Fig. 7A). Likewise, PGC-1α mRNA expression was significantly increased 6.6-8.4-fold in both treatment groups stimulated for 2 or 7 days, with no difference in mRNA induction observed as a result of drug administration (Fig. 7B). To reinforce these data, we measured the protein expression of Uqcrc2 and found similar 1.7-2-fold increases in the stimulated leg relative to control across all groups as CCA exhibited a main effect in all conditions ($P<0.05$; Fig. 7C). Akin to our earlier findings, p62 mRNA exhibited a significant increase of approximately 1.7-fold after 2 days of stimulation in animals administered the drug (Fig. 8A). These trends in p62 were also evident at the protein level at 2 days in vehicle-, and TUDCA-treated animals, respectively ($P<0.05$; Fig. 8C), and were completely attenuated after 7 days of CCA. LC3 mRNA and protein levels displayed no change in any condition/time point (Fig. 8B, D).

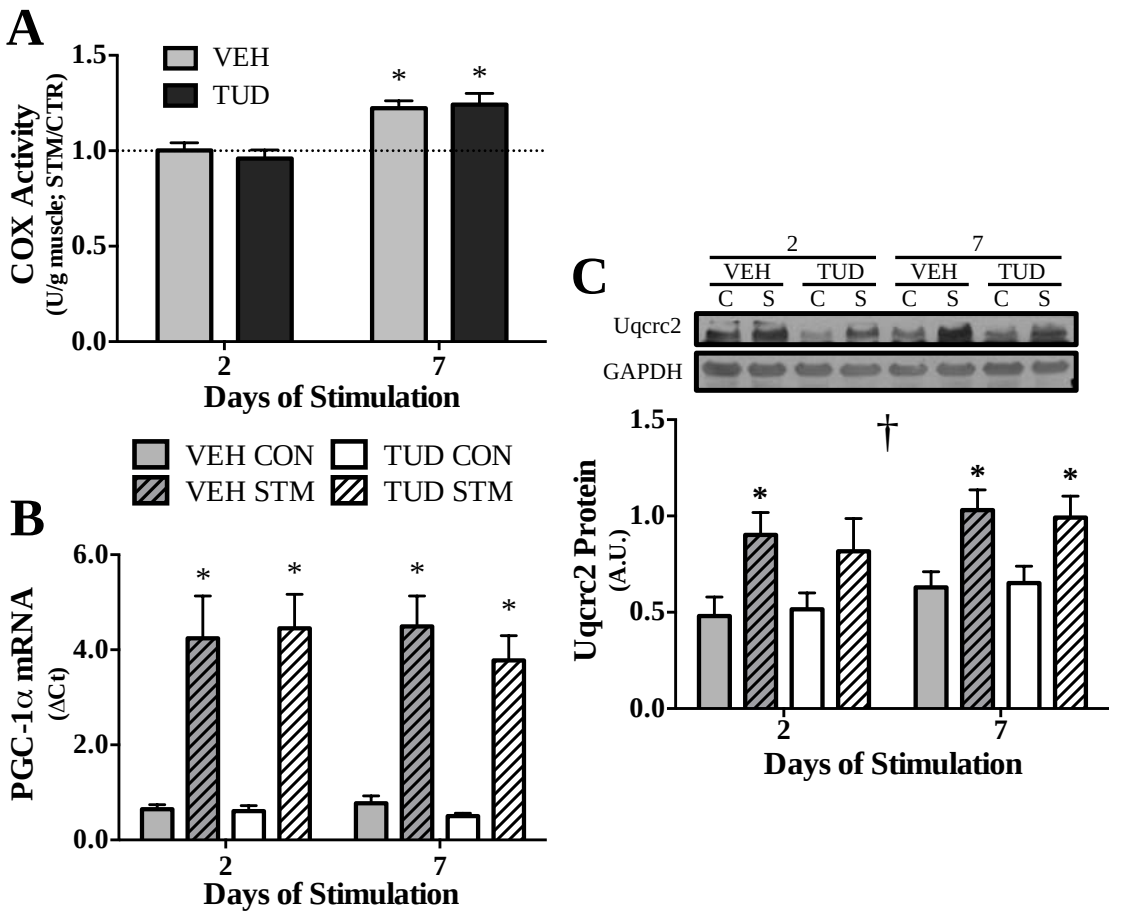

Figure 7. Effect of TUDCA treatment on CCA-induced mitochondrial content and biogenesis. (A) Relative changes in mitochondrial content observed via COX activity (n=8, per day/treatment) following 2 and 7 days of CCA in both vehicle-, and TUDCA-treated rats. **(B)** Coactivator of mitochondrial biogenesis PGC-1α mRNA levels (n=8, per day/condition) and **(C)** protein expression of nuclear-encoded complex III subunit 2, Uqcrc2 (n=7, per day/condition). For the COX activity graph, grey, and black, bars represent vehicle-, and TUDCA-treated animals, respectively, expressed as fold-change in stimulated muscle relative to matched control. For mRNA and protein graphs, open grey, and open white bars represent control muscle in vehicle-, and TUDCA-treated animals, respectively; hatched grey, and hatched white bars represent stimulated muscle in vehicle-, and TUDCA-treated animals, respectively. Values represent means ± SEM. **P*<0.05, stimulated vs. control TA muscle at a given time point and treatment. †*P*<0.05, main effect of CCA relative to control across all conditions.

Fig. 8

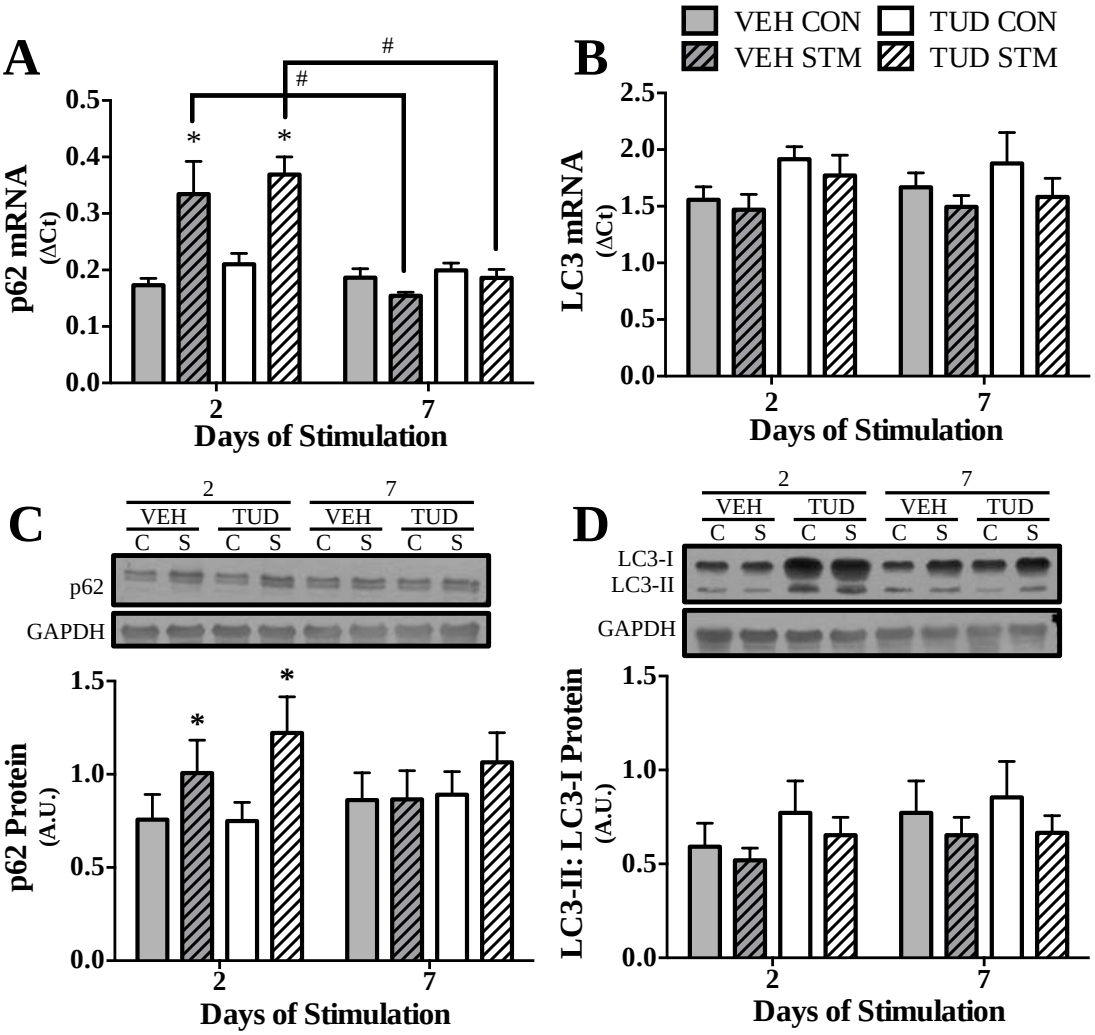

Figure 8. Effect of TUDCA on CCA-induced autophagy induction. Relative mRNA expression of **(A)** p62 and **(B)** LC3 in vehicle-, and TUDCA-treated animals following either 2 or 7 days of CCA (p62, n=6; LC3, n=7, per day/treatment). Corresponding protein levels in **(C)** p62, and **(D)** ratio of lipidated LC3-II to inactive LC3-I (p62, n=7; LC3-II:I, n=8). Open grey, and open white bars represent control muscle in vehicle-, and TUDCA-treated animals, respectively; hatched grey, and hatched white bars represent stimulated muscle in vehicle-, and TUDCA-treated animals, respectively. Values represent means ± SEM. **P*<0.05, stimulated vs. control TA muscle at a given time point and treatment. #*P*<0.05, 2 days stimulated vs. 7 days stimulated for the same drug treatment.

DISCUSSION

Skeletal muscle accounts for a majority of the body mass, and thus is an important determinant of metabolic status and overall health (14, 27). Exercise has been studied for its ability to produce adaptations in skeletal muscle to achieve greater oxidative capacity as a byproduct of enhanced mitochondrial volume. However, the mechanism by which muscle achieves this new phenotype has yet to be fully resolved. Recently, the unfolded protein response (UPR) has been implicated in exercise, which suggests that it plays a role in sensing and initiating adaptive responses (31, 32, 41, 61). In this study, we set out to analyze the signaling events that facilitate skeletal muscle adaptations to exercise over a 7-day time-course of repeated bouts of contractile activity, employing a chronic contractile activity (CCA) model of exercise (33, 56).

CCA over the course of 7 days established an enhanced mitochondrial pool, corroborating previous work from our laboratory using this protocol (13, 18, 42, 56). Our observed increase in COX activity of 30% by day 7 is similar to the level of adaptation achieved with 6 weeks of regular endurance training (23), indicating that our 7-day protocol of chronic stimulation provides us with a useful time-course of the signaling responses as they contribute to a new muscle phenotype. Of particular note, mitochondrial biogenesis-specific signaling, indicated by increased PGC-1α mRNA, was markedly induced following a single bout of CCA. However, this induction did not manifest into detectable increases in mitochondrial content until day 3. Therefore, this 3-day window of signaling preceding adaptation is of particular interest, since PGC-1α plays a fundamental role in regulating transcriptional activity of a host of nuclear-encoded mitochondrial proteins integral to organelle biosynthesis (34). While it is known

that PGC-1α regulates mitochondrial content, only recently has it been suggested that it might also have a more functional role in balancing other adaptive responses such as autophagy, and the UPR through interaction with ATF6 (59–61).

When considering the beneficial adaptations to exercise, it is important to acknowledge the balance between mitochondrial biogenesis and autophagy in effectively maintaining a healthy organelle pool (22, 60). Autophagy is gaining recognition for its role in maintaining cell quality and viability beyond simply degradation (10). Evidence suggests that lack of adequate autophagy results in muscle degeneration, wasting, and reduced strength, as well as the accumulation of protein aggregates and dysfunctional organelles contributing to excessive oxidative stress (10, 19, 36, 37). Our data reinforce the notion of autophagy as a quality control mechanism in muscle adaptation, as we detected concomitant changes in autophagy markers from days 3-7 following CCA, matching the timing of the increases we observed in mitochondrial content. Specifically, the enhanced mRNA expression of p62 at day 2, followed by elevated protein at day 3 suggests an increase in transcriptional drive to enhance the level of this adapter protein in readiness for autophagy. Consistent with this, we detected a reduction of LC3-II: LC3-I protein levels from days 3-7, as well as a return to control values by day 5 in p62 protein, indicating the subsequent degradation of these autophagosomal components as they are decomposed by the lysosome.

Given these observations, we proposed that an intermediate response could modulate, and coordinate, the balance between synthesis and degradation. In particular, we focused on the UPR^{ER}, and the UPR^{mt}, as they have been implicated in mitochondrial adaptations (9, 38, 47, 54), and autophagy (5, 40, 45) in the presence of cellular stress.

We hypothesized that the drive for nuclear-encoded mitochondrial proteins through enhanced PGC-1α signaling may perturb the protein environment within the cell, and therefore, that the UPR would be integral to exercise-induced mitochondrial remodeling. Our observations indicate that the UPR responds to the CCA stimulus acutely, and persists to provide a level of adaptation to chronic stimulation. The UPR^{ER} transcription factors, ATF4 and XBP1s, were significantly induced from 1-3 days of CCA, preceding changes in mitochondria and autophagy, thus providing an early signaling response. Likewise, the transcription factor CHOP, which regulates cell fate by monitoring cellular stress (4), displayed marked elevations in both mRNA and protein throughout 1-7 days of CCA, implying a role for the protein in shifting from acute signaling, to chronic adaptations. The mRNA and protein expression changes of the ER and cytosolic chaperones BiP and HSP70 substantiate CHOP data, as they were also induced from 1-7 days in response to CCA. Altogether, our results provide the first time-course relationship of UPR signaling over a period of progressive adaptation in skeletal muscle mitochondria, through exercise.

Another unique finding of our study was the parallel contractile activity-induced responses observed in both the UPR^{ER} and the UPR^{mt} in skeletal muscle. To date, far less emphasis has been placed on the UPR^{mt}, particularly in mammalian cells. Nonetheless, we were interested in this response, as it pertains directly to the protein folding capacity within mitochondria (11, 38). Our laboratory has previously found that mitochondrial-specific chaperones are induced as an adaptive response to 7 days of CCA (42). Our current data confirm these results and suggest that, similar to the time-course of the UPR^{ER}, mitochondrial factors are induced immediately following a single bout of CCA,

and remain elevated throughout repeated contractile episodes. This further establishes the phasic nature of the UPR in providing rapid and adaptive protein handling relief within multiple subcellular compartments upon alterations in exercise-induced changes in proteostasis.

Our results suggest that the UPR signaling is initiated early in the CCA protocol and precedes mitochondrial adaptations and cellular remodeling, and therefore may play a direct role in initiating and/or facilitating these events. As such, we utilized the chaperone mimetic drug TUDCA, a naturally occurring bile acid produced at low levels in the liver which is used in the treatment of various ER stress-associated diseases (2, 17, 44). The effectiveness in TUDCA treatment is predominantly through augmenting protein handling, and by suppressing CHOP-, and caspase-12-mediated apoptosis during chronic ER stress (16, 35, 44, 57, 62). We found that TUDCA treatment was able to sufficiently attenuate the increase in CHOP protein expression after 2 days of CCA, and provided a similar reduction in HSP70 levels. Despite this, mRNA levels of both CHOP and HSP70 were unaffected by drug treatment, which corroborates the proposed mechanism of TUDCA action on protein handling and translation (8, 15). TUDCA also had no effect on the mRNA expression of UPR^{ER} transcription factors ATF4 and activated XBP1s, as well as the ER chaperone BiP, which all displayed similar increases in response to CCA in TUDCA-, and vehicle-treated animals. Since TUDCA facilitates protein handling, we next investigated the potential effect that it could have on the activation of the UPR^{mt}. However, no effects on the signaling of mitochondrial protein quality control machinery ClpP, HSP60, and CPN10 were observed, indicating that the UPR^{mt} responds separately from the UPR^{ER}.

While various UPR targets were still induced in response to CCA in the presence of TUDCA treatment, we wanted to investigate whether the attenuation in CHOP protein could affect the outcome of mitochondrial remodeling. CHOP has been implicated as a regulator of cell fate during chronic stress (4), as well as in exercise-induced apoptosis (61), indicating that it is capable of monitoring the intensity and duration of cellular stress, and provide signaling towards either remodeling (autophagy) or degradation (apoptosis). Despite effective attenuation of the CCA-induced CHOP expression by TUDCA, we observed no changes in mitochondrial content measured by COX enzyme activity and protein expression of the nuclear-encoded mitochondrial complex III subunit, Uqcrc2. Likewise, mitochondrial biogenesis signaling was unaffected, as PGC-1α mRNA was considerably induced across all conditions. We also found that autophagy was unaffected by TUDCA treatment, despite the reduced activation of CHOP, as p62 and LC3 responded similarly to our initial time-course findings.

A limiting factor in the application of TUDCA treatment is the lack of specificity in inhibiting the three main branches/factors of the UPR. Instead, TUDCA helps modulate protein handling within the cell to reduce the burden on the ER to prevent enhanced UPR activation, and subsequent apoptosis. Therefore, specifically knocking out upstream UPR factors would be worthy of pursuit in the context of exercise adaptations. However, given the usefulness of TUDCA in diminishing CHOP protein increases, we were able to analyze the role that CHOP has on CCA-induced adaptations in mitochondrial content, and autophagy as a process of cellular quality control. Our findings suggest that the potential UPR^{ER} regulation of mitochondrial biogenesis acts independently of CHOP in our CCA model of exercise. However, this does not exclude

the possibility that another UPR^{ER}-associated factor could influence this process. Specifically, ATF6 has been implicated in PGC-1α signaling (61), however we were unable to observe any notable changes in ATF6 as a result of CCA in our study (data not shown), possibly as a result of the transient nature of UPR activation. Future work to examine a time-course of UPR signaling following acute exercise would be useful to best elucidate which factors are the primary responders. The same study linking ATF6 and PGC-1α found that CHOP ablation partially rescued the exercise intolerance of muscle-specific PGC-1α knockout mice. Our data suggest that CHOP attenuation had no impact, positive or negative, on the mitochondrial or autophagic adaptations to contractile activity. It is important to note that the CCA stimulus is low frequency (10Hz) stimulation localized to the tibialis anterior and extensor digitorum longus muscles, rather than whole body, maximal exercise. In studies of whole body exercise, it has recently been observed that the UPR is sensitive to exercise intensity, as the higher the intensity, or novelty, of the stimulus the greater the response (32, 41). We confirmed this trend, as UPR^{ER} transcription factor mRNAs returned to control levels by 5 days concomitant with enhanced protein handling ability and mitochondrial content. Therefore, future research avenues could investigate the effect that TUDCA has on adaptations during an enhanced CCA stimulus, either in duration or intensity to elicit a more stressful condition in the muscle and possibly inducing an increased reliance on CHOP activation. Conversely, inducing ER stress in order to activate the UPR prior to an exercise protocol could further demonstrate its functional role in adaptation. As it is clear that the UPR is involved in some capacity in exercise-induced remodeling, elucidating the specific mechanism of action will be of particular interest as it relates to whole body metabolic health.

ACKNOWLEDGEMENTS

This work was supported by funding from the Natural Sciences and Engineering Research Council of Canada (NSERC) to D. A. Hood. D. A. Hood is also the holder of a Canada Research Chair in Cell Physiology. J.M. Memme was a recipient of NSERC – Canada Graduate Scholarship.

REFERENCES

1. **Al-furoukh N**, **Ianni A**, **Nolte H**, **Hölper S**, **Krüger M**. ClpX stimulates the mitochondrial unfolded protein response (UPR) in mammalian cells. *Biochim Biophys Acta* 1853: 2015, 2015.

2. **Amaral JD**, **Viana RJS**, **Ramalho RM**, **Steer CJ**, **Rodrigues CMP**. Bile acids: regulation of apoptosis by ursodeoxycholic acid. *J Lipid Res* 50: 1721–1734, 2009.

3. **Anderson S**, **Bankier AT**, **Barrell BG**, **de Bruijn MH**, **Coulson AR**, **Drouin J**, **Eperon IC**, **Nierlich DP**, **Roe BA**, **Sanger F**, **Schreier PH**, **Smith AJ**, **Staden R**, **Young IG**. Sequence and organization of the human mitochondrial genome. *Nature* 290: 457–465, 1981.

4. **B'chir W**, **Chaveroux C**, **Carraro V**, **Averous J**, **Maurin AC**, **Jousse C**, **Muranishi Y**, **Parry L**, **Fafournoux P**, **Bruhat A**. Dual role for CHOP in the crosstalk between autophagy and apoptosis to determine cell fate in response to amino acid deprivation. *Cell Signal* 26: 1385–1391, 2014.

5. **B'chir W**, **Maurin A-C**, **Carraro V**, **Averous J**, **Jousse C**, **Muranishi Y**, **Parry L**, **Stepien G**, **Fafournoux P**, **Bruhat A**. The eIF2 /ATF4 pathway is essential for stress-induced autophagy gene expression. *Nucleic Acids Res* 41: 7683–7699, 2013.

6. **Baker BM**, **Haynes CM**. Mitochondrial protein quality control during biogenesis and aging. *Trends Biochem Sci* 36: 254–261, 2011.

7. **Belkin AM**, **Klimanskaya I V**, **Lukashev ME**, **Lilley K**, **Critchley DR**, **Koteliansky VE**. A novel phosphoglucomutase-related protein is concentrated in adherens junctions of muscle and nonmuscle cells. *J Cell Sci* 107: 159–173, 1994.

8. **Berger E**, **Haller D**. Structure-function analysis of the tertiary bile acid TUDCA for the resolution of endoplasmic reticulum stress in intestinal epithelial cells. *Biochem Biophys Res Commun* 409: 610–5, 2011.

9. **de Brito OM**, **Scorrano L**. Mitofusin 2 tethers endoplasmic reticulum to mitochondria. *Nature* 456: 605–610, 2008.

10. **Cecconi F**, **Levine B**. The Role of Autophagy in Mammalian Development: Cell Makeover Rather than Cell Death. *Dev Cell* 15: 344–357, 2008.

11. **Cerutti R**, **Pirinen E**, **Lamperti C**, **Marchet S**, **Sauve AA**, **Li W**, **Leoni V**, **Schon EA**, **Dantzer F**, **Auwerx J**, **Viscomi C**, **Zeviani M**. NAD+-Dependent Activation of Sirt1 Corrects the Phenotype in a Mouse Model of Mitochondrial Disease. *Cell Metab* 19: 1042–1049, 2014.

12. **Fan ACY**, **Bhangoo MK**, **Young JC**. Hsp90 Functions in the Targeting and Outer Membrane Translocation Steps of Tom70-mediated Mitochondrial Import. *J Biol Chem* 281: 33313–33324, 2006.

13. **Freyssenet D**, **Connor MK**, **Takahashi M**, **Hood DA**. Cytochrome c transcriptional activation and mRNA stability during contractile activity in skeletal muscle. *Am J Physiol Endocrinol Metab* 277: E26–32, 1999.

14. **Frontera WR**, **Ochala J**. Skeletal Muscle: A Brief Review of Structure and Function. *Calcif Tissue Int* 96: 183–195, 2015.

15. **Gani AR**, **Uppala JK**, **Ramaiah KVA**. Tauroursodeoxycholic acid prevents stress induced aggregation of proteins in vitro and promotes PERK activation in HepG2 cells. *Arch Biochem Biophys* 568: 8–15, 2015.

16. **Gao X**, **Fu L**, **Xiao M**, **Xu C**, **Sun L**, **Zhang T**, **Zheng F**, **Mei C**. The Nephroprotective Effect of Tauroursodeoxycholic Acid on Ischaemia/Reperfusion-Induced Acute Kidney Injury by Inhibiting Endoplasmic Reticulum Stress. *Basic Clin Pharmacol Toxicol* 111: 14–23, 2012.

17. **Gaspar JM**, **Martins A**, **Cruz R**, **Rodrigues CMP**, **Ambrósio AF**, **Santiago AR**. Tauroursodeoxycholic acid protects retinal neural cells from cell death induced by prolonged exposure to elevated glucose. *Neuroscience* 253: 380–389, 2013.

18. **Gordon JW**, **Rungi AA**, **Inagaki H**, **Hood DA**. Effects of contractile activity on mitochondrial transcription factor A expression in skeletal muscle. *J Appl Physiol* 90: 389–396, 2001.

19. **Grumati P**, **Bonaldo P**. Autophagy in Skeletal Muscle Homeostasis and in Muscular Dystrophies. *Cells* 1: 325–345, 2012.

20. **Handschin C**, **Spiegelman BM**. Peroxisome Proliferator-Activated Receptor γ Coactivator 1 Coactivators, Energy Homeostasis, and Metabolism. *Endocr Rev* 27: 728–735, 2006.

21. **Haynes CM**, **Ron D**. The mitochondrial UPR - protecting organelle protein homeostasis. *J Cell Sci* 123: 3849–55, 2010.

22. **He C**, **Bassik MC**, **Moresi V**, **Sun K**, **Wei Y**, **Zou Z**, **An Z**, **Loh J**, **Fisher J**, **Sun Q**, **Korsmeyer S**, **Packer M**, **May HI**, **Hill JA**, **Virgin HW**, **Gilpin C**, **Xiao G**, **Bassel-Duby R**, **Scherer PE**, **Levine B**. Exercise-induced BCL2-regulated autophagy is required for muscle glucose homeostasis. *Nature* 481: 511–515, 2012.

23. **Henriksson J**, **Reitman JS**. Time course of changes in human skeletal muscle succinate dehydrogenase and cytochrome oxidase activities and maximal oxygen uptake with physical activity and inactivity. *Acta Physiol Scand* 99: 91–97, 1977.

24. **Hock MB**, **Kralli A**. Transcriptional control of mitochondrial biogenesis and function. *Annu Rev Physiol* 71: 177–203, 2009.

25. **Hood DA**, **Adhihetty PJ**, **Colavecchia M**, **Gordon JW**, **Irrcher I**, **Joseph A-M**, **Lowe ST**, **Rungi AA**. Mitochondrial biogenesis and the role of the protein import pathway. *Med Sci Sports Exerc* 35: 86–94, 2003.

26. **Hood DA**, **Zak R**, **Pette D**. Chronic stimulation of rat skeletal muscle induces coordinate increases in mitochondrial and nuclear mRNAs of cytochrome-c-oxidase subunits. *Eur J Biochem* 179: 275–280, 1989.

27. **Hood DA**. Invited Review: Contractile activity-induced mitochondrial biogenesis in skeletal muscle. *J Appl Physiol* 90: 1137–1157, 2001.

28. **Irrcher I**, **Adhihetty PJ**, **Joseph A-M**, **Ljubicic V**, **Hood DA**. Regulation of mitochondrial biogenesis in muscle by endurance exercise. *Sports Med* 33: 783–93, 2003.

29. **Jäger R**, **Bertrand MJM**, **Gorman AM**, **Vandenabeele P**, **Samali A**. The unfolded protein response at the crossroads of cellular life and death during endoplasmic reticulum stress. *Biol Cell* 104: 259–70, 2012.

30. **Joseph A-M**, **Hood DA**. Plasticity of TOM complex assembly in skeletal muscle mitochondria in response to chronic contractile activity. *Mitochondrion* 12: 305–12, 2012.

31. **Kim HJ**, **Jamart C**, **Deldicque L**, **An G**, **Lee YH**, **Kim CK**, **Raymackers J**, **Francaux M**. Endoplasmic reticulum stress markers and ubiquitin–proteasome pathway activity in response to a 200-km run. *Med Sci Sports Exerc* 43: 18–25, 2011.

32. **Kim K**, **Kim Y-H**, **Lee S-H**, **Jeon M-J**, **Park S-Y**, **Doh K-O**. Effect of exercise intensity on unfolded protein response in skeletal muscle of rat. *Korean J Physiol Pharmacol* 18: 211–6, 2014.

33. **Ljubicic V**, **Adhihetty PJ**, **Hood DA**. Application of Animal Models: Chronic Electrical Stimulation-Induced Contractile Activity. *Can J Appl Physiol* 30: 625–643, 2005.

34. **Ljubicic V**, **Joseph A-M**, **Saleem A**, **Uguccioni G**, **Collu-Marchese M**, **Lai RYJ**, **Nguyen LM-D**, **Hood DA**. Transcriptional and post-transcriptional regulation of mitochondrial biogenesis in skeletal muscle: Effects of exercise and aging. *Biochim Biophys Acta - Gen Subj* 1800: 223–234, 2010.

35. **Malo A**, **Krüger B**, **Seyhun E**, **Schäfer C**, **Hoffmann RT**, **Göke B**, **Kubisch CH**. Tauroursodeoxycholic acid reduces endoplasmic reticulum stress , trypsin activation , and acinar cell apoptosis while increasing secretion in rat pancreatic acini. *Am J Physiol - Gastrointest Liver Physiol* 299: G877–G886, 2010.

36. **Masiero E**, **Agatea L**, **Mammucari C**, **Blaauw B**, **Loro E**, **Komatsu M**, **Metzger D**, **Reggiani C**, **Schiaffino S**, **Sandri M**. Autophagy is required to maintain muscle mass. *Cell Metab* 10: 507–515, 2009.

37. **Masiero E**, **Sandri M**. Autophagy inhibition induces atrophy and myopathy in adult skeletal muscles. *Autophagy* 6: 307–309, 2014.

38. **Mouchiroud L**, **Houtkooper RH**, **Moullan N**, **Katsyuba E**, **Ryu D**, **Canto C**, **Mottis A**, **Jo YS**, **Viswanathan M**, **Schoonjans K**, **Guarente L**, **Auwerx J**. The NAD(+)/Sirtuin Pathway Modulates Longevity through Activation of Mitochondrial UPR and FOXO Signaling. *Cell* 154: 430–441, 2013.

39. **O'Leary MFN**, **Hood DA**. Effect of prior chronic contractile activity on mitochondrial function and apoptotic protein expression in denervated muscle. *J Appl Physiol* 105: 114–20, 2008.

40. **Ogata M**, **Hino S**, **Saito A**, **Morikawa K**, **Kondo S**, **Kanemoto S**, **Murakami T**, **Taniguchi M**, **Tanii I**, **Yoshinaga K**, **Shiosaka S**, **Hammarback JA**, **Urano F**, **Imaizumi K**. Autophagy is activated for cell survival after endoplasmic reticulum stress. *Mol Cell Biol* 26: 9220–31, 2006.

41. **Ogborn DI**, **McKay BR**, **Crane JD**, **Parise G**, **Tarnopolsky MA**. The unfolded protein response is triggered following a single, unaccustomed resistance-exercise bout. *Am J Physiol Regul Integr Comp Physiol* 307: R664–9, 2014.

42. **Ornatsky OI**, **Connor MK**, **Hood DA**. Expression of stress proteins and mitochondrial chaperonins in chronically stimulated skeletal muscle. *Biochem J* 311 (Pt 1: 119–23, 1995.

43. **Ostojic O**, **O'Leary MFN**, **Singh K**, **Menzies KJ**, **Vainshtein A**, **Hood DA**. The effects of chronic muscle use and disuse on cardiolipin metabolism. *J Appl Physiol* 114: 444–52, 2013.

44. **Ozcan U**, **Yilmaz E**, **Ozcan L**, **Furuhashi M**, **Vaillancourt E**, **Smith RO**, **Görgün CZ**, **Hotamisligil GS**. Chemical chaperones reduce ER stress and restore glucose homeostasis in a mouse model of type 2 diabetes. *Science* 313: 1137–1140, 2006.

45. **Papa L**, **Germain D**. SirT3 regulates the mitochondrial unfolded protein response. *Mol Cell Biol* 34: 699–710, 2014.

46. **Pellegrino MW**, **Nargund AM**, **Haynes CM**. Signaling the mitochondrial unfolded protein response. *Biochim Biophys Acta* 1833: 410–6, 2013.

47. **Rainbolt TK**, **Saunders JM**, **Wiseman RL**. Stress-responsive regulation of mitochondria through the ER unfolded protein response. *Trends Endocrinol. Metab.* (July 2014). doi: 10.1016/j.tem.2014.06.007.

48. **Ron D**, **Walter P**. Signal integration in the endoplasmic reticulum unfolded protein response. *Nat Rev Mol Cell Biol* 8: 519–529, 2007.

49. **Sanchez AM**, **Bernardi H**, **Py G**, **Candau R**. Autophagy is essential to support skeletal muscle plasticity in response to endurance exercise. *Am. J. Physiol. Regul. Integr. Comp. Physiol.* (August 13, 2014). doi: 10.1152/ajpregu.00187.2014.

50. **Scarpulla RC**, **Vega RB**, **Kelly DP**. Transcriptional integration of mitochondrial biogenesis. *Trends Endocrinol Metab* 23: 459–466, 2012.

51. **Scarpulla RC**. Transcriptional Paradigms in Mammalian Mitochondrial Biogenesis and Function. (2008). doi: 10.1152/physrev.00025.2007.

52. **Scarpulla RC**. Metabolic control of mitochondrial biogenesis through the PGC-1 family regulatory network. *Biochim Biophys Acta* 1813: 1269–78, 2011.

53. **Schröder M**, **Kaufman RJ**. ER stress and the unfolded protein response. *Mutat Res* 569: 29–63, 2005.

54. **Senft D**, **Ronai ZA**. UPR, autophagy, and mitochondria crosstalk underlies the ER stress response. *Trends Biochem Sci* 40: 141–148, 2015.

55. **Shao M**, **Shan B**, **Liu Y**, **Deng Y**, **Yan C**, **Wu Y**, **Mao T**, **Qiu Y**, **Zhou Y**, **Jiang S**, **Jia W**, **Li J**, **Li J**, **Rui L**, **Yang L**, **Liu Y**. Hepatic IRE1α regulates fasting-induced metabolic adaptive programs through the XBP1s-PPARα axis signalling. *Nat Commun* 5: 3528, 2014.

56. **Takahashi M**, **Hood DA**. Chronic stimulation-induced changes in mitochondria and performance in rat skeletal muscle. *J Appl Physiol* 74: 934–941, 1993.

57. **Tanaka Y**, **Ishitsuka Y**, **Hayasaka M**, **Yamada Y**, **Miyata K**, **Endo M**, **Kondo Y**, **Moriuchi H**, **Irikura M**, **Tanaka K-I**, **Mizushima T**, **Oike Y**, **Irie T**. The exacerbating roles of CCAAT/enhancer-binding protein homologous protein (CHOP) in the development of bleomycin-induced pulmonary fibrosis and the preventive effects of tauroursodeoxycholic acid (TUDCA) against pulmonary fibrosis in mice. *Pharmacol Res* 99: 52–62, 2015.

58. **Tatsuta T**, **Langer T**. Quality control of mitochondria: protection against neurodegeneration and ageing. *EMBO J* 27: 306–314, 2008.

59. **Vainshtein A**, **Desjardins EM**, **Armani A**, **Sandri M**, **Hood DA**. PGC-1α modulates denervation-induced mitophagy in skeletal muscle. *Skelet Muscle* 5: 9, 2015.

60. **Vainshtein A**, **Tryon LD**, **Pauly M**, **Hood DA**. Role of PGC-1α during acute exercise-induced autophagy and mitophagy in skeletal muscle. *Am J Physiol - Cell Physiol* 308: C710–C719, 2015.

61. **Wu J**, **Ruas JL**, **Estall JL**, **Rasbach KA**, **Choi JH**, **Ye L**, **Boström P**, **Tyra HM**, **Crawford RW**, **Campbell KP**, **Rutkowski DT**, **Kaufman RJ**, **Spiegelman BM**. The unfolded protein response mediates adaptation to exercise in skeletal muscle through a PGC-1α/ATF6α complex. *Cell Metab* 13: 160–9, 2011.

62. **Xie Q**, **Khaoustov VI**, **Chung CC**, **Sohn J**, **Krishnan B**, **Lewis DE**, **Yoffe B**. Effect of tauroursodeoxycholic acid on endoplasmic reticulum stress-induced caspase-12 activation. *Hepatology* 36: 592–601, 2002.

63. **Young JC**, **Hoogenraad NJ**, **Hartl FU**. Molecular Chaperones Hsp90 and Hsp70 Deliver Preproteins to the Mitochondrial Import Receptor Tom70. *Cell* 112: 41–50, 2003.

FUTURE WORK

1. Our data indicate that the UPR^{ER} and the UPR^{mt} are involved in exercise-induced adaptations as both responses were induced from 1-7 days of CCA, and are capable of providing acute and chronic protein handling relief in the form of enhanced chaperones and proteases. However the specific mechanism that the UPR plays in exercise adaptations remains incompletely understood. We utilized TUDCA treatment as a global blockade of UPR activation through reduced ER stress, which was unable to diminish the activation of multiple UPR transcripts. However, the attenuated increase in CHOP had no effect in level of adaptation observed compared to vehicle-treated animals. With this considered, a potential avenue of future research would be to inhibit various downstream and upstream effectors of the UPR. Recently it has been found that ATF6 is coactivated by PGC-1α to help mediate adaptation, therefore this could provide a useful knockout target, likewise other transcription factors such as ATF4 or XBP1 could provide meaningful avenues of pursuit in the context of mitochondrial adaptations to exercise.
2. In contrast to knocking out UPR factors, future work could take the opposite approach of transgenic/knock-in models in order to induce a heightened UPR activation. This would provide us the ability to observe whether a greater level of adaptation can be achieved. Furthermore, ER stress can be induced prior to a training program by administering potent ER stressors such as thapsigargin or tunicamycin, in order to elicit an early UPR^{ER} to similarly observe any impact this would have on the level of adaptation as the muscle is presumably more inclined to match the rates of protein synthesis.

3. Given the transient nature of the UPR and the dependence on kinase phosphorylation, it remains possible that our sampling of tissue 3 hours following the final bout of contractile activity was outside of the optimal window of UPR activation/signaling. We had difficulty obtaining consistent western blot results in phospho-proteins as well as ATF6 induction. Therefore, it would be equally useful to examine the acute signaling that takes place following a single bout of muscle stimulation by sampling over a time-course of 0, 3, 6, 12, and 24 hours after cessation of muscle contraction. In this way, we can elucidate the primary responders associated with UPR activation.
4. Our study investigated the UPR^{ER} and the UPR^{mt} by separately sampling the specific effectors of either pathway. It would be of benefit to observe the level of coordination of the two pathways by disturbing nuclear- and mitochondrial-derived protein incorporation into the mitochondrion. One way in which to accomplish this is by blocking import of nuclear transcribed proteins. This will ultimately create a backlog of proteins in multiple subcellular compartments and could provide some indication of the level of independence/integration of these signaling pathways. Particularly, studying this coordination within mammalian systems would be of special relevance given the lack of available literature.
5. Our model of CCA has two distinct advantages: 1) stimulation of the peroneal nerve recruits all motor units that are innervated downstream, and 2) the level of intensity of stimulation mimics that found in slow-twitch type I motor units. Therefore it is possible that the adaptation we observe in our model is principally found in the glycolytic fast-twitch muscle fibers, which are less accustomed to exercise, while

having a minor effect in type I fibers. A potential avenue of investigation could elicit a stimulation of greater intensity or duration in order to completely fatigue all muscle fibers and achieve an even greater level of adaptation similar to high intensity, maximal exercise. Under this condition of hyper-activated protein synthesis leading to a more pronounced increase in mitochondrial content, it is possible that the UPR would be of even greater importance in establishing a new adaptive phenotype. Here, we could manipulate the protein-folding environment, similar to our current study, to once again analyze the impact of the UPR.

6. Finally, the sampling of UPR^{ER} and UPR^{mt} factors in this study were limited to protein and mRNA expression in order to establish a time-course and to get a framework of some of the most sensitive responders to proteotoxic stress within contracting muscle, as the UPR had not been well defined in this tissue. However, future research could expand the sampling to include more UPR^{mt} factors in particular including transcription factors UBL5 and Sat5B, which are transcription factors involved in upregulating mitochondrial genes. Furthermore, it would also be useful to corroborate data on UPR activation with protein synthesis rates in contracting muscle. This could help establish a dose-response relationship between intensity of stimulation, protein synthesis, UPR activation, and subsequent adaptation.

APPENDIX A: DATA AND STATISTICAL ANALYSIS

Table 1: Cytochrome c oxidase activity during 7-day CCA time-course.

	Cytochrome c Oxidase Activity (U/g muscle)									
	1 Day		2 Days		3 Days		5 Days		7 Days	
n	CTR	STM	CTR	STM	CTR	STM	CTR	STM	CTR	STM
1	18.69	15.42	21.89	19.19	18.4	20.82	22.89	26.2	17.84	24.68
2	19.07	18.99	22.6	20.14	18	24.8	21.75	25.03	16.96	22.37
3	16.3	16.5	17.81	19.4	20.85	23.47	19.92	25.26	19.19	23.03
4	12.8	14.59	16.43	15.49	21.23	22.57	18.19	23.01	17.49	24.04
5	18.18	20.9	15.48	15.42	21.37	21.58	20.8	22.02	19.21	27.13
6	20.83	18.03	13.99	15.49	20.73	19.56	18.27	20.34	19.02	23.41
X	17.64	17.4	18.04	17.52	20.1	22.14	20.3	23.64	18.29	24.11
SEM	1.138	0.963	1.428	0.928	0.609	0.769	0.77	0.913	0.4	0.687

RM 2-Way ANOVA - Control vs CCA Stim			
Source of Variation	P value	P value summary	Significant ?
Interaction	0.0003	***	Yes
Days	< 0.0001	****	Yes
CCA	0.0001	***	Yes
Matching	0.0049	**	Yes

Bonferroni Post Hoc Test - Control vs CCA Stim				
Days	Difference	t	P value	Summary
1	0.2392	0.282	P > 0.05	ns
2	0.5121	0.6036	P > 0.05	ns
3	-2.038	2.402	P = 0.06	ns
5	-3.342	3.939	P < 0.05	**
7	-5.823	6.862	P < 0.05	****

Table 2A: mRNA expression of PGC-1α during 7-day CCA time-course.

	PGC-1α mRNA - Control vs. CCA Stim (ΔCt)									
	1 Day		2 Days		3 Days		5 Days		7 Days	
n	CTR	STM	CTR	STM	CTR	STM	CTR	STM	CTR	STM
1	0.004	0.057	0.005	0.005	0.006	0.067	0.004	0.042	0.006	0.075
2	0.006	0.057	0.006	0.052	0.007	0.062	0.007	0.046	0.004	0.041
3	0.005	0.031	0.005	0.04	0.007	0.059	0.004	0.036	0.005	0.03
4	0.004	0.054	0.006	0.045	0.004	0.087	0.007	0.038	0.005	0.042
5	0.006	0.108	0.007	0.065	0.007	0.068	0.007	0.046	0.004	0.05
6	0.004	0.084	0.006	0.038	0.004	0.058	0.006	0.051	0.003	0.037
X	0.005	0.065	0.006	0.041	0.006	0.067	0.006	0.043	0.004	0.046
SEM	4E-04	0.011	3E-04	0.008	5E-04	0.004	6E-04	0.002	3E-04	0.006

RM 2-Way ANOVA - Control vs CCA Stim			
Source of Variation	P value	P value summary	Significant ?
Interaction	4.244	*	Yes
Days	4.176	*	Yes
CCA	74.5	****	Yes
Matching	8.831	ns	No

Bonferroni Post Hoc Test - Control vs CCA Stim				
Days	Difference	t	P value	Summary
1	-0.06029	8.607	P < 0.05	****
2	-0.03534	5.045	P < 0.05	***
3	-0.06095	8.701	P < 0.05	****
5	-0.03728	5.322	P < 0.05	****
7	-0.04154	5.93	P < 0.05	****

Table 2B: mRNA expression of autophagy genes during 7-day CCA time-course.

	p62 mRNA - Control vs. CCA Stim (ΔCt)									
	1 Day		2 Days		3 Days		5 Days		7 Days	
n	CTR	STM	CTR	STM	CTR	STM	CTR	STM	CTR	STM
1	0.195	0.207	0.081	0.362	0.172	0.231	0.199	0.144	0.143	0.125
2	0.185	0.22	0.152	0.305	0.159	0.216	0.19	0.17	0.184	0.193
3	0.125	0.18	0.097	0.192	0.137	0.197	0.132	0.119	0.158	0.119
4	0.217	0.281	0.121	0.199	0.173	0.179	0.15	0.136	0.136	0.105
5	0.101	0.19	0.069	0.15	0.099	0.125	0.088	0.087	0.127	0.118
6	0.107	0.14	0.156	0.237	0.121	0.216	0.104	0.128	0.106	0.108
X	0.155	0.203	0.113	0.241	0.144	0.194	0.144	0.131	0.142	0.128
SEM	0.02	0.019	0.015	0.032	0.012	0.016	0.018	0.011	0.011	0.013

RM 2-Way ANOVA - Control vs CCA Stim			
Source of Variation	P value	P value summary	Significant ?
Interaction	0.0292	*	Yes
Days	0.0396	*	Yes
CCA	< 0.0001	****	Yes
Matching	0.4327	ns	No

Bonferroni Post Hoc Test - Control vs CCA Stim				
Days	Difference	t	P value	Summary
1	-0.04819	2.767	P > 0.05	ns
2	-0.1281	7.356	P < 0.05	****
3	-0.05064	2.908	P < 0.05	*
5	0.01309	0.7513	P > 0.05	ns
7	0.0143	0.821	P > 0.05	ns

	LC3 mRNA - Control vs. CCA Stim (ΔCt)									
	1 Day		2 Days		3 Days		5 Days		7 Days	
n	CTR	STM	CTR	STM	CTR	STM	CTR	STM	CTR	STM
1	0.209	0.157	0.188	0.282	0.213	0.176	0.2	0.13	0.189	0.161
2	0.138	0.141	0.856	0.125	0.168	0.151	0.166	0.137	0.221	0.169
3	0.116	0.114	0.122	0.121	0.151	0.106	0.16	0.117	0.174	0.141
4	0.174	0.166	0.136	0.104	0.138	0.123	0.148	0.113	0.117	0.089
5	0.182	0.207	0.169	0.144	0.139	0.106	0.176	0.139	0.141	0.168
6	0.169	0.196	0.205	0.149	0.187	0.165	0.178	0.144	0.217	0.2
X	0.165	0.163	0.279	0.154	0.166	0.138	0.171	0.13	0.176	0.155
SEM	0.013	0.014	0.116	0.026	0.012	0.012	0.007	0.005	0.017	0.015

RM 2-Way ANOVA - Control vs CCA Stim			
Source of Variation	P value	P value summary	Significant ?
Interaction	0.5735	ns	No
Days	0.4487	ns	No
CCA	0.0917	ns	No
Matching	0.4994	ns	No

Bonferroni Post Hoc Test - Control vs CCA Stim				
Days	Difference	t	P value	Summary
1	0.00135	0.02419	P > 0.05	ns
2	0.1252	2.252	P > 0.05	ns
3	0.02825	0.5083	P > 0.05	ns
5	0.04137	0.7442	P > 0.05	ns
7	0.0219	0.3941	P > 0.05	ns

Table 2C: mRNA expression of UPR^{ER} genes during 7-day CCA time-course.

	ATF4 mRNA - Control vs. CCA Stim (ΔCt)									
	1 Day		2 Days		3 Days		5 Days		7 Days	
n	CTR	STM	CTR	STM	CTR	STM	CTR	STM	CTR	STM
1	0.059	0.055	0.069	0.067	0.073	0.125	0.071	0.053	0.084	0.052
2	0.066	0.086	0.074	0.132	0.094	0.141	0.098	0.079	0.082	0.06
3	0.104	0.159	0.124	0.178	0.082	0.134	0.095	0.125	0.107	0.08
4	0.136	0.208	0.21	0.445	0.18	0.349	0.196	0.216	0.172	0.115
5	0.09	0.118	0.094	0.229	0.098	0.129	0.111	0.089	0.113	0.073
6	0.058	0.071	0.057	0.111	0.079	0.086	0.05	0.061	0.07	0.082
X	0.085	0.116	0.105	0.194	0.101	0.161	0.103	0.104	0.105	0.077
SEM	0.013	0.024	0.023	0.055	0.016	0.038	0.021	0.025	0.015	0.009

RM 2-Way ANOVA - Control vs CCA Stim			
Source of Variation	P value	P value summary	Significant ?
Interaction	0.003	**	Yes
Days	0.4711	ns	No
CCA	0.0022	**	Yes
Matching	< 0.0001	****	Yes

Bonferroni Post Hoc Test - Control vs CCA Stim				
Days	Difference	t	P value	Summary
1	-0.0309	1.544	P > 0.05	ns
2	-0.08887	4.441	P < 0.05	***
3	-0.05976	2.987	P < 0.05	*
5	-0.00058	0.02904	P > 0.05	ns
7	0.02772	1.385	P > 0.05	ns

	XBP1s mRNA - Control vs. CCA Stim (ΔCt)									
	1 Day		2 Days		3 Days		5 Days		7 Days	
n	CTR	STM	CTR	STM	CTR	STM	CTR	STM	CTR	STM
1	0.002	0.004	7E-04	0.001	0.001	0.002	0.002	9E-04	0.001	6E-04
2	0.002	0.004	0.001	0.006	0.001	0.002	0.001	0.001	0.001	9E-04
3	0.001	0.001	0.002	0.004	0.002	0.005	0.002	9E-04	0.002	0.001
4	8E-04	0.001	0.002	0.004	0.003	0.003	0.002	0.001	0.002	8E-04
5	0.001	0.005	1E-03	0.002	0.001	0.002	0.001	8E-04	0.002	0.001
6	0.001	0.003	0.002	0.012	0.002	0.008	0.002	0.002	0.002	8E-04
X	0.001	0.003	0.001	0.005	0.002	0.004	0.002	0.001	0.002	9E-04
SEM	2E-04	6E-04	2E-04	0.002	2E-04	0.001	1E-04	2E-04	1E-04	9E-05

RM 2-Way ANOVA - Control vs CCA Stim			
Source of Variation	P value	P value summary	Significant ?
Interaction	0.0057	**	Yes
Days	0.0629	ns	No
CCA	0.0053	**	Yes
Matching	0.235	ns	No

Bonferroni Post Hoc Test - Control vs CCA Stim				
Days	Difference	t	P value	Summary
1	-0.00163	1.973	P > 0.05	ns
2	-0.00349	4.224	P < 0.05	**
3	-0.00186	2.256	P > 0.05	ns
5	0.00057	0.6887	P > 0.05	ns
7	0.00077	0.9366	P > 0.05	ns

	CHOP mRNA - Control vs. CCA Stim (ΔCt)									
	1 Day		2 Days		3 Days		5 Days		7 Days	
n	CTR	STM	CTR	STM	CTR	STM	CTR	STM	CTR	STM
1	0.005	0.031	0.007	0.006	0.007	0.021	0.006	0.016	0.009	0.025
2	0.007	0.018	0.007	0.026	0.01	0.024	0.008	0.016	0.011	0.015
3	0.008	0.018	0.007	0.022	0.009	0.021	0.004	0.013	0.007	0.013
4	0.006	0.016	0.008	0.022	0.005	0.035	0.008	0.02	0.008	0.016
5	0.012	0.043	0.017	0.05	0.014	0.037	0.017	0.029	0.01	0.03
6	0.01	0.057	0.014	0.043	0.015	0.044	0.016	0.023	0.016	0.036
X	0.008	0.03	0.01	0.028	0.01	0.03	0.01	0.019	0.01	0.022
SEM	0.001	0.007	0.002	0.007	0.002	0.004	0.002	0.002	0.001	0.004

RM 2-Way ANOVA - Control vs CCA Stim			
Source of Variation	P value	P value summary	Significant ?
Interaction	0.1664	ns	No
Days	0.7006	ns	No
CCA	< 0.0001	****	Yes
Matching	0.0231	*	Yes

Bonferroni Post Hoc Test - Control vs CCA Stim				
Days	Difference	t	P value	Summary
1	-0.02244	5.461	P < 0.05	****
2	-0.01801	4.383	P < 0.05	***
3	-0.02039	4.961	P < 0.05	***
5	-0.00949	2.309	P > 0.05	ns
7	-0.01229	2.991	P < 0.05	*

	BiP mRNA - Control vs. CCA Stim (ΔCt)									
	1 Day		2 Days		3 Days		5 Days		7 Days	
n	CTR	STM	CTR	STM	CTR	STM	CTR	STM	CTR	STM
1	0.058	0.128	0.044	0.039	0.053	0.117	0.045	0.071	0.059	0.073
2	0.066	0.128	0.064	0.32	0.059	0.145	0.062	0.078	0.051	0.112
3	0.047	0.067	0.049	0.217	0.058	0.288	0.068	0.069	0.063	0.097
4	0.036	0.075	0.054	0.184	0.048	0.068	0.049	0.067	0.046	0.074
5	0.07	0.118	0.054	0.134	0.082	0.119	0.068	0.074	0.076	0.107
6	0.079	0.201	0.072	0.479	0.076	0.395	0.103	0.137	0.103	0.102
X	0.059	0.119	0.056	0.229	0.063	0.188	0.066	0.083	0.066	0.094
SEM	0.006	0.02	0.004	0.063	0.005	0.051	0.009	0.011	0.008	0.007

RM 2-Way ANOVA - Control vs CCA Stim			
Source of Variation	P value	P value summary	Significant ?
Interaction	0.0192	*	Yes
Days	0.1088	ns	No
CCA	< 0.0001	****	Yes
Matching	0.2165	ns	No

Bonferroni Post Hoc Test - Control vs CCA Stim				
Days	Difference	t	P value	Summary
1	-0.06004	1.707	P < 0.05	*
2	-0.1726	4.907	P < 0.05	***
3	-0.1258	3.575	P < 0.05	**
5	-0.01701	0.4835	P > 0.05	ns
7	-0.02792	0.7935	P < 0.05	*

	HSP70 mRNA - Control vs. CCA Stim (ΔCt)									
	1 Day		2 Days		3 Days		5 Days		7 Days	
n	CTR	STM	CTR	STM	CTR	STM	CTR	STM	CTR	STM
1	0.464	36.36	0.278	0.365	0.422	1.867	0.458	3.726	0.476	1.315
2	0.439	20.25	0.428	17	0.421	3.394	0.568	2.213	0.401	2.829
3	0.191	2.107	0.224	4.412	0.237	1.45	0.36	1.495	0.249	2.217
4	0.307	42.6	0.498	8.475	0.349	1.752	0.455	1.049	0.39	0.892
5	0.091	8.773	0.163	7.049	0.117	0.811	0.13	0.576	0.115	0.596
6	0.111	5.74	0.102	3.414	0.232	0.866	0.075	0.545	0.057	0.385
X	0.267	19.3	0.282	6.785	0.296	1.69	0.341	1.601	0.281	1.372
SEM	0.066	6.892	0.063	2.348	0.05	0.385	0.08	0.496	0.069	0.394

RM 2-Way ANOVA - Control vs CCA Stim			
Source of Variation	P value	P value summary	Significant ?
Interaction	0.0022	**	Yes
Days	0.0028	**	Yes
CCA	0.0005	***	Yes
Matching	0.4656	ns	No

Bonferroni Post Hoc Test - Control vs CCA Stim				
Days	Difference	t	P value	Summary
1	-19.04	5.867	P < 0.05	****
2	-6.503	2.004	P > 0.05	ns
3	-1.394	0.4296	P > 0.05	ns
5	-1.26	0.3882	P > 0.05	ns
7	-1.091	0.3362	P > 0.05	ns

Table 2D: mRNA expression of UPR^{mt} genes during 7-day CCA time-course.

	ClpP mRNA - Control vs. CCA Stim (ΔCt)									
	1 Day		2 Days		3 Days		5 Days		7 Days	
n	CTR	STM	CTR	STM	CTR	STM	CTR	STM	CTR	STM
1	0.029	0.032	0.029	0.118	0.032	0.047	0.03	0.042	0.034	0.043
2	0.034	0.023	0.03	0.049	0.039	0.05	0.034	0.05	0.035	0.051
3	0.026	0.043	0.032	0.047	0.03	0.051	0.025	0.041	0.035	0.039
4	0.099	0.105	0.036	0.049	0.029	0.044	0.037	0.06	0.03	0.044
5	0.055	0.06	0.043	0.048	0.066	0.057	0.054	0.078	0.029	0.052
6	0.038	0.045	0.049	0.05	0.046	0.077	0.041	0.059	0.041	0.07
7	0.039	0.059	0.041	0.059	0.063	0.07	0.049	0.068	0.041	0.048
8	0.028	0.036	0.033	0.045	0.035	0.059	0.028	0.037	0.023	0.046
X	0.044	0.05	0.037	0.058	0.042	0.057	0.037	0.054	0.034	0.049
SEM	0.009	0.009	0.003	0.009	0.005	0.004	0.004	0.005	0.002	0.003

RM 2-Way ANOVA - Control vs CCA Stim			
Source of Variation	P value	P value summary	Significant ?
Interaction	0.4015	ns	No
Days	0.8394	ns	No
CCA	< 0.0001	****	Yes
Matching	< 0.0001	****	Yes

Bonferroni Post Hoc Test - Control vs CCA Stim				
Days	Difference	t	P value	Summary
1	-0.00677	1.283	P > 0.05	ns
2	-0.02153	4.082	P < 0.05	**
3	-0.01436	2.724	P > 0.05	ns
5	-0.01707	3.237	P < 0.05	*
7	-0.01564	2.966	P < 0.05	*

	CPN10 mRNA - Control vs. CCA Stim (ΔCt)									
	1 Day		2 Days		3 Days		5 Days		7 Days	
n	CTR	STM	CTR	STM	CTR	STM	CTR	STM	CTR	STM
1	0.095	0.177	0.076	0.152	0.102	0.201	0.102	0.205	0.109	0.161
2	0.098	0.157	0.097	0.209	0.103	0.182	0.106	0.18	0.111	0.236
3	0.095	0.113	0.093	0.157	0.099	0.214	0.095	0.162	0.1	0.234
4	0.251	0.276	0.224	0.283	0.182	0.255	0.229	0.27	0.218	0.284
5	0.208	0.241	0.111	0.241	0.14	0.272	0.168	0.258	0.118	0.23
6	0.135	0.204	0.135	0.238	0.15	0.273	0.155	0.238	0.166	0.223
X	0.147	0.195	0.122	0.213	0.129	0.233	0.143	0.219	0.137	0.228
SEM	0.027	0.024	0.022	0.021	0.014	0.016	0.021	0.018	0.019	0.016

RM 2-Way ANOVA - Control vs CCA Stim			
Source of Variation	P value	P value summary	Significant ?
Interaction	0.0214	*	Yes
Days	0.9741	ns	No
CCA	< 0.0001	****	Yes
Matching	< 0.0001	****	Yes

Bonferroni Post Hoc Test - Control vs CCA Stim				
Days	Difference	t	P value	Summary
1	-0.04771	4.184	P < 0.05	**
2	-0.09069	7.952	P < 0.05	****
3	-0.1033	9.06	P < 0.05	****
5	-0.07636	6.695	P < 0.05	****
7	-0.09076	7.958	P < 0.05	****

	HSP60 mRNA - Control vs. CCA Stim (ΔCt)									
	1 Day		2 Days		3 Days		5 Days		7 Days	
n	CTR	STM	CTR	STM	CTR	STM	CTR	STM	CTR	STM
1	0.055	0.114	0.079	0.122	0.075	0.088	0.058	0.103	0.077	0.11
2	0.101	0.151	0.098	0.138	0.093	0.109	0.106	0.121	0.09	0.147
3	0.082	0.077	0.075	0.101	0.071	0.143	0.062	0.092	0.057	0.125
4	0.058	0.115	0.094	0.106	0.061	0.095	0.087	0.116	0.088	0.119
5	0.155	0.222	0.106	0.196	0.183	0.225	0.145	0.221	0.1	0.144
6	0.111	0.199	0.221	0.173	0.161	0.184	0.176	0.167	0.167	0.202
7	0.064	0.105	0.06	0.107	0.055	0.08	0.081	0.098	0.057	0.077
8	0.058	0.071	0.057	0.111	0.079	0.086	0.05	0.061	0.07	0.082
X	0.085	0.132	0.099	0.132	0.097	0.126	0.096	0.122	0.088	0.126
SEM	0.012	0.019	0.019	0.012	0.017	0.019	0.016	0.018	0.013	0.014

RM 2-Way ANOVA - Control vs CCA Stim			
Source of Variation	P value	P value summary	Significant ?
Interaction	0.6459	ns	No
Days	0.9961	ns	No
CCA	< 0.0001	****	Yes
Matching	< 0.0001	****	Yes

Bonferroni Post Hoc Test - Control vs CCA Stim				
Days	Difference	t	P value	Summary
1	-0.04649	4.722	P < 0.05	***
2	-0.03295	3.347	P < 0.05	**
3	-0.02908	2.954	P < 0.05	*
5	-0.02685	2.727	P < 0.05	*
7	-0.03757	3.817	P < 0.05	**

	mtHSP70 mRNA - Control vs. CCA Stim (ΔCt)									
	1 Day		2 Days		3 Days		5 Days		7 Days	
n	CTR	STM	CTR	STM	CTR	STM	CTR	STM	CTR	STM
1	0.048	0.065	0.046	0.087	0.061	0.091	0.05	0.095	0.053	0.1
2	0.057	0.041	0.05	0.071	0.046	0.079	0.064	0.082	0.041	0.075
3	0.052	0.046	0.05	0.074	0.071	0.104	0.048	0.07	0.038	0.078
4	0.032	0.042	0.058	0.069	0.045	0.072	0.062	0.086	0.044	0.063
5	0.032	0.043	0.019	0.027	0.026	0.036	0.031	0.029	0.022	0.038
6	0.033	0.055	0.049	0.055	0.041	0.075	0.045	0.073	0.036	0.055
7	0.028	0.042	0.029	0.035	0.018	0.043	0.051	0.064	0.047	0.047
8	0.021	0.024	0.02	0.036	0.027	0.033	0.02	0.028	0.019	0.032
X	0.038	0.045	0.04	0.057	0.042	0.067	0.046	0.066	0.037	0.061
SEM	0.005	0.004	0.005	0.008	0.006	0.009	0.005	0.009	0.004	0.008

RM 2-Way ANOVA - Control vs CCA Stim			
Source of Variation	P value	P value summary	Significant ?
Interaction	0.0618	ns	No
Days	0.4909	ns	No
CCA	< 0.0001	****	Yes
Matching	< 0.0001	****	Yes

Bonferroni Post Hoc Test - Control vs CCA Stim				
Days	Difference	t	P value	Summary
1	-0.00683	1.491	P > 0.05	ns
2	-0.01625	3.548	P < 0.05	**
3	-0.02488	5.433	P < 0.05	****
5	-0.01943	4.242	P < 0.05	***
7	-0.02357	5.146	P < 0.05	****

Table 3A: Protein expression of mitochondrial content and biogenesis markers following 7 days of CCA.

	7 Day CCA PGC-1α, Uqcrc2, COX IV - Control vs CCA Stim					
	PGC-1α		Uqcrc2		COX IV	
n	CTR	STM	CTR	STM	CTR	STM
1	1.31984	1.87118	1.38979	1.24491	2.05575	2.36908
2	1.19298	1.15656	2.05575	2.36908	0.82086	1.05333
3	0.38098	0.8092	0.82086	1.05333	0.80999	1.36698
4	2.42568	1.90626	1.79755	1.64915	0.66357	0.80608
5	0.63097	1.13614	0.80999	1.36698	0.62852	0.85471
6			0.62852	0.85471	0.68635	1.0843
X	1.19009	1.37587	1.25041	1.42302	0.94417	1.25575
SEM	0.35432	0.21833	0.24032	0.21914	0.22462	0.23702

RM 2-Way ANOVA - Control vs CCA Stim			
Source of Variation	P value	P value summary	Significant ?
Interaction	0.0165	*	Yes
Days	0.9794	ns	No
CCA	0.0005	***	Yes
Matching	< 0.0001	****	Yes

Bonferroni Post Hoc Test - Control vs CCA Stim				
Days	Difference	t	P value	Summary
PGC-1α	-0.1858	1.176	P > 0.05	ns
COXIV	-0.1683	1.261	P > 0.05	ns
Uqcrc2	-0.7254	5.435	P < 0.05	***

Table 3B: Protein expression of autophagy markers during 7-day CCA time-course.

	p62 Protein - Control vs. CCA Stim									
	1 Day		2 Days		3 Days		5 Days		7 Days	
n	CTR	STM	CTR	STM	CTR	STM	CTR	STM	CTR	STM
1	1.207	0.833	0.609	1.104	0.633	1.233	1.123	1.609	1.121	0.848
2	0.965	0.644	0.924	1.387	0.967	1.175	1.065	1.197	0.983	0.881
3	1.538	1.284	0.706	0.834	0.616	1.015	0.509	0.619	0.683	0.72
4	1.329	0.742	0.749	0.949	0.713	0.854	0.756	1.074	0.714	0.861
5	0.792	0.996	0.635	0.663	0.501	2.456	1.539	1.849	1.274	1.519
6	1.551	2.701	2.797	2.282	2.132	3.029	1.325	1.686	2.591	2.592
7	0.889	0.88	0.783	0.978	0.911	1.479	3.169	1.134	1.013	1.116
X	1.182	1.154	1.029	1.171	0.925	1.606	1.355	1.31	1.197	1.22
SEM	0.116	0.269	0.297	0.204	0.211	0.309	0.329	0.162	0.246	0.249

RM 2-Way ANOVA - Control vs CCA Stim			
Source of Variation	P value	P value summary	Significant ?
Interaction	0.1266	ns	No
Days	0.9566	ns	No
CCA	0.1212	ns	No
Matching	< 0.0001	****	Yes

Bonferroni Post Hoc Test - Control vs CCA Stim				
Days	Difference	t	P value	Summary
1	0.02747	0.1267	P > 0.05	ns
2	-0.1421	0.6554	P > 0.05	ns
3	-0.6813	3.142	P < 0.05	*
5	0.04522	0.2086	P > 0.05	ns
7	-0.0225	0.1038	P > 0.05	ns

	LC3-II:LC3-I Protein - Control vs. CCA Stim									
	1 Day		2 Days		3 Days		5 Days		7 Days	
n	CTR	STM	CTR	STM	CTR	STM	CTR	STM	CTR	STM
1	1.728	0.801	1.132	0.96	1.772	0.562	1.368	0.556	1.178	0.532
2	1.013	1.566	1.111	0.311	1.171	0.482	1.746	0.596	1.022	0.226
3	1.256	0.696	2.182	0.722	2.036	0.673	2.04	0.48	0.984	0.447
4	1.038	0.77	0.677	0.475	1.423	0.494	1.44	0.573	0.688	0.346
5	0.812	0.539	0.364	0.359	1.922	0.607	0.849	0.571	1.663	0.786
6	2.266	0.649	0.847	0.591	0.747	0.262	0.847	0.369	0.677	0.462
X	1.352	0.837	1.052	0.57	1.512	0.513	1.382	0.524	1.035	0.467
SEM	0.223	0.151	0.254	0.099	0.202	0.058	0.195	0.035	0.149	0.077

RM 2-Way ANOVA - Control vs CCA Stim			
Source of Variation	P value	P value summary	Significant ?
Interaction	0.3047	ns	No
Days	0.2985	ns	No
CCA	< 0.0001	****	Yes
Matching	0.1566	ns	No

Bonferroni Post Hoc Test - Control vs CCA Stim				
Days	Difference	t	P value	Summary
1	0.5155	2.537	P > 0.05	ns
2	0.4824	2.374	P > 0.05	ns
3	0.9983	4.914	P < 0.05	***
5	0.8574	4.22	P < 0.05	**
7	0.5688	2.8	P < 0.05	*

Table 3C: Protein expression of UPR^{ER} markers during 7-day CCA time-course.

	CHOP Protein - Control vs. CCA Stim									
	1 Day		2 Days		3 Days		5 Days		7 Days	
n	CTR	STM	CTR	STM	CTR	STM	CTR	STM	CTR	STM
1	0.213	0.265	0.184	0.322	0.488	0.545	0.417	0.506	0.87	0.657
2	0.187	0.183	0.361	0.627	0.242	0.382	0.22	0.468	0.28	0.402
3	0.678	0.722	0.706	0.854	0.376	0.603	0.868	1.255	0.564	0.844
4	0.306	0.134	0.209	0.431	0.304	0.804	0.363	0.576	0.254	0.385
5	0.885	1.381	0.894	0.97	1.036	0.955	0.76	1.352	0.441	1.053
6	0.099	0.602	0.247	0.397	0.483	0.667	0.5	0.901	0.415	1.511
7	0.937	1.225	1.009	1.585	1.051	1.601	1.734	1.728	1.252	1.396
X	0.472	0.645	0.516	0.741	0.569	0.794	0.695	0.97	0.582	0.893
SEM	0.133	0.189	0.131	0.168	0.127	0.151	0.193	0.184	0.136	0.17

RM 2-Way ANOVA - Control vs CCA Stim			
Source of Variation	P value	P value summary	Significant ?
Interaction	0.8985	ns	No
Days	0.7542	ns	No
CCA	< 0.0001	****	Yes
Matching	< 0.0001	****	Yes

Bonferroni Post Hoc Test - Control vs CCA Stim				
Days	Difference	t	P value	Summary
1	-0.1726	1.682	P > 0.05	ns
2	-0.225	2.193	P > 0.05	ns
3	-0.2252	2.195	P > 0.05	ns
5	-0.2748	2.679	P > 0.05	ns
7	-0.3103	3.025	P < 0.05	*

	BiP Protein - Control vs. CCA Stim									
	1 Day		2 Days		3 Days		5 Days		7 Days	
n	CTR	STM	CTR	STM	CTR	STM	CTR	STM	CTR	STM
1	1.459	1.297	0.921	0.198	0.59	0.819	0.844	0.826	0.667	0.856
2	0.699	0.634	0.631	0.443	0.519	0.575	0.646	0.789	1.036	0.891
3	1.149	1.223	0.838	0.821	1.245	1.458	1.883	1.198	0.866	1.639
4	3.324	3.167	2.075	2.557	2.929	1.992	2.545	2.228	1.442	1.708
5	0.681	0.658	0.843	0.778	0.746	0.744	0.543	0.577	0.803	1.48
6	0.825	0.503	0.434	0.345	0.549	0.501	0.422	0.703	0.309	0.697
7	0.674	0.355	0.401	0.046	0.604	0.759	0.877	0.637	0.558	0.534
X	1.259	1.119	0.877	0.741	1.026	0.978	1.109	0.994	0.811	1.115
SEM	0.362	0.367	0.214	0.321	0.331	0.206	0.3	0.219	0.137	0.182

RM 2-Way ANOVA - Control vs CCA Stim			
Source of Variation	P value	P value summary	Significant ?
Interaction	0.0824	ns	No
Days	0.8982	ns	No
CCA	0.6322	ns	No
Matching	< 0.0001	****	Yes

Bonferroni Post Hoc Test - Control vs CCA Stim				
Days	Difference	t	P value	Summary
1	0.1394	1.121	P > 0.05	ns
2	0.1363	1.096	P > 0.05	ns
3	0.04771	0.3838	P > 0.05	ns
5	0.1145	0.9209	P > 0.05	ns
7	-0.3034	2.441	P > 0.05	ns

	HSP70 Protein - Control vs. CCA Stim									
	1 Day		2 Days		3 Days		5 Days		7 Days	
n	CTR	STM	CTR	STM	CTR	STM	CTR	STM	CTR	STM
1	0.359	1.027	1.022	1.067	0.848	1.304	1.086	1.525	0.294	1.581
2	0.445	0.875	0.287	0.659	0.462	1.035	0.48	0.957	0.677	1.037
3	0.55	1.109	0.327	0.557	0.368	1.09	0.415	1.262	0.373	0.823
4	2.216	2.876	1.449	5.155	2.134	1.93	1.255	4.156	0.794	2.001
5	0.32	0.39	0.251	0.804	0.67	1.255	0.33	0.986	0.547	1.628
6	0.271	0.465	0.322	1.01	0.444	1.129	0.519	1.305		
X	0.693	1.124	0.609	1.542	0.821	1.291	0.681	1.698	0.537	1.414
SEM	0.307	0.37	0.206	0.727	0.272	0.134	0.158	0.499	0.093	0.213

RM 2-Way ANOVA - Control vs CCA Stim			
Source of Variation	P value	P value summary	Significant ?
Interaction	0.6049	ns	No
Days	0.9766	ns	No
CCA	< 0.0001	****	Yes
Matching	0.0012	**	Yes

Bonferroni Post Hoc Test - Control vs CCA Stim				
Days	Difference	t	P value	Summary
1	-0.4305	1.31	P > 0.05	ns
2	-0.9325	2.838	P < 0.05	*
3	-0.4696	1.429	P > 0.05	ns
5	-1.018	3.098	P < 0.05	*
7	-0.8768	2.436	P > 0.05	ns

Figure 3D: Protein expression of UPR^{mt} markers during 7-day CCA time-course.

	SirT3 Protein - Control vs. CCA Stim									
	1 Day		2 Days		3 Days		5 Days		7 Days	
n	CTR	STM	CTR	STM	CTR	STM	CTR	STM	CTR	STM
1	0.633	0.751	0.427	0.702	0.564	0.729	0.783	0.778	1.044	1.087
2	0.958	0.443	0.884	1.237	0.886	0.889	0.89	1.167	0.99	1.047
3	1.162	1.04	0.726	0.489	0.71	0.996	1.09	1.181	0.891	0.875
4	0.677	0.488	1.04	0.895	0.708	0.734	0.677	1.201	0.791	1.298
5	0.472	0.733	1.079	0.926	1.149	3.097	2.497	2.645	1.429	1.883
6	0.387	0.153	0.349	0.296	0.249	0.417	0.366	0.288	0.299	0.621
7	1.089	0.599	0.656	0.683	1.22	1.141	1.977	1.654	1.165	1.718
8	0.943	1.294	1.353	1.832	2.435	2.959	2.444	2.373	1.396	2.968
X	0.79	0.688	0.814	0.882	0.99	1.37	1.34	1.411	1.001	1.437
SEM	0.102	0.126	0.121	0.169	0.234	0.37	0.297	0.278	0.128	0.264

RM 2-Way ANOVA - Control vs CCA Stim			
Source of Variation	P value	P value summary	Significant ?
Interaction	0.085	ns	No
Days	0.2014	ns	No
CCA	0.0176	*	Yes
Matching	< 0.0001	****	Yes

Bonferroni Post Hoc Test - Control vs CCA Stim				
Days	Difference	t	P value	Summary
1	0.1024	0.6687	P > 0.05	ns
2	-0.06817	0.4451	P > 0.05	ns
3	-0.3803	2.483	P > 0.05	ns
5	-0.07031	0.4591	P > 0.05	ns
7	-0.4367	2.851	P < 0.05	*

	CPN10 Protein - Control vs. CCA Stim									
	1 Day		2 Days		3 Days		5 Days		7 Days	
n	CTR	STM	CTR	STM	CTR	STM	CTR	STM	CTR	STM
1	0.706	0.838	0.718	1.435	0.466	0.713	0.732	0.738	0.315	0.509
2	0.546	0.931	0.545	0.756	0.471	0.936	0.92	1.12	1.098	1.714
3	0.911	0.795	1.17	0.852	1.274	1.391	1.725	2.804	1.335	3.33
4	1.716	1.508	1.276	1.257	1.455	0.922	0.545	0.989	0.873	1.292
5	1.302	1.075	1.883	1.21	0.913	1.452	0.891	1.663	0.956	1.484
6	0.564	0.689	0.535	0.658	0.521	0.503	0.354	0.31	0.524	0.8
7	1.214	2.017	1.967	2.4	2.3	2.664	2.005	1.916	1.65	3.314
X	0.994	1.122	1.156	1.224	1.057	1.226	1.025	1.363	0.964	1.778
SEM	0.165	0.18	0.226	0.224	0.256	0.272	0.231	0.315	0.173	0.427

RM 2-Way ANOVA - Control vs CCA Stim			
Source of Variation	P value	P value summary	Significant ?
Interaction	0.0509	ns	No
Days	0.9213	ns	No
CCA	0.0009	***	Yes
Matching	< 0.0001	****	Yes

Bonferroni Post Hoc Test - Control vs CCA Stim				
Days	Difference	t	P value	Summary
1	-0.128	0.6923	P > 0.05	ns
2	-0.06789	0.3673	P > 0.05	ns
3	-0.1685	0.9117	P > 0.05	ns
5	-0.3382	1.829	P > 0.05	ns
7	-0.8132	4.399	P < 0.05	***

	HSP60 Protein - Control vs. CCA Stim									
	1 Day		2 Days		3 Days		5 Days		7 Days	
n	CTR	STM	CTR	STM	CTR	STM	CTR	STM	CTR	STM
1	0.822	1.307	1.14	1.49	1.409	1.803	1.204	1.335	1.444	1.804
2	0.786	0.824	0.761	0.757	0.884	1.104	1.044	0.895	1.011	0.967
3	0.55	1.068	0.304	0.421	0.577	0.92	0.766	0.975	0.375	0.576
4	4.081	3.879	4.091	4.354	3.747	2.65	2.52	3.164	1.883	2.406
5	0.419	0.453	0.629	1.168	0.989	1.159	0.845	1.104	0.544	1.192
6	1.032	0.969	1.255	1.102	1.247	1.166	1.089	1.145	1.22	1.149
7	0.718	0.723	0.878	0.747	1.255	1.356	1.266	1.128	1.375	1.509
X	1.201	1.318	1.294	1.434	1.444	1.451	1.248	1.392	1.122	1.372
SEM	0.486	0.439	0.481	0.504	0.398	0.226	0.223	0.3	0.199	0.227

RM 2-Way ANOVA - Control vs CCA Stim			
Source of Variation	P value	P value summary	Significant ?
Interaction	0.7539	ns	No
Days	0.9948	ns	No
CCA	0.026	*	Yes
Matching	< 0.0001	****	Yes

Bonferroni Post Hoc Test - Control vs CCA Stim				
Days	Difference	t	P value	Summary
1	-0.1166	0.9275	P > 0.05	ns
2	-0.1402	1.115	P > 0.05	ns
3	-0.00704	0.05601	P > 0.05	ns
5	-0.1447	1.152	P > 0.05	ns
7	-0.2499	1.989	P > 0.05	ns

	mtHSP70 Protein - Control vs. CCA Stim									
	1 Day		2 Days		3 Days		5 Days		7 Days	
n	CTR	STM	CTR	STM	CTR	STM	CTR	STM	CTR	STM
1	0.512	0.649	0.683	0.719	0.579	0.629	0.643	0.683	0.633	0.692
2	1.857	0.161	1.187	1.12	1.218	1.377	1.497	1.777	1.59	1.823
3	1.245	0.895	0.941	0.891	1.026	1.457	0.937	1.41	0.842	0.944
4	1.084	0.876	1.26	1.214	0.974	1.266	1.125	1.358	0.996	1.352
5	0.472	0.617	0.875	0.741	0.827	1.271	0.187	0.335	0.273	0.449
6	0.316	0.327	0.332	0.353	0.273	0.371	0.692	0.8	0.774	1.631
7	1.093	1.521	2.074	3.186	3.19	3.385	3.08	2.941	2.906	3.456
X	0.94	0.721	1.05	1.175	1.155	1.394	1.166	1.329	1.145	1.478
SEM	0.205	0.167	0.207	0.352	0.359	0.366	0.355	0.327	0.33	0.379

RM 2-Way ANOVA - Control vs CCA Stim			
Source of Variation	P value	P value summary	Significant ?
Interaction	0.1414	ns	No
Days	0.7951	ns	No
CCA	0.0715	ns	No
Matching	< 0.0001	****	Yes

Bonferroni Post Hoc Test - Control vs CCA Stim				
Days	Difference	t	P value	Summary
1	0.219	1.428	P > 0.05	ns
2	-0.1245	0.8121	P > 0.05	ns
3	-0.2388	1.557	P > 0.05	ns
5	-0.1632	1.064	P > 0.05	ns
7	-0.3333	2.173	P > 0.05	ns

Table 4. Cytochome c oxidase activity following TUDCA/vehicle treatment with 2 or 7 days of CCA.

	Cytochrome c Oxidase Activity (U/g muscle)							
	VEHICLE				TUDCA			
	2 Days		7 Days		2 Days		7 Days	
n	CTR	STM	CTR	STM	CTR	STM	CTR	STM
1	17.395	19.783	21.165	25.567	18.888	18.922	19.382	24.68
2	14.69	16.857	11.056	14.537	21.686	17.497	14.392	21.14
3	16.166	16.431	18.188	21.652	19.613	14.81	17.378	22.334
4	20.926	20.517	21.635	25.977	18.009	19.715	19.911	21.259
5	27.529	24.057	17.761	23.929	24.356	22.274	24.407	26.898
6	20.065	16.763	18.58	19.954	19.161	19.434	14.383	18.043
X	19.462	19.068	18.064	21.936	20.285	18.775	18.309	22.392
SEM	1.8753	1.2201	1.5476	1.7535	0.9554	1.0156	1.5549	1.2558

RM 2-Way ANOVA - VEHICLE - Control vs CCA Stim			
Source of Variation	P value	Summary	Significant?
Interaction	0.0567	ns	No
Days	0.9047	ns	No
CCA	0.0965	ns	No
Matching	< 0.0001	****	Yes

Bonferroni Post Hoc Test - VEHICLE - Control vs CCA Stim				
Days	Difference	t	P value	Summary
2	0.1909	0.2086	P > 0.05	ns
7	-2.496	2.729	P < 0.05	*

RM 2-Way ANOVA - TUDCA- Control vs CCA Stim			
Source of Variation	P value	Summary	Significant?
Interaction	0.0042	**	Yes
Days	0.5565	ns	No
CCA	0.1122	ns	No
Matching	< 0.0001	****	Yes

Bonferroni Post Hoc Test - TUDCA - Control vs CCA Stim				
Days	Difference	t	P value	Summary
2	1.05	1.212	P > 0.05	ns
7	-3.128	3.609	P < 0.05	**

Bonferroni Post Hoc Test - MULTIPLE COMPARISONS - Control vs CCA Stim				
Comparison	Difference	t	P value	Summary
2 Days :VEH CON vs. 2 Days :TUD CON	-0.8233	0.406	P > 0.05	ns
2 Days :VEH CON vs. 7 Days :VEH CON	1.398	0.69	P > 0.05	ns
2 Days :VEH STM vs. 2 Days :TUD STM	0.2929	0.145	P > 0.05	ns
2 Days :VEH STM vs. 7 Days :VEH STM	-2.868	1.416	P > 0.05	ns
2 Days :TUD CON vs. 7 Days :TUD CON	1.976	0.976	P > 0.05	ns
2 Days :TUD STM vs. 7 Days :TUD STM	-3.617	1.786	P > 0.05	ns
7 Days :VEH CON vs. 7 Days :TUD CON	-0.2446	0.121	P > 0.05	ns
7 Days :VEH STM vs. 7 Days :TUD STM	-0.4564	0.225	P > 0.05	ns

Table 5A: mRNA expression of UPR^{ER} markers following TUDCA/vehicle treatment with 2 or 7 days of CCA.

	CHOP mRNA - Control vs. CCA Stim (ΔCt)							
	VEHICLE				TUDCA			
	2 Days		7 Days		2 Days		7 Days	
n	CTR	STM	CTR	STM	CTR	STM	CTR	STM
1	0.7556	3.0221	0.823	0.38	1.3124	0.836	4.516	0.4109
2	0.8686	1.5147	1.0954	1.9107	0.9891	4.7321	1.0056	3.3428
3	0.8125	1.3205	0.7376	1.3482	0.7296	2.6633	0.6332	1.4906
4	1.1784	6.1581	0.9642	1.4267	1.1372	3.739	0.7254	1.6876
5	0.9282	1.8541	0.8711	1.1735	0.7785	3.2835	0.7335	1.7946
6	1.0973	3.3295	0.7676	1.0135	1.0911	4.0555	0.7447	1.5544
7	0.9473	2.926	1.1452	1.845	0.8943	3.242	0.3711	1.1107
8	1.028	2.4799	0.9784	1.7837	0.7733	1.6287	0.7331	1.5663
X	0.952	2.8256	0.9228	1.3602	0.9632	3.0225	1.1828	1.6197
SEM	0.0507	0.5421	0.0526	0.1812	0.073	0.4526	0.4801	0.2912

RM 2-Way ANOVA - VEHICLE - Control vs CCA Stim			
Source of Variation	P value	Summary	Significant?
Interaction	0.0165	*	Yes
Days	0.0304	*	Yes
CCA	0.0006	***	Yes
Matching	0.2756	ns	No

Bonferroni Post Hoc Test - VEHICLE - Control vs CCA Stim				
Days	Difference	t	P value	Summary
2	-0.0187	5.021	P < 0.05	***
7	-0.0044	1.172	P > 0.05	ns

Bonferroni Post Hoc Test - MULTIPLE COMPARISONS - Control vs CCA Stim				
Comparison	Difference	t	P value	Summary
2:VEH CON vs. 2:TUD CON	-0.0112	0.024	P > 0.05	ns
2:VEH CON vs. 7:VEH CON	0.02917	0.063	P > 0.05	ns
2:VEH STM vs. 2:TUD STM	-0.1969	0.425	P > 0.05	ns
2:VEH STM vs. 7:VEH STM	1.465	3.165	P > 0.05	ns
2:TUD CON vs. 7:TUD CON	-0.2196	0.474	P > 0.05	ns
2:TUD STM vs. 7:TUD STM	1.403	3.03	P > 0.05	ns
7:VEH CON vs. 7:TUD CON	-0.26	0.562	P > 0.05	ns
7:VEH STM vs. 7:TUD STM	-0.2596	0.561	P > 0.05	ns

RM 2-Way ANOVA - TUDCA- Control vs CCA Stim			
Source of Variation	P value	Summary	Significant?
Interaction	0.0677	ns	No
Days	0.0754	ns	No
CCA	0.0087	**	Yes
Matching	0.8511	ns	No

Bonferroni Post Hoc Test - TUDCA - Control vs CCA Stim				
Days	Difference	t	P value	Summary
2	-0.0206	3.554	P < 0.05	**
7	-0.0044	0.7541	P > 0.05	ns

	CHOP mRNA - CCA Stim/Cotnrol (ΔΔCt)			
	2 Days		7 Days	
n	VEH	TUD	VEH	TUD
1	4	0.637	0.462	0.091
2	1.744	4.784	1.744	3.324
3	1.625	3.65	1.828	2.354
4	5.226	3.288	1.48	2.326
5	1.998	4.218	1.347	2.447
6	1.998	3.717	1.32	2.087
7	3.089	3.625	1.611	2.993
8	2.412	2.106	1.823	2.137
X	2.7615	3.25313	1.45188	2.21988
SEM	0.4498	0.46188	0.15805	0.33949

2-Way ANOVA - RELATIVE CHANGE - CCA Stim/Control			
Source of Variation	P value	Summary	Significant?
Interaction	0.7137	ns	No
Days	0.0039	**	Yes
TUDCA	0.1022	ns	No

Bonferroni Post Hoc Test - MULTIPLE COMPARISONS - Control vs CCA Stim				
Comparison	Difference	t	P value	Summary
2 Days :VEH vs. 2 Days :TUD	-0.4916	0.9325	P > 0.05	ns
2 Days :VEH vs. 7 Days :VEH	1.31	2.484	P > 0.05	ns
2 Days :VEH vs. 7 Days :TUD	0.5416	1.027	P > 0.05	ns
2 Days :TUD vs. 7 Days :VEH	1.801	3.417	P < 0.05	*
2 Days :TUD vs. 7 Days :TUD	1.033	1.96	P > 0.05	ns
7 Days :VEH vs. 7 Days :TUD	-0.768	1.457	P > 0.05	ns

HSP70 mRNA - Control vs. CCA Stim (ΔCt)								
	VEHICLE				TUDCA			
	2 Days		7 Days		2 Days		7 Days	
n	CTR	STM	CTR	STM	CTR	STM	CTR	STM
1	0.2424	2.9989	0.3419	1.9592	0.2059	1.2149	0.6123	1.1165
2	0.5869	1.7258	0.2175	2.6524	0.252	23.212	0.4771	1.9475
3	0.4947	6.4169	0.3472	2.0077	0.9513	21.779	0.3551	2.5401
4	0.3531	21.721	1.2849	3.1979	0.3637	15.662	0.7513	3.9477
5	0.7259	15.7	0.4929	1.5292	0.5966	31.539	0.6546	4.0914
6	0.4607	35.105	1.7355	1.794	0.8391	9.0968	0.3734	3.8304
7	0.6024	32.807	0.6616	1.0653	0.6164	22.857	0.8875	4.4458
8	0.4611	9.663	0.6383	2.517	0.3373	3.541	0.4239	2.3536
X	0.4909	15.767	0.715	2.0903	0.5203	16.113	0.5669	3.0341
SEM	0.0533	4.5994	0.1864	0.2391	0.0974	3.7687	0.0678	0.4256

RM 2-Way ANOVA - VEHICLE - Control vs CCA Stim			
Source of Variation	P value	Summary	Significant?
Interaction	0.0091	**	Yes
Days	0.0114	*	Yes
CCA	0.0028	**	Yes
Matching	0.4933	ns	No

Bonferroni Post Hoc Test - VEHICLE - Control vs CCA Stim				
Days	Difference	t	P value	Summary
2	-0.1528	4.697	P < 0.05	***
7	-0.0138	0.4229	P > 0.05	ns

Bonferroni Post Hoc Test - MULTIPLE COMPARISONS - Control vs CCA Stim				
Comparison	Difference	t	P value	Summary
2:VEH CON vs. 2:TUD CON	-0.0294	0.01	P > 0.05	ns
2:VEH CON vs. 7:VEH CON	-0.2241	0.075	P > 0.05	ns
2:VEH STM vs. 2:TUD STM	-0.3455	0.116	P > 0.05	ns
2:VEH STM vs. 7:VEH STM	13.68	4.581	P < 0.05	***
2:TUD CON vs. 7:TUD CON	-0.0466	0.016	P > 0.05	ns
2:TUD STM vs. 7:TUD STM	13.08	4.381	P < 0.05	**
7:VEH CON vs. 7:TUD CON	0.1481	0.05	P > 0.05	ns
7:VEH STM vs. 7:TUD STM	-0.9438	0.316	P > 0.05	ns

Source of Variation	P value	Summary	Significant?
Interaction	0.0036	**	Yes
Days	0.0043	**	Yes
CCA	0.0003	***	Yes
Matching	0.4711	ns	No

Bonferroni Post Hoc Test - TUDCA - Control vs CCA Stim				
Days	Difference	t	P value	Summary
2	-0.1559	5.869	P < 0.05	****
7	-0.0247	0.9287	P > 0.05	ns

HSP70 mRNA - CCA Stim/Cotnrol (ΔΔCt)				
	2 Days		7 Days	
n	VEH	TUD	VEH	TUD
1	12.369	5.899	5.73	1.823
2	2.941	92.107	12.196	4.082
3	12.971	22.895	5.782	7.152
4	61.512	43.063	2.489	5.255
5	21.629	52.867	3.103	6.251
6	21.629	10.841	1.034	10.259
7	54.462	37.078	1.61	5.01
8	20.957	10.498	3.943	5.553
X	26.0588	34.406	4.48588	5.67313
SEM	7.34614	10.1983	1.26105	0.86122

2-Way ANOVA - RELATIVE CHANGE - CCA Stim/Control			
Source of Variation	P value	Summary	Significant?
Interaction	0.5762	ns	No
Days	0.0005	***	Yes
TUDCA	0.4577	ns	No

Bonferroni Post Hoc Test - MULTIPLE COMPARISONS - Control vs CCA Stim				
Comparison	Difference	t	P value	Summary
2 Days :VEH vs. 2 Days :TUD	-8.347	0.9324	P > 0.05	ns
2 Days :VEH vs. 7 Days :VEH	21.57	2.41	P > 0.05	ns
2 Days :VEH vs. 7 Days :TUD	20.39	2.277	P > 0.05	ns
2 Days :TUD vs. 7 Days :VEH	29.92	3.342	P < 0.05	*
2 Days :TUD vs. 7 Days :TUD	28.73	3.209	P < 0.05	*
7 Days :VEH vs. 7 Days :TUD	-1.187	0.1326	P > 0.05	ns

ATF4 mRNA - Control vs. CCA Stim (ΔCt)								
	VEHICLE				TUDCA			
	2 Days		7 Days		2 Days		7 Days	
n	CTR	STM	CTR	STM	CTR	STM	CTR	STM
1	1.2427	1.0687	1.4504	0.9628	1.1063	0.5357	1.1515	1.1509
2	0.7392	0.9041	1.2853	0.7277	1.3618	2.4292	0.9743	0.8947
3	1.0459	1.2385	1.6621	0.8984	1.0541	2.2443	1.2012	0.6639
4	1.2263	2.6754	1.1224	0.6334	0.4517	0.9621	1.0916	0.6583
5	1.1267	1.5339	1.0007	0.7826	1.2297	2.2519	1.0024	0.9637
6	1.1044	2.8245	1.0664	0.8071	1.5141	2.9653	1.0892	0.8491
7	1.0587	1.9735	1.349	1.0472	1.3313	2.7157	1.0799	0.9028
8	0.8863	1.0281	1.101	0.773	1.1061	0.6183	1.0155	0.6649
X	1.0538	1.6558	1.2547	0.829	1.1444	1.8403	1.0757	0.8435
SEM	0.0598	0.2672	0.0796	0.0472	0.1132	0.3453	0.0271	0.0618

RM 2-Way ANOVA - VEHICLE - Control vs CCA Stim			
Source of Variation	P value	Summary	Significant?
Interaction	0.0011	**	Yes
Days	0.0732	ns	No
CCA	0.4926	ns	No
Matching	0.1756	ns	No

Bonferroni Post Hoc Test - VEHICLE - Control vs CCA Stim				
Days	Difference	t	P value	Summary
2	-0.0602	3.4	P < 0.05	**
7	0.04256	2.404	P > 0.05	ns

Bonferroni Post Hoc Test - MULTIPLE COMPARISONS - Control vs CCA Stim				
Comparison	Difference	t	P value	Summary
2:VEH CON vs. 2:TUD CON	-0.0906	0.3862	P > 0.05	ns
2:VEH CON vs. 7:VEH CON	-0.2009	0.8562	P > 0.05	ns
2:VEH STM vs. 2:TUD STM	-0.1845	0.7863	P > 0.05	ns
2:VEH STM vs. 7:VEH STM	0.8268	3.524	P < 0.05	*
2:TUD CON vs. 7:TUD CON	0.0687	0.2928	P > 0.05	ns
2:TUD STM vs. 7:TUD STM	0.9968	4.249	P < 0.05	**
7:VEH CON vs. 7:TUD CON	0.1789	0.7627	P > 0.05	ns
7:VEH STM vs. 7:TUD STM	-0.0145	0.0618	P > 0.05	ns

RM 2-Way ANOVA - TUDCA- Control vs CCA Stim			
Source of Variation	P value	Summary	Significant?
Interaction	0.007	**	Yes
Days	0.0272	*	Yes
CCA	0.137	ns	No
Matching	0.0807	ns	No

Bonferroni Post Hoc Test - TUDCA - Control vs CCA Stim				
Days	Difference	t	P value	Summary
2	-0.0696	3.348	P < 0.05	**
7	0.02322	1.117	P > 0.05	ns

ATF4 mRNA - CCA Stim/Cotnrol (ΔΔCt)				
	2 Days		7 Days	
n	VEH	TUD	VEH	TUD
1	0.86	0.484	0.664	1
2	1.223	1.784	0.566	0.918
3	1.184	2.129	0.541	0.553
4	2.182	2.13	0.564	0.603
5	1.361	1.831	0.782	0.961
6	1.361	1.958	0.757	0.78
7	1.864	2.04	0.776	0.836
8	1.16	0.559	0.702	0.655
X	1.399	1.61438	0.669	0.78825
SEM	0.15	0.24265	0.03563	0.05995

2-Way ANOVA - RELATIVE CHANGE - CCA Stim/Control			
Source of Variation	P value	Summary	Significant?
Interaction	0.7467	ns	No
Days	< 0.0001	****	Yes
TUDCA	0.2645	ns	No

Bonferroni Post Hoc Test - MULTIPLE COMPARISONS - Control vs CCA Stim				
Comparison	Difference	t	P value	Summary
2 Days :VEH vs. 2 Days :TUD	-0.215	1.036	P > 0.05	ns
2 Days :VEH vs. 7 Days :VEH	0.7304	3.518	P < 0.05	**
2 Days :VEH vs. 7 Days :TUD	0.6111	2.944	P < 0.05	*
2 Days :TUD vs. 7 Days :VEH	0.9454	4.554	P < 0.05	***
2 Days :TUD vs. 7 Days :TUD	0.8261	3.98	P < 0.05	**
7 Days :VEH vs. 7 Days :TUD	-0.1193	0.5744	P > 0.05	ns

XBP1s mRNA - Control vs. CCA Stim (ΔCt)								
	VEHICLE				TUDCA			
	2 Days		7 Days		2 Days		7 Days	
n	CTR	STM	CTR	STM	CTR	STM	CTR	STM
1	1.1404	0.8391	1.5421	0.9739	1.4351	0.7626	1.3222	0.8147
2	0.9079	2.5276	1.3647	0.555	1.3707	10.266	0.9619	0.6891
3	0.9757	1.8008	2.7715	0.7353	1.4031	9.7295	1.8532	0.8036
4	1.4397	14.92	1.3271	0.564	1.018	1.7526	1.6922	0.8009
5	1.8593	6.9837	1.7803	1.0854	1.7778	14.615	2.1868	1.4964
6	1.2686	15.608	1.7756	0.5811	1.7186	10.526	1.0303	0.9786
7	0.9078	4.9679	1.2307	0.6995	1.2403	12.081	2.5317	1.3751
8	1.3393	1.8933	1.2302	1.1316	1.2661	1.499	1.2797	0.5763
X	1.2298	6.1926	1.6278	0.7907	1.4037	7.6539	1.6072	0.9418
SEM	0.1145	2.0994	0.1811	0.0844	0.0882	1.9255	0.198	0.1157

RM 2-Way ANOVA - VEHICLE - Control vs CCA Stim			
Source of Variation	P value	Summary	Significant?
Interaction	0.014	*	Yes
Days	0.036	*	Yes
CCA	0.0657	ns	No
Matching	0.4373	ns	No

Bonferroni Post Hoc Test - VEHICLE - Control vs CCA Stim				
Days	Difference	t	P value	Summary
2	-0.005	3.397	P < 0.05	**
7	0.00084	0.5729	P > 0.05	ns

Bonferroni Post Hoc Test - MULTIPLE COMPARISONS - Control vs CCA Stim				
Comparison	Difference	t	P value	Summary
2:VEH CON vs. 2:TUD CON	-0.1739	0.1212	P > 0.05	ns
2:VEH CON vs. 7:VEH CON	-0.3979	0.2775	P > 0.05	ns
2:VEH STM vs. 2:TUD STM	-1.461	1.019	P > 0.05	ns
2:VEH STM vs. 7:VEH STM	5.402	3.766	P < 0.05	*
2:TUD CON vs. 7:TUD CON	-0.2035	0.1419	P > 0.05	ns
2:TUD STM vs. 7:TUD STM	6.712	4.68	P < 0.05	***
7:VEH CON vs. 7:TUD CON	0.0205	0.0143	P > 0.05	ns
7:VEH STM vs. 7:TUD STM	-0.1511	0.1054	P > 0.05	ns

RM 2-Way ANOVA - TUDCA- Control vs CCA Stim			
Source of Variation	P value	Summary	Significant?
Interaction	0.0025	**	Yes
Days	0.0058	**	Yes
CCA	0.0101	*	Yes
Matching	0.4093	ns	No

Bonferroni Post Hoc Test - TUDCA - Control vs CCA Stim				
Days	Difference	t	P value	Summary
2	-0.0063	4.703	P < 0.05	***
7	0.00067	0.5006	P > 0.05	ns

XBP1s mRNA - CCA Stim/Cotnrol (ΔΔCt)				
	2 Days		7 Days	
n	VEH	TUD	VEH	TUD
1	0.736	0.531	0.632	0.616
2	2.784	7.489	0.407	0.716
3	1.846	6.934	0.265	0.434
4	10.363	1.722	0.425	0.473
5	3.756	8.221	0.61	0.684
6	3.756	6.125	0.327	0.95
7	5.473	9.741	0.568	0.543
8	1.414	1.184	0.92	0.45
X	3.766	5.24338	0.51925	0.60825
SEM	1.08396	1.25966	0.07404	0.06155

2-Way ANOVA - RELATIVE CHANGE - CCA Stim/Control			
Source of Variation	P value	Summary	Significant?
Interaction	0.4113	ns	No
Days	< 0.0001	****	Yes
TUDCA	0.3548	ns	No

Bonferroni Post Hoc Test - MULTIPLE COMPARISONS - Control vs CCA Stim				
Comparison	Difference	t	P value	Summary
2 Days :VEH vs. 2 Days :TUD	-1.477	1.255	P > 0.05	ns
2 Days :VEH vs. 7 Days :VEH	3.247	2.758	P > 0.05	ns
2 Days :VEH vs. 7 Days :TUD	3.158	2.683	P > 0.05	ns
2 Days :TUD vs. 7 Days :VEH	4.724	4.013	P < 0.05	**
2 Days :TUD vs. 7 Days :TUD	4.635	3.938	P < 0.05	**
7 Days :VEH vs. 7 Days :TUD	-0.089	0.07561	P > 0.05	ns

BiP mRNA - Control vs. CCA Stim (ΔCt)								
	VEHICLE				TUDCA			
	2 Days		7 Days		2 Days		7 Days	
n	CTR	STM	CTR	STM	CTR	STM	CTR	STM
1	0.4285	0.587	0.5028	0.682	0.4293	0.7316	0.397	0.5709
2	0.6006	1.2042	0.7097	1.0213	0.5976	3.8707	0.6839	1.1851
3	0.471	0.6815	0.6863	0.5473	0.5272	2.9145	0.5929	0.6007
4	0.6866	4.5322	0.5513	0.7854	0.9404	3.0976	0.6007	0.6895
5	0.5274	0.8216	0.5614	0.5356	0.5651	2.5362	0.6072	0.7256
6	0.4417	3.7677	0.6617	0.6413	0.4635	1.6914	0.4918	0.7315
7	0.4862	1.3579	0.6043	0.7422	0.5156	2.8782	0.3627	0.6107
8	0.5265	1.5411	0.496	0.6511	0.4518	1.2224	0.5129	0.6808
X	0.5211	1.8116	0.5967	0.7008	0.5613	2.3678	0.5312	0.7244
SEM	0.0306	0.5284	0.0291	0.0549	0.0578	0.3738	0.0392	0.0691

RM 2-Way ANOVA - VEHICLE - Control vs CCA Stim			
Source of Variation	P value	Summary	Significant?
Interaction	0.0379	*	Yes
Days	0.0797	ns	No
CCA	0.0174	*	Yes
Matching	0.4171	ns	No

Bonferroni Post Hoc Test - VEHICLE - Control vs CCA Stim				
Days	Difference	t	P value	Summary
2	-0.1291	3.527	P < 0.05	**
7	-0.0104	0.2844	P > 0.05	ns

Bonferroni Post Hoc Test - MULTIPLE COMPARISONS - Control vs CCA Stim				
Comparison	Difference	t	P value	Summary
2:VEH CON vs. 2:TUD CON	-0.0403	0.1223	P > 0.05	ns
2:VEH CON vs. 7:VEH CON	-0.0757	0.2298	P > 0.05	ns
2:VEH STM vs. 2:TUD STM	-0.5562	1.69	P > 0.05	ns
2:VEH STM vs. 7:VEH STM	1.111	3.375	P < 0.05	*
2:TUD CON vs. 7:TUD CON	0.0302	0.0916	P > 0.05	ns
2:TUD STM vs. 7:TUD STM	1.643	4.993	P < 0.05	***
7:VEH CON vs. 7:TUD CON	0.0656	0.1992	P > 0.05	ns
7:VEH STM vs. 7:TUD STM	-0.0236	0.0716	P > 0.05	ns

RM 2-Way ANOVA - TUDCA- Control vs CCA Stim			
Source of Variation	P value	Summary	Significant?
Interaction	0.0004	***	Yes
Days	0.0014	**	Yes
CCA	< 0.0001	****	Yes
Matching	0.2395	ns	No

Bonferroni Post Hoc Test - TUDCA - Control vs CCA Stim				
Days	Difference	t	P value	Summary
2	-0.1807	7.348	P < 0.05	****
7	-0.0193	0.7858	P > 0.05	ns

BiP mRNA - CCA Stim/Cotnrol (ΔΔCt)				
	2 Days		7 Days	
n	VEH	TUD	VEH	TUD
1	1.37	1.704	1.356	1.438
2	2.005	6.478	1.439	1.733
3	1.447	5.529	0.797	1.013
4	6.601	3.294	1.425	1.148
5	1.558	4.488	0.954	1.195
6	1.558	3.649	0.969	1.487
7	2.793	5.582	1.228	1.684
8	2.927	2.705	1.313	1.327
X	2.53238	4.17863	1.18513	1.37813
SEM	0.61938	0.5753	0.08662	0.09037

2-Way ANOVA - RELATIVE CHANGE - CCA Stim/Control			
Source of Variation	P value	Summary	Significant?
Interaction	0.1001	ns	No
Days	< 0.0001	****	Yes
TUDCA	0.0401	*	Yes

Bonferroni Post Hoc Test - MULTIPLE COMPARISONS - Control vs CCA Stim				
Comparison	Difference	t	P value	Summary
2 Days :VEH vs. 2 Days :TUD	-1.646	2.724	P > 0.05	ns
2 Days :VEH vs. 7 Days :VEH	1.347	2.23	P > 0.05	ns
2 Days :VEH vs. 7 Days :TUD	1.154	1.91	P > 0.05	ns
2 Days :TUD vs. 7 Days :VEH	2.994	4.954	P < 0.05	***
2 Days :TUD vs. 7 Days :TUD	2.801	4.635	P < 0.05	***
7 Days :VEH vs. 7 Days :TUD	-0.193	0.3194	P > 0.05	ns

Table 5B: mRNA expression of UPR^{mt} markers following TUDCA/vehicle treatment with 2 or 7 days of CCA.

	CPN10 mRNA - Control vs. CCA Stim (ΔCt)							
	VEHICLE				TUDCA			
	2 Days		7 Days		2 Days		7 Days	
n	CTR	STM	CTR	STM	CTR	STM	CTR	STM
1	0.8172	1.6738	1.0066	2.0313	0.7933	1.1418	0.7987	2.0462
2	0.7691	1.0536	0.9909	1.7024	0.7477	1.6532	0.8827	1.6976
3	0.8135	1.1151	0.9123	1.5452	0.8842	1.5434	0.9051	1.5103
4	1.1842	1.9704	1.0257	1.3504	0.9551	1.8814	0.9497	1.2744
5	0.8703	1.2898	0.9527	1.4215	0.9141	1.6442	0.8925	1.4726
6	0.8477	1.5045	0.8099	1.3706	0.828	1.3843	0.7508	1.24
7	0.8591	1.7832	0.8448	1.5171	0.8343	1.217	0.7477	1.364
8	1.0285	1.6342	1.0251	1.4356	0.855	1.1686	0.7417	1.3419
X	0.8987	1.5031	0.946	1.5468	0.8515	1.4542	0.8336	1.4934
SEM	0.0489	0.115	0.0293	0.0799	0.0234	0.0951	0.0294	0.0945

RM 2-Way ANOVA - VEHICLE - Control vs CCA Stim			
Source of Variation	P value	Summary	Significant?
Interaction	0.9759	ns	No
Days	0.6199	ns	No
CCA	< 0.0001	****	Yes
Matching	0.0587	ns	No

Bonferroni Post Hoc Test - VEHICLE - Control vs CCA Stim				
Days	Difference	t	P value	Summary
2	-0.0604	7.34	P < 0.05	****
7	-0.0601	7.297	P < 0.05	****

Bonferroni Post Hoc Test - MULTIPLE COMPARISONS - Control vs CCA Stim				
Comparison	Difference	t	P value	Summary
2:VEH CON vs. 2:TUD CON	0.0472	0.4595	P > 0.05	ns
2:VEH CON vs. 7:VEH CON	-0.0473	0.4602	P > 0.05	ns
2:VEH STM vs. 2:TUD STM	0.0488	0.4751	P > 0.05	ns
2:VEH STM vs. 7:VEH STM	-0.0437	0.4253	P > 0.05	ns
2:TUD CON vs. 7:TUD CON	0.0179	0.1737	P > 0.05	ns
2:TUD STM vs. 7:TUD STM	-0.0391	0.3808	P > 0.05	ns
7:VEH CON vs. 7:TUD CON	0.1124	1.093	P > 0.05	ns
7:VEH STM vs. 7:TUD STM	0.0534	0.5196	P > 0.05	ns

RM 2-Way ANOVA - TUDCA- Control vs CCA Stim			
Source of Variation	P value	Summary	Significant?
Interaction	0.6667	ns	No
Days	0.8879	ns	No
CCA	< 0.0001	****	Yes
Matching	0.3105	ns	No

Bonferroni Post Hoc Test - TUDCA - Control vs CCA Stim				
Days	Difference	t	P value	Summary
2	-0.0603	6.579	P < 0.05	****
7	-0.066	7.202	P < 0.05	****

	CPN10 mRNA - CCA Stim/Cotnrol (ΔΔCt)			
	2 Days		7 Days	
n	VEH	TUD	VEH	TUD
1	2.048	1.439	2.018	2.562
2	1.37	2.211	1.718	1.923
3	1.371	1.746	1.694	1.669
4	1.664	1.97	1.317	1.342
5	1.482	1.799	1.492	1.65
6	1.482	1.672	1.692	1.652
7	2.076	1.459	1.796	1.824
8	1.589	1.367	1.4	1.809
X	1.635	1.70788	1.64088	1.80388
SEM	0.1	0.10206	0.08048	0.12447

2-Way ANOVA - RELATIVE CHANGE - CCA Stim/Control			
Source of Variation	P value	Summary	Significant?
Interaction	0.6637	ns	No
Days	0.6251	ns	No
TUDCA	0.2616	ns	No

Bonferroni Post Hoc Test - MULTIPLE COMPARISONS - Control vs CCA Stim				
Comparison	Difference	t	P value	Summary
2 Days :VEH vs. 2 Days :TUD	-0.0726	0.4994	P > 0.05	ns
2 Days :VEH vs. 7 Days :VEH	-0.0056	0.03868	P > 0.05	ns
2 Days :VEH vs. 7 Days :TUD	-0.1686	1.16	P > 0.05	ns
2 Days :TUD vs. 7 Days :VEH	0.067	0.4607	P > 0.05	ns
2 Days :TUD vs. 7 Days :TUD	-0.096	0.6602	P > 0.05	ns
7 Days :VEH vs. 7 Days :TUD	-0.163	1.121	P > 0.05	ns

HSP60 mRNA - Control vs. CCA Stim (ΔCt)								
	VEHICLE				TUDCA			
	2 Days		7 Days		2 Days		7 Days	
n	CTR	STM	CTR	STM	CTR	STM	CTR	STM
1	0.7626	1.1203	0.9245	0.9393	0.5555	0.6962	0.5842	1.1922
2	0.8107	0.8606	1.0075	1.2533	0.8232	1.3092	0.8939	1.2347
3	0.7871	0.5311	0.8341	1.091	0.5666	0.8757	0.6863	0.9249
4	0.9361	0.7659	0.7373	1.0466	0.7774	0.7736	0.7718	0.8036
5	0.8269	1.272	0.7842	1.2159	0.878	0.9313	0.3786	0.5789
6	0.8405	0.8602	0.7853	0.9514	0.64	0.6523	0.6068	1.0878
X	0.8273	0.9017	0.8455	1.0829	0.7068	0.8731	0.6536	0.9703
SEM	0.0246	0.1071	0.0415	0.0535	0.0562	0.0972	0.072	0.1026

RM 2-Way ANOVA - VEHICLE - Control vs CCA Stim			
Source of Variation	P value	Summary	Significant?
Interaction	0.23	ns	No
Days	0.1578	ns	No
CCA	0.0346	*	Yes
Matching	0.4714	ns	No

Bonferroni Post Hoc Test - VEHICLE - Control vs CCA Stim				
Days	Difference	t	P value	Summary
2	-0.0074	0.8243	P > 0.05	ns
7	-0.0237	2.632	P > 0.05	ns

Bonferroni Post Hoc Test - MULTIPLE COMPARISONS - Control vs CCA Stim				
Comparison	Difference	t	P value	Summary
2:VEH CON vs. 2:TUD CON	0.1392	1.578	P > 0.05	ns
2:VEH CON vs. 7:VEH CON	-0.0242	0.2741	P > 0.05	ns
2:VEH STM vs. 2:TUD STM	-0.0754	0.8552	P > 0.05	ns
2:VEH STM vs. 7:VEH STM	-0.1437	1.628	P > 0.05	ns
2:TUD CON vs. 7:TUD CON	0.0187	0.2115	P > 0.05	ns
2:TUD STM vs. 7:TUD STM	-0.0381	0.4322	P > 0.05	ns
7:VEH CON vs. 7:TUD CON	0.182	2.063	P > 0.05	ns
7:VEH STM vs. 7:TUD STM	0.0301	0.3411	P > 0.05	ns

RM 2-Way ANOVA - TUDCA- Control vs CCA Stim			
Source of Variation	P value	Summary	Significant?
Interaction	0.2228	ns	No
Days	0.8363	ns	No
CCA	0.0019	**	Yes
Matching	0.0391	*	Yes

Bonferroni Post Hoc Test - TUDCA - Control vs CCA Stim				
Days	Difference	t	P value	Summary
2	-0.0166	2.032	P > 0.05	ns
7	-0.0317	3.87	P < 0.05	**

HSP60 mRNA - CCA Stim/Cotnrol (ΔΔCt)				
	2 Days		7 Days	
n	VEH	TUD	VEH	TUD
1	1.469	1.253	1.016	2.041
2	1.062	1.59	1.244	1.381
3	0.675	1.546	1.308	1.348
4	0.933	0.995	1.42	1.041
5	1.538	1.061	1.551	1.529
6	1.023	1.019	1.212	1.793
X	1.11667	1.244	1.29183	1.52217
SEM	0.13444	0.1091	0.07497	0.14426

2-Way ANOVA - RELATIVE CHANGE - CCA Stim/Control			
Source of Variation	P value	Summary	Significant?
Interaction	0.6692	ns	No
Days	0.0708	ns	No
TUDCA	0.1477	ns	No

Bonferroni Post Hoc Test - MULTIPLE COMPARISONS - Control vs CCA Stim				
Comparison	Difference	t	P value	Summary
2 Days :VEH vs. 2 Days :TUD	-0.1273	0.7582	P > 0.05	ns
2 Days :VEH vs. 7 Days :VEH	-0.1752	1.043	P > 0.05	ns
2 Days :VEH vs. 7 Days :TUD	-0.4055	2.414	P > 0.05	ns
2 Days :TUD vs. 7 Days :VEH	-0.0478	0.2848	P > 0.05	ns
2 Days :TUD vs. 7 Days :TUD	-0.2782	1.656	P > 0.05	ns
7 Days :VEH vs. 7 Days :TUD	-0.2303	1.371	P > 0.05	ns

ClpP mRNA - Control vs. CCA Stim (ΔCt)								
	VEHICLE				TUDCA			
	2 Days		7 Days		2 Days		7 Days	
n	CTR	STM	CTR	STM	CTR	STM	CTR	STM
1	0.3004	0.4236	0.4319	0.5045	0.3104	0.8868	0.1992	0.4481
2	0.2907	0.4503	0.3279	0.4404	0.2838	0.523	0.3509	0.5195
3	0.2983	0.2891	0.3249	0.322	0.2707	0.4009	0.1934	0.3876
4	0.4186	1.461	0.4481	0.4375	2.1871	2.703	0.3477	0.543
5	0.2547	0.3298	0.3237	0.3433	0.279	0.3421	0.3357	0.4186
6	0.2619	0.4014	0.2259	0.4181	0.3201	0.3646	0.3029	0.4957
7	0.2694	0.2953	0.2365	0.5865	0.2844	0.4144	0.1865	0.2293
8	0.4594	0.5123	0.3949	0.6037	0.3135	0.7982	0.3257	0.54
X	0.3192	0.5203	0.3392	0.457	0.5311	0.8041	0.2803	0.4477
SEM	0.0271	0.1372	0.0291	0.0363	0.2367	0.2807	0.0261	0.0371

RM 2-Way ANOVA - VEHICLE - Control vs CCA Stim			
Source of Variation	P value	Summary	Significant?
Interaction	0.5307	ns	No
Days	0.7946	ns	No
CCA	0.0276	*	Yes
Matching	0.2011	ns	No

Bonferroni Post Hoc Test - VEHICLE - Control vs CCA Stim				
Days	Difference	t	P value	Summary
2	-0.0002	2.193	P > 0.05	ns
7	-0.0001	1.284	P > 0.05	ns

Bonferroni Post Hoc Test - MULTIPLE COMPARISONS - Control vs CCA Stim				
Comparison	Difference	t	P value	Summary
2:VEH CON vs. 2:TUD CON	-0.212	1.065	P > 0.05	ns
2:VEH CON vs. 7:VEH CON	-0.0201	0.1007	P > 0.05	ns
2:VEH STM vs. 2:TUD STM	-0.2838	1.425	P > 0.05	ns
2:VEH STM vs. 7:VEH STM	0.0634	0.3181	P > 0.05	ns
2:TUD CON vs. 7:TUD CON	0.2509	1.26	P > 0.05	ns
2:TUD STM vs. 7:TUD STM	0.3564	1.79	P > 0.05	ns
7:VEH CON vs. 7:TUD CON	0.059	0.2961	P > 0.05	ns
7:VEH STM vs. 7:TUD STM	0.0093	0.0465	P > 0.05	ns

RM 2-Way ANOVA - TUDCA- Control vs CCA Stim			
Source of Variation	P value	Summary	Significant?
Interaction	0.2139	ns	No
Days	0.2596	ns	No
CCA	< 0.0001	****	Yes
Matching	< 0.0001	****	Yes

Bonferroni Post Hoc Test - TUDCA - Control vs CCA Stim				
Days	Difference	t	P value	Summary
2	-0.0003	4.764	P < 0.05	***
7	-0.0002	2.923	P < 0.05	*

ClpP mRNA - CCA Stim/Cotnrol (ΔΔCt)				
	2 Days		7 Days	
n	VEH	TUD	VEH	TUD
1	1.41	2.857	1.168	2.25
2	1.549	1.843	1.343	1.48
3	0.969	1.481	0.991	2.004
4	3.49	1.236	0.976	1.562
5	1.295	1.226	1.061	1.247
6	1.295	1.139	1.851	1.637
7	1.096	1.457	2.48	1.23
8	1.115	2.546	1.529	1.658
X	1.52738	1.72313	1.42488	1.6335
SEM	0.28791	0.22883	0.18422	0.12384

2-Way ANOVA - RELATIVE CHANGE - CCA Stim/Control			
Source of Variation	P value	Summary	Significant?
Interaction	0.9763	ns	No
Days	0.6581	ns	No
TUDCA	0.3546	ns	No

Bonferroni Post Hoc Test - MULTIPLE COMPARISONS - Control vs CCA Stim				
Comparison	Difference	t	P value	Summary
2 Days :VEH vs. 2 Days :TUD	-0.1958	0.6444	P > 0.05	ns
2 Days :VEH vs. 7 Days :VEH	0.1025	0.3374	P > 0.05	ns
2 Days :VEH vs. 7 Days :TUD	-0.1061	0.3494	P > 0.05	ns
2 Days :TUD vs. 7 Days :VEH	0.2983	0.9819	P > 0.05	ns
2 Days :TUD vs. 7 Days :TUD	0.08963	0.2951	P > 0.05	ns
7 Days :VEH vs. 7 Days :TUD	-0.2086	0.6868	P > 0.05	ns

Table 5C: mRNA expression of PGC-1α following TUDCA/vehicle treatment with 2 or 7 days of CCA.

PGC-1α mRNA - Control vs. CCA Stim (ΔCt)								
	VEHICLE				TUDCA			
	2 Days		7 Days		2 Days		7 Days	
n	CTR	STM	CTR	STM	CTR	STM	CTR	STM
1	0.408	6.5656	0.5495	3.0756	0.2388	0.9916	0.2522	4.7204
2	0.6022	2.3407	0.8689	6.5926	0.7103	6.0618	0.7161	6.417
3	0.4973	3.2151	0.4761	5.1879	0.2678	4.4429	0.4061	3.9583
4	0.4166	1.1524	0.656	2.4948	0.422	4.3953	0.4133	1.758
5	0.7844	4.4202	0.8264	2.3656	0.8827	4.9149	0.6749	3.3711
6	0.56	2.5276	0.4495	5.3152	0.661	4.7758	0.5398	2.5571
7	1.2298	8.8428	1.7781	7.0187	1.2111	7.5937	0.4025	4.5247
8	0.7	4.8954	0.5854	3.9069	0.4658	2.4299	0.6242	2.9293
X	0.6498	4.245	0.7737	4.4946	0.6074	4.4507	0.5037	3.7795
SEM	0.0948	0.8882	0.1532	0.6383	0.1164	0.7177	0.0569	0.5158

RM 2-Way ANOVA - VEHICLE - Control vs CCA Stim			
Source of Variation	P value	Summary	Significant?
Interaction	0.9023	ns	No
Days	0.7607	ns	No
CCA	< 0.0001	****	Yes
Matching	0.2557	ns	No

Bonferroni Post Hoc Test - VEHICLE - Control vs CCA Stim				
Days	Difference	t	P value	Summary
2	-0.036	5.057	P < 0.05	***
7	-0.0372	5.233	P < 0.05	***

Bonferroni Post Hoc Test - MULTIPLE COMPARISONS - Control vs CCA Stim				
Comparison	Difference	t	P value	Summary
2:VEH CON vs. 2:TUD CON	0.0424	0.0595	P > 0.05	ns
2:VEH CON vs. 7:VEH CON	-0.1239	0.1741	P > 0.05	ns
2:VEH STM vs. 2:TUD STM	-0.2058	0.2891	P > 0.05	ns
2:VEH STM vs. 7:VEH STM	-0.2497	0.3508	P > 0.05	ns
2:TUD CON vs. 7:TUD CON	0.1038	0.1458	P > 0.05	ns
2:TUD STM vs. 7:TUD STM	0.6712	0.943	P > 0.05	ns
7:VEH CON vs. 7:TUD CON	0.2701	0.3794	P > 0.05	ns
7:VEH STM vs. 7:TUD STM	0.7152	1.005	P > 0.05	ns

RM 2-Way ANOVA - TUDCA- Control vs CCA Stim			
Source of Variation	P value	Summary	Significant?
Interaction	0.495	ns	No
Days	0.4375	ns	No
CCA	< 0.0001	****	Yes
Matching	0.2546	ns	No

Bonferroni Post Hoc Test - TUDCA - Control vs CCA Stim				
Days	Difference	t	P value	Summary
2	-0.0384	6.711	P < 0.05	****
7	-0.0328	5.72	P < 0.05	***

PGC-1α mRNA - CCA Stim/Cotnrol (ΔΔCt)				
	2 Days		7 Days	
n	VEH	TUD	VEH	TUD
1	16.093	4.152	5.597	18.716
2	3.887	8.535	7.587	8.961
3	6.465	16.591	10.898	9.746
4	2.766	10.416	3.803	4.254
5	5.635	5.568	2.862	4.995
6	5.635	7.225	11.826	4.737
7	7.19	6.27	3.947	11.243
8	6.994	5.217	6.673	4.693
X	6.83313	7.99675	6.64913	8.41813
SEM	1.42757	1.41414	1.16943	1.75545

2-Way ANOVA - RELATIVE CHANGE - CCA Stim/Control			
Source of Variation	P value	Summary	Significant?
Interaction	0.8369	ns	No
Days	0.9356	ns	No
TUDCA	0.3227	ns	No

Bonferroni Post Hoc Test - MULTIPLE COMPARISONS - Control vs CCA Stim				
Comparison	Difference	t	P value	Summary
2 Days :VEH vs. 2 Days :TUD	-1.164	0.5649	P > 0.05	ns
2 Days :VEH vs. 7 Days :VEH	0.184	0.08932	P > 0.05	ns
2 Days :VEH vs. 7 Days :TUD	-1.585	0.7694	P > 0.05	ns
2 Days :TUD vs. 7 Days :VEH	1.348	0.6542	P > 0.05	ns
2 Days :TUD vs. 7 Days :TUD	-0.4214	0.2046	P > 0.05	ns
7 Days :VEH vs. 7 Days :TUD	-1.769	0.8588	P > 0.05	ns

Table 5D: mRNA expression of autophagy markers following TUDCA/vehicle treatment with 2 or 7 days of CCA.

p62 mRNA - Control vs. CCA Stim (ΔCt)								
	VEHICLE				TUDCA			
	2 Days		7 Days		2 Days		7 Days	
n	CTR	STM	CTR	STM	CTR	STM	CTR	STM
1	0.1468	0.2505	0.2503	0.1662	0.1785	0.3055	0.2148	0.1583
2	0.2137	0.4475	0.1973	0.1719	0.293	0.3647	0.2067	0.2233
3	0.1397	0.226	0.1432	0.1374	0.16	0.2755	0.1503	0.1282
4	0.1914	0.5728	0.205	0.1663	0.2353	0.4854	0.2015	0.1844
5	0.1565	0.2483	0.1665	0.1422	0.1935	0.3625	0.2439	0.2036
6	0.1916	0.2605	0.1564	0.1423	0.1998	0.4213	0.1798	0.2186
X	0.1733	0.3343	0.1864	0.1544	0.21	0.3692	0.1995	0.1861
SEM	0.0121	0.0581	0.016	0.0062	0.0195	0.0312	0.013	0.0151

RM 2-Way ANOVA - VEHICLE - Control vs CCA Stim			
Source of Variation	P value	Summary	Significant?
Interaction	0.0038	**	Yes
Days	0.0397	*	Yes
CCA	0.0315	*	Yes
Matching	0.1693	ns	No

Bonferroni Post Hoc Test - VEHICLE - Control vs CCA Stim				
Days	Difference	t	P value	Summary
2	-0.161	4.413	P < 0.05	**
7	0.03206	0.8789	P > 0.05	ns

Bonferroni Post Hoc Test - MULTIPLE COMPARISONS - Control vs CCA Stim				
Comparison	Difference	t	P value	Summary
2:VEH CON vs. 2:TUD CON	-0.0368	0.9853	P > 0.05	ns
2:VEH CON vs. 7:VEH CON	-0.0132	0.3534	P > 0.05	ns
2:VEH STM vs. 2:TUD STM	-0.0349	0.9353	P > 0.05	ns
2:VEH STM vs. 7:VEH STM	0.1799	4.822	P < 0.05	***
2:TUD CON vs. 7:TUD CON	0.0105	0.2824	P > 0.05	ns
2:TUD STM vs. 7:TUD STM	0.1831	4.908	P < 0.05	***
7:VEH CON vs. 7:TUD CON	-0.013	0.3496	P > 0.05	ns
7:VEH STM vs. 7:TUD STM	-0.0317	0.8492	P > 0.05	ns

RM 2-Way ANOVA - TUDCA- Control vs CCA Stim			
Source of Variation	P value	Summary	Significant?
Interaction	0.0002	***	Yes
Days	0.0032	**	Yes
CCA	0.0009	***	Yes
Matching	0.0736	ns	No

Bonferroni Post Hoc Test - TUDCA - Control vs CCA Stim				
Days	Difference	t	P value	Summary
2	-0.1591	7.223	P < 0.05	****
7	0.01342	0.6092	P > 0.05	ns

p62 mRNA - CCA Stim/Cotnrol (ΔΔCt)				
	2 Days		7 Days	
n	VEH	TUD	VEH	TUD
1	1.706	1.711	0.664	0.737
2	2.094	1.245	0.871	1.08
3	1.618	1.722	0.96	0.853
4	1.618	2.063	0.811	0.915
5	1.587	1.873	0.854	0.835
6	1.36	2.108	0.91	1.216
X	1.664	1.787	0.845	0.93933
SEM	0.098	0.12785	0.04168	0.07216

2-Way ANOVA - RELATIVE CHANGE - CCA Stim/Control			
Source of Variation	P value	Summary	Significant?
Interaction	0.8754	ns	No
Days	< 0.0001	****	Yes
TUDCA	0.2447	ns	No

Bonferroni Post Hoc Test - MULTIPLE COMPARISONS - Control vs CCA Stim				
Comparison	Difference	t	P value	Summary
2 Days :VEH vs. 2 Days :TUD	-0.1232	0.9598	P > 0.05	ns
2 Days :VEH vs. 7 Days :VEH	0.8188	6.381	P < 0.05	****
2 Days :VEH vs. 7 Days :TUD	0.7245	5.646	P < 0.05	****
2 Days :TUD vs. 7 Days :VEH	0.942	7.341	P < 0.05	****
2 Days :TUD vs. 7 Days :TUD	0.8477	6.606	P < 0.05	****
7 Days :VEH vs. 7 Days :TUD	-0.0943	0.7351	P > 0.05	ns

LC3 mRNA - Control vs. CCA Stim (ΔCt)								
	VEHICLE				TUDCA			
	2 Days		7 Days		2 Days		7 Days	
n	CTR	STM	CTR	STM	CTR	STM	CTR	STM
1	0.9199	0.8327	1.2557	1.0074	1.3838	0.9313	1.0577	0.8917
2	1.615	1.7059	2.2917	1.8048	2.1117	1.8999	2.666	1.7513
3	1.7717	1.4959	1.8096	1.5554	2.2806	2.1897	1.555	1.6048
4	1.546	1.7037	1.624	1.7522	1.7705	1.4413	1.8206	1.8198
5	1.7087	1.854	1.7494	1.4282	2.0739	2.0252	1.6722	1.4487
6	1.5564	1.1371	1.3593	1.3817	1.8834	1.6563	3.0556	2.2654
7	1.7905	1.5522	1.5825	1.5342	1.9061	2.2628	1.3162	1.3005
X	1.5583	1.4688	1.6675	1.4948	1.9157	1.7724	1.8776	1.5832
SEM	0.1127	0.1365	0.1282	0.1003	0.1093	0.1776	0.2737	0.1638

RM 2-Way ANOVA - VEHICLE - Control vs CCA Stim			
Source of Variation	P value	Summary	Significant?
Interaction	0.497	ns	No
Days	0.6788	ns	No
CCA	0.0474	*	Yes
Matching	0.0009	***	Yes

Bonferroni Post Hoc Test - VEHICLE - Control vs CCA Stim				
Days	Difference	t	P value	Summary
2	0.00895	1.067	P > 0.05	ns
7	0.01726	2.057	P > 0.05	ns

Bonferroni Post Hoc Test - MULTIPLE COMPARISONS - Control vs CCA Stim				
Comparison	Difference	t	P value	Summary
2:VEH CON vs. 2:TUD CON	-0.3574	1.586	P > 0.05	ns
2:VEH CON vs. 7:VEH CON	-0.1092	0.4845	P > 0.05	ns
2:VEH STM vs. 2:TUD STM	-0.3036	1.347	P > 0.05	ns
2:VEH STM vs. 7:VEH STM	-0.026	0.1156	P > 0.05	ns
2:TUD CON vs. 7:TUD CON	0.0381	0.1692	P > 0.05	ns
2:TUD STM vs. 7:TUD STM	0.1892	0.8398	P > 0.05	ns
7:VEH CON vs. 7:TUD CON	-0.2101	0.9328	P > 0.05	ns
7:VEH STM vs. 7:TUD STM	-0.0883	0.392	P > 0.05	ns

RM 2-Way ANOVA - TUDCA- Control vs CCA Stim			
Source of Variation	P value	Summary	Significant?
Interaction	0.4138	ns	No
Days	0.6628	ns	No
CCA	0.0304	*	Yes
Matching	0.0005	***	Yes

Bonferroni Post Hoc Test - TUDCA - Control vs CCA Stim				
Days	Difference	t	P value	Summary
2	0.01434	1.136	P > 0.05	ns
7	0.02945	2.333	P > 0.05	ns

LC3 mRNA - CCA Stim/Cotnrol (ΔΔCt)				
	2 Days		7 Days	
n	VEH	TUD	VEH	TUD
1	0.905	0.673	0.802	0.843
2	1.056	0.9	0.788	0.657
3	0.844	0.96	0.86	1.032
4	1.102	0.814	1.079	1
5	1.102	0.977	0.816	0.866
6	0.731	0.879	1.016	0.741
7	0.867	1.187	0.969	0.988
X	0.944	0.91286	0.90429	0.87529
SEM	0.055	0.05978	0.0439	0.05337

2-Way ANOVA - RELATIVE CHANGE - CCA Stim/Control			
Source of Variation	P value	Summary	Significant?
Interaction	0.9852	ns	No
Days	0.4757	ns	No
TUDCA	0.5782	ns	No

Bonferroni Post Hoc Test - MULTIPLE COMPARISONS - Control vs CCA Stim				
Comparison	Difference	t	P value	Summary
2 Days :VEH vs. 2 Days :TUD	0.031	0.4118	P > 0.05	ns
2 Days :VEH vs. 7 Days :VEH	0.03957	0.5257	P > 0.05	ns
2 Days :VEH vs. 7 Days :TUD	0.06857	0.911	P > 0.05	ns
2 Days :TUD vs. 7 Days :VEH	0.00857	0.1139	P > 0.05	ns
2 Days :TUD vs. 7 Days :TUD	0.03757	0.4991	P > 0.05	ns
7 Days :VEH vs. 7 Days :TUD	0.029	0.3853	P > 0.05	ns

Table 6A: Protein expression of UPR^{ER} markers following TUDCA/vehicle treatment with 2 or 7 days of CCA.

CHOP Protein - Control vs. CCA Stim								
	VEHICLE				TUDCA			
	2 Days		7 Days		2 Days		7 Days	
n	CTR	STM	CTR	STM	CTR	STM	CTR	STM
1	0.2548	1.1821	0.6716	1.2495	0.2591	0.5041	0.5048	0.9653
2	0.3759	0.5395	0.5872	0.9137	0.568	0.7024	0.4526	0.8297
3	0.8474	1.219	0.9031	1.6216	0.4841	0.7203	1.1661	1.7257
4	0.5119	1.1257	1.2902	1.3714	0.3329	0.588	0.5861	0.8635
5	0.6491	1.422	0.6407	1.3778	0.6865	0.9926	0.3667	0.9291
6	0.0562	0.3674	0.3387	0.4361	0.3378	0.4293	0.213	0.4553
7	0.1793	0.8262	0.7364	0.8384	0.5166	1.0974	0.5074	1.445
X	0.4107	0.9546	0.7383	1.1155	0.455	0.7192	0.5424	1.0305
SEM	0.1049	0.1466	0.1121	0.1533	0.0573	0.0933	0.1135	0.1595

RM 2-Way ANOVA - VEHICLE - Control vs CCA Stim			
Source of Variation	P value	Summary	Significant?
Interaction	0.4342	ns	No
Days	0.0888	ns	No
CCA	< 0.0001	****	Yes
Matching	0.0061	**	Yes

Bonferroni Post Hoc Test - VEHICLE - Control vs CCA Stim				
Days	Difference	t	P value	Summary
2	-0.4821	4.664	P < 0.05	***
7	-0.3644	3.526	P < 0.05	**

Bonferroni Post Hoc Test - MULTIPLE COMPARISONS - Control vs CCA Stim				
Comparison	Difference	t	P value	Summary
2:VEH CON vs. 2:TUD CON	-0.1067	0.6623	P > 0.05	ns
2:VEH CON vs. 7:VEH CON	-0.3301	2.048	P > 0.05	ns
2:VEH STM vs. 2:TUD STM	0.1024	0.6355	P > 0.05	ns
2:VEH STM vs. 7:VEH STM	-0.2124	1.318	P > 0.05	ns
2:TUD CON vs. 7:TUD CON	-0.0329	0.2041	P > 0.05	ns
2:TUD STM vs. 7:TUD STM	-0.2093	1.299	P > 0.05	ns
7:VEH CON vs. 7:TUD CON	0.1905	1.182	P > 0.05	ns
7:VEH STM vs. 7:TUD STM	0.1055	0.6548	P > 0.05	ns

RM 2-Way ANOVA - TUDCA- Control vs CCA Stim			
Source of Variation	P value	Summary	Significant?
Interaction	0.102	ns	No
Days	0.4288	ns	No
CCA	< 0.0001	****	Yes
Matching	0.0001	***	Yes

Bonferroni Post Hoc Test - TUDCA - Control vs CCA Stim				
Days	Difference	t	P value	Summary
2	-0.273	3.83	P < 0.05	**
7	-0.4494	6.305	P < 0.05	****

CHOP Protein - CCA Stim/Cotnrol				
	2 Days		7 Days	
n	VEH	TUD	VEH	TUD
1	4.639	1.946	1.86	1.912
2	1.435	1.237	1.556	1.833
3	1.439	1.488	1.796	1.48
4	2.199	1.767	1.063	1.473
5	2.191	1.446	2.15	2.533
6	6.541	1.271	1.287	2.138
7	4.607	2.124	1.139	2.848
X	3.293	1.61129	1.55014	2.031
SEM	0.746	0.12887	0.15368	0.19514

2-Way ANOVA - RELATIVE CHANGE - CCA Stim/Control			
Source of Variation	P value	Summary	Significant?
Interaction	0.0121	*	Yes
Days	0.1099	ns	No
TUDCA	0.1449	ns	No

Bonferroni Post Hoc Test - MULTIPLE COMPARISONS - Control vs CCA Stim				
Comparison	Difference	t	P value	Summary
2:VEH vs. 2:TUD	1.682	2.984	P < 0.05	*
2:VEH vs. 7:VEH	1.743	3.093	P < 0.05	*
2:VEH vs. 7:TUD	1.262	2.239	P > 0.05	ns
2:TUD vs. 7:VEH	0.06114	0.1085	P > 0.05	ns
2:TUD vs. 7:TUD	-0.4197	0.7448	P > 0.05	ns
7:VEH vs. 7:TUD	-0.4809	0.8533	P > 0.05	ns

HSP70 Protein - Control vs. CCA Stim								
	VEHICLE				TUDCA			
	2 Days		7 Days		2 Days		7 Days	
n	CTR	STM	CTR	STM	CTR	STM	CTR	STM
1	0.2217	0.7085	0.4166	1.0958	0.412	0.6684	0.5515	0.7848
2	0.3986	1.1017	0.5246	1.1224	0.8067	1.4004	0.7528	2.1326
3	0.5772	1.5342	0.6707	1.6621	0.8221	1.5232	0.6456	0.9512
4	0.5468	1.3475	1.2406	1.3867	0.7142	1.4061	0.6427	0.826
5	0.6559	1.1109	0.6641	0.9862	0.5059	0.863	0.4821	0.9494
6	0.3257	0.8324	0.4207	0.9951	0.4748	0.8548	0.473	1.0483
7	0.3619	0.8942	0.4628	0.9656	0.4826	0.7714	0.3948	1.2394
X	0.4543	1.1059	0.6562	1.2081	0.6226	1.1193	0.5913	1.1154
SEM	0.0678	0.1258	0.1254	0.1084	0.0735	0.1487	0.0444	0.2071

RM 2-Way ANOVA - VEHICLE - Control vs CCA Stim			
Source of Variation	P value	Summary	Significant?
Interaction	0.226	ns	No
Days	0.2773	ns	No
CCA	< 0.0001	****	Yes
Matching	0.0341	*	Yes

Bonferroni Post Hoc Test - VEHICLE - Control vs CCA Stim				
Days	Difference	t	P value	Summary
2	-0.7045	7.757	P < 0.05	****
7	-0.5419	5.966	P < 0.05	****

Bonferroni Post Hoc Test - MULTIPLE COMPARISONS - Control vs CCA Stim				
Comparison	Difference	t	P value	Summary
2:VEH CON vs. 2:TUD CON	-0.1428	1.028	P > 0.05	ns
2:VEH CON vs. 7:VEH CON	-0.2018	1.452	P > 0.05	ns
2:VEH STM vs. 2:TUD STM	0.0613	0.4413	P > 0.05	ns
2:VEH STM vs. 7:VEH STM	-0.0391	0.2815	P > 0.05	ns
2:TUD CON vs. 7:TUD CON	0.0343	0.2466	P > 0.05	ns
2:TUD STM vs. 7:TUD STM	-0.0986	0.71	P > 0.05	ns
7:VEH CON vs. 7:TUD CON	0.0932	0.671	P > 0.05	ns
7:VEH STM vs. 7:TUD STM	0.0018	0.0128	P > 0.05	ns

RM 2-Way ANOVA - TUDCA- Control vs CCA Stim			
Source of Variation	P value	Summary	Significant?
Interaction	0.442	ns	No
Days	0.8032	ns	No
CCA	< 0.0001	****	Yes
Matching	0.0677	ns	No

Bonferroni Post Hoc Test - TUDCA - Control vs CCA Stim				
Days	Difference	t	P value	Summary
2	-0.5004	4.214	P < 0.05	**
7	-0.6333	5.333	P < 0.05	***

HSP70 Protein - CCA Stim/Cotnrol				
	2 Days		7 Days	
n	VEH	TUD	VEH	TUD
1	3.196	1.623	2.63	1.423
2	2.764	1.736	2.14	2.833
3	2.658	1.853	2.478	1.473
4	2.464	1.969	1.118	1.285
5	1.694	1.706	1.485	1.969
6	2.555	1.8	2.365	2.216
7	2.47	1.599	2.086	3.14
X	2.543	1.75514	2.04314	2.04843
SEM	0.171	0.04927	0.20792	0.27371

2-Way ANOVA - RELATIVE CHANGE - CCA Stim/Control			
Source of Variation	P value	Summary	Significant?
Interaction	0.0514	ns	No
Days	0.5983	ns	No
TUDCA	0.0544	ns	No

Bonferroni Post Hoc Test - MULTIPLE COMPARISONS - Control vs CCA Stim				
Comparison	Difference	t	P value	Summary
2:VEH vs. 2:TUD	0.7879	2.88	P < 0.05	*
2:VEH vs. 7:VEH	0.4999	1.827	P > 0.05	ns
2:VEH vs. 7:TUD	0.4946	1.808	P > 0.05	ns
2:TUD vs. 7:VEH	-0.288	1.053	P > 0.05	ns
2:TUD vs. 7:TUD	-0.2933	1.072	P > 0.05	ns
7:VEH vs. 7:TUD	-0.0053	0.01932	P > 0.05	ns

Table 6B: Protein expression of UPR^{mt} markers following TUDCA/vehicle treatment with 2 or 7 days of CCA.

CPN10 Protein - Control vs. CCA Stim								
	VEHICLE				TUDCA			
	2 Days		7 Days		2 Days		7 Days	
n	CTR	STM	CTR	STM	CTR	STM	CTR	STM
1	0.7959	1.3119	1.0376	1.5589	1.0277	1.6373	1.1594	1.3506
2	0.7109	0.8269	0.4714	0.9839	0.7437	0.8444	0.6442	1.0828
3	0.4732	0.4977	0.6995	1.0928	0.6797	0.9713	1.0027	1.355
4	0.5749	0.5273	0.6086	0.7993	0.5294	0.6235	0.5725	1.0751
5	0.825	0.8583	0.6212	0.8346	0.907	0.7624	0.573	1.0622
6	1.009	0.8205	0.4018	0.5259	0.5165	0.4711	0.386	0.7618
7	0.7535	0.9437	0.9157	1.4559	0.9561	0.8933	0.7571	1.31
8	0.2139	0.4872	1.0516	1.5728	0.8485	1.1231	0.9846	1.8714
X	0.6695	0.7842	0.7259	1.103	0.7761	0.9158	0.7599	1.2336
SEM	0.0865	0.099	0.0881	0.1379	0.0677	0.1253	0.0938	0.115

RM 2-Way ANOVA - VEHICLE - Control vs CCA Stim			
Source of Variation	P value	Summary	Significant?
Interaction	0.018	*	Yes
Days	0.2019	ns	No
CCA	0.0002	***	Yes
Matching	0.0002	***	Yes

Bonferroni Post Hoc Test - VEHICLE - Control vs CCA Stim				
Days	Difference	t	P value	Summary
2	-0.1146	1.655	P > 0.05	ns
7	-0.3771	5.445	P < 0.05	***

Bonferroni Post Hoc Test - MULTIPLE COMPARISONS - Control vs CCA Stim				
Comparison	Difference	t	P value	Summary
2:VEH CON vs. 2:TUD CON	-0.1065	0.725	P > 0.05	ns
2:VEH CON vs. 7:VEH CON	-0.0564	0.3838	P > 0.05	ns
2:VEH STM vs. 2:TUD STM	-0.1316	0.8957	P > 0.05	ns
2:VEH STM vs. 7:VEH STM	-0.3188	2.17	P > 0.05	ns
2:TUD CON vs. 7:TUD CON	0.0161	0.1097	P > 0.05	ns
2:TUD STM vs. 7:TUD STM	-0.3178	2.163	P > 0.05	ns
7:VEH CON vs. 7:TUD CON	-0.034	0.2315	P > 0.05	ns
7:VEH STM vs. 7:TUD STM	-0.1306	0.8888	P > 0.05	ns

RM 2-Way ANOVA - TUDCA- Control vs CCA Stim			
Source of Variation	P value	Summary	Significant?
Interaction	0.01	*	Yes
Days	0.2798	ns	No
CCA	< 0.0001	****	Yes
Matching	0.0012	**	Yes

Bonferroni Post Hoc Test - TUDCA - Control vs CCA Stim				
Days	Difference	t	P value	Summary
2	-0.1397	1.761	P > 0.05	ns
7	-0.4737	5.97	P < 0.05	****

CPN10 Protein - CCA Stim/Cotnrol				
	2 Days		7 Days	
n	VEH	TUD	VEH	TUD
1	1.648	1.593	1.502	1.165
2	1.163	1.135	2.087	1.681
3	1.052	1.429	1.562	1.351
4	0.917	1.178	1.313	1.878
5	1.04	0.841	1.343	1.854
6	0.813	0.912	1.309	1.973
7	1.252	0.934	1.59	1.73
8	2.278	1.324	1.496	1.901
X	1.27	1.16825	1.52525	1.69163
SEM	0.169	0.09463	0.0894	0.10169

2-Way ANOVA - RELATIVE CHANGE - CCA Stim/Control			
Source of Variation	P value	Summary	Significant?
Interaction	0.2659	ns	No
Days	0.0027	**	Yes
TUDCA	0.7879	ns	No

Bonferroni Post Hoc Test - MULTIPLE COMPARISONS - Control vs CCA Stim				
Comparison	Difference	t	P value	Summary
2 Days :VEH vs. 2 Days :TUD	0.1021	0.6106	P > 0.05	ns
2 Days :VEH vs. 7 Days :VEH	-0.2549	1.524	P > 0.05	ns
2 Days :VEH vs. 7 Days :TUD	-0.4213	2.519	P > 0.05	ns
2 Days :TUD vs. 7 Days :VEH	-0.357	2.135	P > 0.05	ns
2 Days :TUD vs. 7 Days :TUD	-0.5234	3.129	P < 0.05	*
7 Days :VEH vs. 7 Days :TUD	-0.1664	0.9948	P > 0.05	ns

Table 6C: Protein expression of Uqcrc2 following TUDCA/vehicle treatment with 2 or 7 days of CCA.

Uqcrc2 Protein - Control vs. CCA Stim								
	VEHICLE				TUDCA			
	2 Days		7 Days		2 Days		7 Days	
n	CTR	STM	CTR	STM	CTR	STM	CTR	STM
1	0.9757	1.0663	0.775	1.491	0.2873	0.7757	0.6121	1.2933
2	0.2208	0.4578	0.4772	0.9282	0.1247	0.1744	0.9401	1.1358
3	0.6119	1.0395	0.8522	1.1477	0.5444	0.613	0.8225	0.85
4	0.3453	0.6345	0.4189	0.9534	0.6581	0.7583	0.8349	0.934
5	0.5319	1.2056	0.5053	1.0403	0.6159	1.6533	0.2752	0.8361
6	0.4219	0.6741	0.4532	0.5548	0.6269	0.7067	0.4873	0.5208
7	0.2599	1.2367	0.9255	1.0955	0.751	1.038	0.5942	1.3723
X	0.4811	0.9021	0.6296	1.0301	0.5155	0.8171	0.6523	0.9918
SEM	0.098	0.1166	0.0805	0.1061	0.0851	0.1704	0.0872	0.1119

RM 2-Way ANOVA - VEHICLE - Control vs CCA Stim			
Source of Variation	P value	Summary	Significant?
Interaction	0.888	ns	No
Days	0.2868	ns	No
CCA	< 0.0001	****	Yes
Matching	0.0332	*	Yes

Bonferroni Post Hoc Test - VEHICLE - Control vs CCA Stim				
Days	Difference	t	P value	Summary
2	-0.421	4.177	P < 0.05	**
7	-0.4005	3.974	P < 0.05	**

Bonferroni Post Hoc Test - MULTIPLE COMPARISONS - Control vs CCA Stim				
Comparison	Difference	t	P value	Summary
2:VEH CON vs. 2:TUD CON	-0.0344	0.2205	P > 0.05	ns
2:VEH CON vs. 7:VEH CON	-0.1485	0.9521	P > 0.05	ns
2:VEH STM vs. 2:TUD STM	0.085	0.545	P > 0.05	ns
2:VEH STM vs. 7:VEH STM	-0.128	0.8207	P > 0.05	ns
2:TUD CON vs. 7:TUD CON	-0.1369	0.8773	P > 0.05	ns
2:TUD STM vs. 7:TUD STM	-0.1747	1.12	P > 0.05	ns
7:VEH CON vs. 7:TUD CON	-0.0227	0.1456	P > 0.05	ns
7:VEH STM vs. 7:TUD STM	0.0384	0.2459	P > 0.05	ns

RM 2-Way ANOVA - TUDCA- Control vs CCA Stim			
Source of Variation	P value	Summary	Significant?
Interaction	0.84	ns	No
Days	0.29	ns	No
CCA	0.0044	**	Yes
Matching	0.0758	ns	No

Bonferroni Post Hoc Test - TUDCA - Control vs CCA Stim				
Days	Difference	t	P value	Summary
2	-0.3016	2.327	P > 0.05	ns
7	-0.3394	2.618	P < 0.05	*

Uqcrc2 Protein - CCA Stim/Cotnrol				
	2 Days		7 Days	
n	VEH	TUD	VEH	TUD
1	1.093	2.7	1.924	2.113
2	2.074	1.399	1.945	1.208
3	1.699	1.126	1.347	1.033
4	1.838	1.152	2.276	1.119
5	2.266	2.684	2.059	3.038
6	1.598	1.127	1.224	1.069
7	4.758	1.382	1.184	2.309
X	2.189	1.65286	1.70843	1.69843
SEM	0.451	0.27179	0.16817	0.29898

2-Way ANOVA - RELATIVE CHANGE - CCA Stim/Control			
Source of Variation	P value	Summary	Significant?
Interaction	0.4102	ns	No
Days	0.4949	ns	No
TUDCA	0.3929	ns	No

Bonferroni Post Hoc Test - MULTIPLE COMPARISONS - Control vs CCA Stim				
Comparison	Difference	t	P value	Summary
2 Days :VEH vs. 2 Days :TUD	0.5366	1.208	P > 0.05	ns
2 Days :VEH vs. 7 Days :VEH	0.481	1.083	P > 0.05	ns
2 Days :VEH vs. 7 Days :TUD	0.491	1.105	P > 0.05	ns
2 Days :TUD vs. 7 Days :VEH	-0.0556	0.1251	P > 0.05	ns
2 Days :TUD vs. 7 Days :TUD	-0.0456	0.1026	P > 0.05	ns
7 Days :VEH vs. 7 Days :TUD	0.01	0.02251	P > 0.05	ns

Table 6D: Protein expression of autophagy markers following TUDCA/vehicle treatment with 2 or 7 days of CCA.

p62 Protein - Control vs. CCA Stim								
	VEHICLE				TUDCA			
	2 Days		7 Days		2 Days		7 Days	
n	CTR	STM	CTR	STM	CTR	STM	CTR	STM
1	0.6866	0.9562	1.2332	1.5689	0.8754	2.0209	1.373	1.1471
2	1.1338	1.6761	0.8139	0.8418	0.9243	1.0935	1.0527	1.4119
3	1.3134	1.6527	1.4971	1.1799	1.1734	1.8217	0.9	1.343
4	0.4677	0.666	0.4613	0.6809	0.7539	1.168	0.6132	0.8277
5	0.5058	0.6971	0.4575	0.5821	0.599	0.865	0.4345	0.4852
6	0.8275	0.8513	0.8718	0.3284	0.498	0.9678	1.1535	1.5923
7	0.3664	0.5445	0.6975	0.8735	0.4189	0.6178	0.7062	0.6416
X	0.6626	1.0063	0.754	0.8651	0.6554	1.2221	0.7791	1.0641
SEM	0.1502	0.1771	0.1661	0.1541	0.1276	0.1936	0.1547	0.1584

RM 2-Way ANOVA - VEHICLE - Control vs CCA Stim			
Source of Variation	P value	Summary	Significant?
Interaction	0.0929	ns	No
Days	0.9307	ns	No
CCA	0.0853	ns	No
Matching	0.0002	***	Yes

Bonferroni Post Hoc Test - VEHICLE - Control vs CCA Stim				
Days	Difference	t	P value	Summary
2	-0.249	2.617	P < 0.05	*
7	-0.0033	0.03489	P > 0.05	ns

Bonferroni Post Hoc Test - MULTIPLE COMPARISONS - Control vs CCA Stim				
Comparison	Difference	t	P value	Summary
2:VEH CON vs. 2:TUD CON	0.0083	0.0389	P > 0.05	ns
2:VEH CON vs. 7:VEH CON	-0.1045	0.489	P > 0.05	ns
2:VEH STM vs. 2:TUD STM	-0.2158	1.01	P > 0.05	ns
2:VEH STM vs. 7:VEH STM	0.1412	0.6608	P > 0.05	ns
2:TUD CON vs. 7:TUD CON	-0.1415	0.6621	P > 0.05	ns
2:TUD STM vs. 7:TUD STM	0.158	0.7396	P > 0.05	ns
7:VEH CON vs. 7:TUD CON	-0.0287	0.1342	P > 0.05	ns
7:VEH STM vs. 7:TUD STM	-0.199	0.9316	P > 0.05	ns

RM 2-Way ANOVA - TUDCA- Control vs CCA Stim			
Source of Variation	P value	Summary	Significant?
Interaction	0.09	ns	No
Days	0.9666	ns	No
CCA	0.0018	**	Yes
Matching	0.0026	**	Yes

Bonferroni Post Hoc Test - TUDCA - Control vs CCA Stim				
Days	Difference	t	P value	Summary
2	-0.4731	4.121	P < 0.05	**
7	-0.1737	1.513	P > 0.05	ns

p62 Protein - CCA Stim/Cotnrol				
	2 Days		7 Days	
n	VEH	TUD	VEH	TUD
1	1.393	2.309	1.272	0.835
2	1.478	1.183	1.034	1.341
3	1.258	1.552	0.788	1.492
4	1.424	1.549	1.476	1.35
5	1.378	1.444	1.272	1.117
6	1.029	1.943	0.377	1.38
7	1.486	1.475	1.252	0.909
X	1.349	1.63643	1.06729	1.20343
SEM	0.061	0.14056	0.14147	0.09571

2-Way ANOVA - RELATIVE CHANGE - CCA Stim/Control			
Source of Variation	P value	Summary	Significant?
Interaction	0.517	ns	No
Days	0.0047	**	Yes
TUDCA	0.0774	ns	No

Bonferroni Post Hoc Test - MULTIPLE COMPARISONS - Control vs CCA Stim				
Comparison	Difference	t	P value	Summary
2 Days :VEH vs. 2 Days :TUD	-0.287	1.77	P > 0.05	ns
2 Days :VEH vs. 7 Days :VEH	0.2821	1.74	P > 0.05	ns
2 Days :VEH vs. 7 Days :TUD	0.146	0.9002	P > 0.05	ns
2 Days :TUD vs. 7 Days :VEH	0.5691	3.509	P < 0.05	*
2 Days :TUD vs. 7 Days :TUD	0.433	2.67	P > 0.05	ns
7 Days :VEH vs. 7 Days :TUD	-0.1361	0.8394	P > 0.05	ns

LC3-II: LC3-I Protein - Control vs. CCA Stim								
	VEHICLE				TUDCA			
	2 Days		7 Days		2 Days		7 Days	
n	CTR	STM	CTR	STM	CTR	STM	CTR	STM
1	0.4702	0.9213	0.5324	0.6221	0.8336	0.9733	0.6116	0.6239
2	0.2321	0.3757	0.3971	0.8829	0.4576	0.4232	1.2508	0.9229
3	0.3204	0.3433	0.4988	0.4437	1.1166	0.6296	0.3589	0.4028
4	0.6297	0.4163	0.8418	0.4583	0.782	0.7959	0.2296	0.4209
5	0.9813	0.565	1.2649	0.9449	0.4025	0.2953	0.5844	0.3164
6	0.5357	0.4289	0.7453	0.5335	0.1739	0.2531	1.0657	0.8049
7	0.3309	0.5239	1.6659	1.0351	0.7824	0.6055	1.8978	0.8523
8	1.2385	0.5829	0.233	0.3004	0.1839	0.6949	0.8339	0.9762
X	0.5923	0.5197	0.7724	0.6526	0.5916	0.5839	0.8541	0.665
SEM	0.124	0.0652	0.1696	0.095	0.1196	0.0876	0.1917	0.0916

RM 2-Way ANOVA - VEHICLE - Control vs CCA Stim			
Source of Variation	P value	Summary	Significant?
Interaction	0.7914	ns	No
Days	0.2992	ns	No
CCA	0.2891	ns	No
Matching	0.0336	*	Yes

Bonferroni Post Hoc Test - VEHICLE - Control vs CCA Stim				
Days	Difference	t	P value	Summary
2	0.07269	0.5885	P > 0.05	ns
7	0.1198	0.9698	P > 0.05	ns

Bonferroni Post Hoc Test - MULTIPLE COMPARISONS - Control vs CCA Stim				
Comparison	Difference	t	P value	Summary
2:VEH CON vs. 2:TUD CON	-0.18	0.9612	P > 0.05	ns
2:VEH CON vs. 7:VEH CON	-0.18	0.9612	P > 0.05	ns
2:VEH STM vs. 2:TUD STM	-0.1329	0.7098	P > 0.05	ns
2:VEH STM vs. 7:VEH STM	-0.1329	0.7098	P > 0.05	ns
2:TUD CON vs. 7:TUD CON	-0.0817	0.4362	P > 0.05	ns
2:TUD STM vs. 7:TUD STM	-0.0124	0.0664	P > 0.05	ns
7:VEH CON vs. 7:TUD CON	-0.0817	0.4362	P > 0.05	ns
7:VEH STM vs. 7:TUD STM	-0.0124	0.0664	P > 0.05	ns

RM 2-Way ANOVA - TUDCA- Control vs CCA Stim			
Source of Variation	P value	Summary	Significant?
Interaction	0.3129	ns	No
Days	0.3051	ns	No
CCA	0.2752	ns	No
Matching	0.0132	*	Yes

Bonferroni Post Hoc Test - TUDCA - Control vs CCA Stim				
Days	Difference	t	P value	Summary
2	0.00769	0.06277	P > 0.05	ns
7	0.1891	1.543	P > 0.05	ns

LC3-II: LC3-I Protein - CCA Stim/Cotnrol				
	2 Days		7 Days	
n	VEH	TUD	VEH	TUD
1	1.959	1.168	1.168	1.02
2	1.619	0.925	2.224	0.738
3	1.071	0.564	0.889	1.122
4	0.661	1.018	0.544	1.833
5	0.576	0.734	0.747	0.541
6	0.801	1.456	0.716	0.755
7	1.583	0.774	0.621	0.449
8	0.471	3.778	1.29	1.171
X	1.093	1.30213	1.02488	0.95363
SEM	0.198	0.36696	0.1943	0.15608

2-Way ANOVA - RELATIVE CHANGE - CCA Stim/Control			
Source of Variation	P value	Summary	Significant?
Interaction	0.5679	ns	No
Days	0.3987	ns	No
TUDCA	0.778	ns	No

Bonferroni Post Hoc Test - MULTIPLE COMPARISONS - Control vs CCA Stim				
Comparison	Difference	t	P value	Summary
2 Days :VEH vs. 2 Days :TUD	-0.2095	0.61	P > 0.05	ns
2 Days :VEH vs. 7 Days :VEH	0.06775	0.1973	P > 0.05	ns
2 Days :VEH vs. 7 Days :TUD	0.139	0.4047	P > 0.05	ns
2 Days :TUD vs. 7 Days :VEH	0.2773	0.8072	P > 0.05	ns
2 Days :TUD vs. 7 Days :TUD	0.3485	1.015	P > 0.05	ns
7 Days :VEH vs. 7 Days :TUD	0.07125	0.2074	P > 0.05	ns

APPENDIX B: SUPPLEMENTARY AND ADDITIONAL DATA (STATISTIC TABLES NOT SHOWN)

Fig. S1

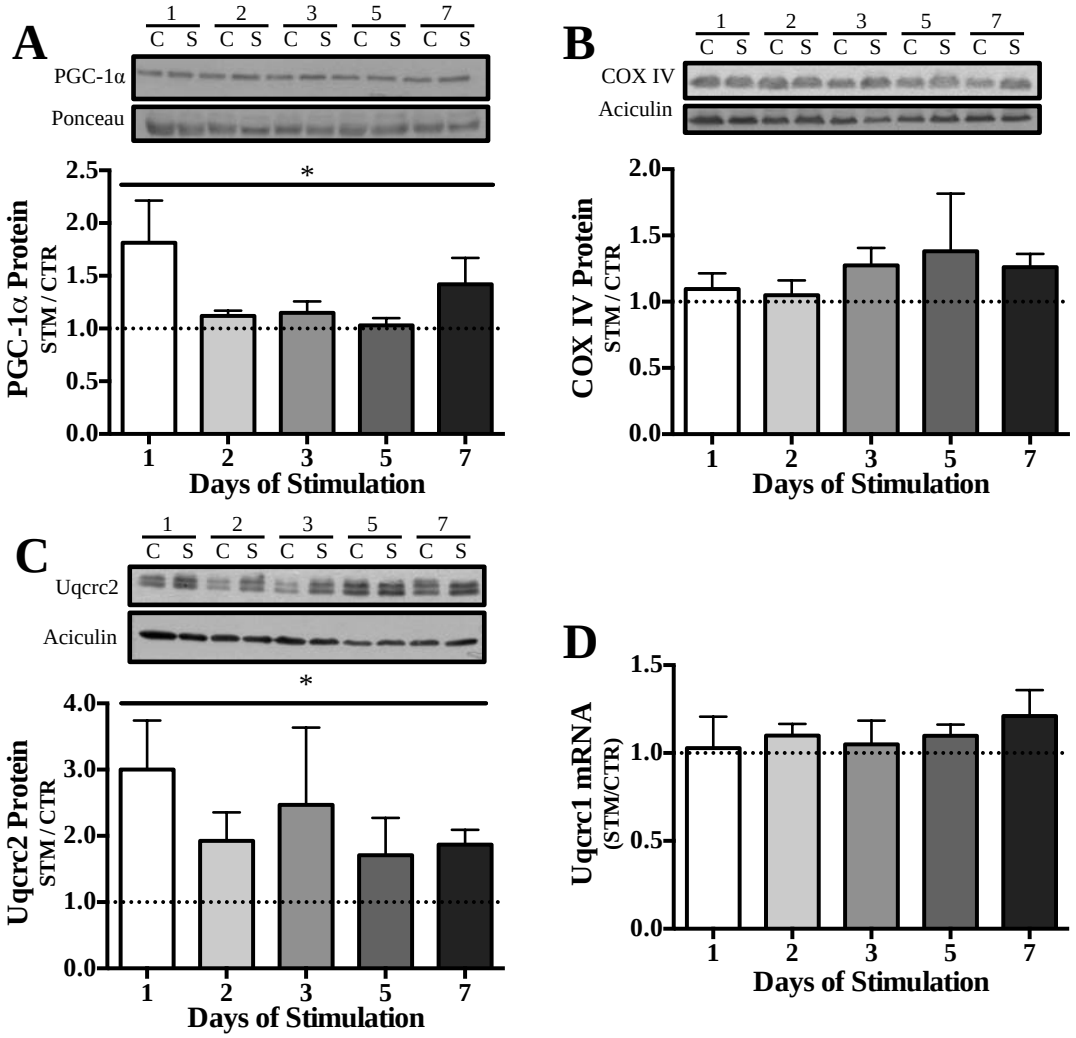

Figure S1. Fold-change in protein level of mitochondrial biogenesis marker **(A)** PGC-1α, and ETC components **(B)** COX IV and **(C)** Uqcrc2 (PGC-1α, n=5; COX IV, Uqcrc2, n=6, per day), and **(D)** mRNA expression of complex III subunit 1, Uqcrc1, throughout 1-7 days of CCA (n=7, per day). Bars represent fold-change in stimulated muscle relative to matched controls; means ± SEM. **P<0.05*, stimulated vs. control TA muscle at a given time point.

Fig. S2

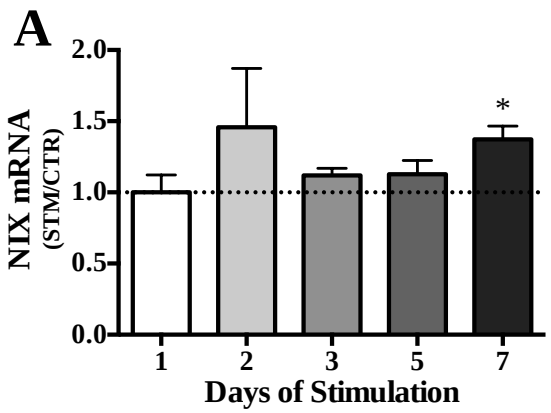

Figure S2. Time-course in the mRNA expression of mitophagy marker NIX following 1-7 days of CCA (n=6, per day). Bars represent fold-change in stimulated muscle relative to matched controls; means ± SEM. *$P<0.05$, stimulated vs. control TA muscle at a given time point.

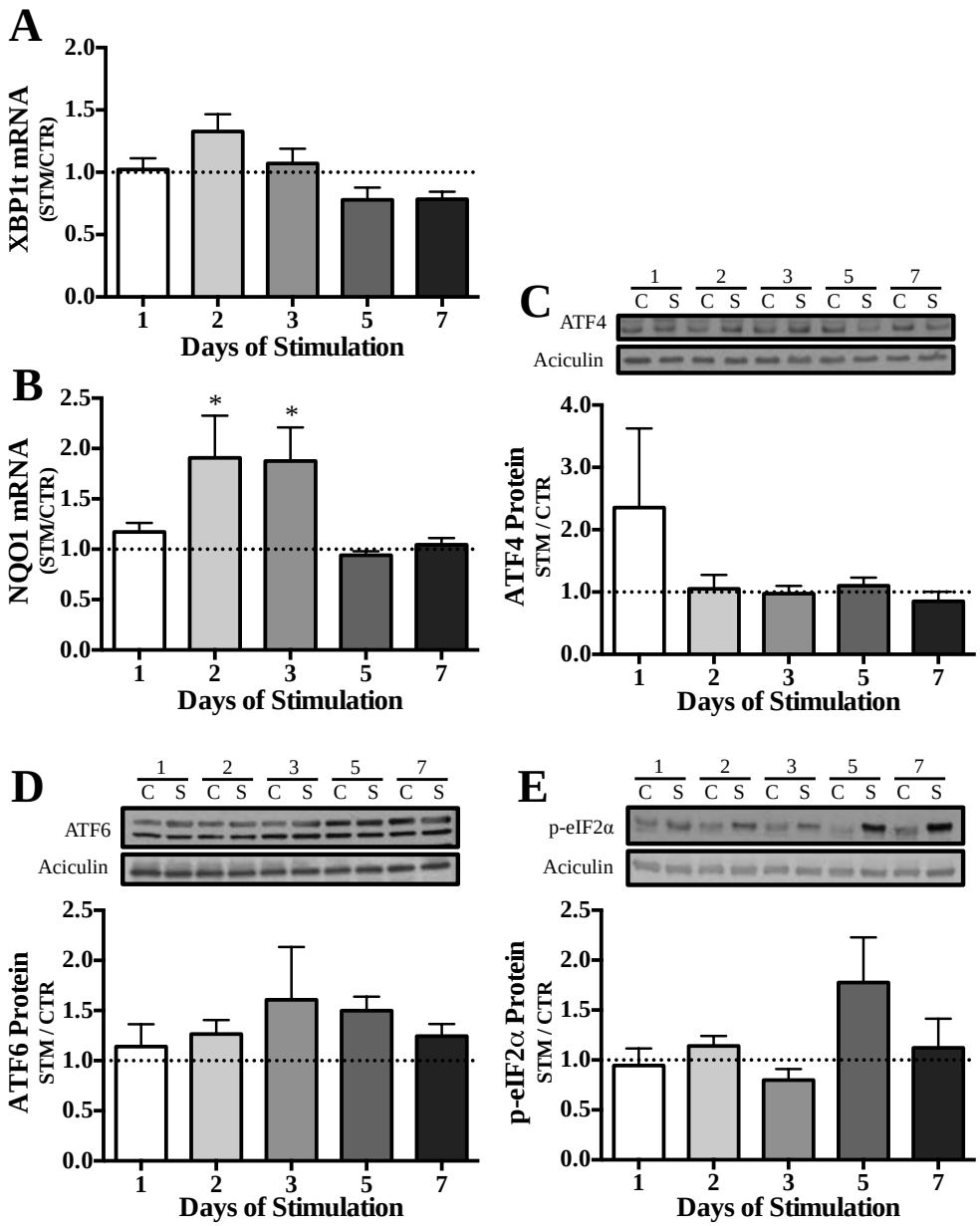

Figure S3. Fold-change in the **(A)** full length mRNA expression of UPR^{ER} transcription factor XBP1t, and **(B)** the antioxidant transcript NQO1, following repeated contractile bouts from 1-7 days (XBP1t, and NQO1, n=6). Associated protein expression of **(C)** ATF4, **(D)** ATF6, and **(E)** p-eIF2α (ATF6, n=7; p-eIF2α, and ATF4, n=6, per day). Bars represent fold-change in stimulated muscle relative to matched controls; means ± SEM. **P<0.05,* stimulated vs. control TA muscle at a given time point.

Fig. S4

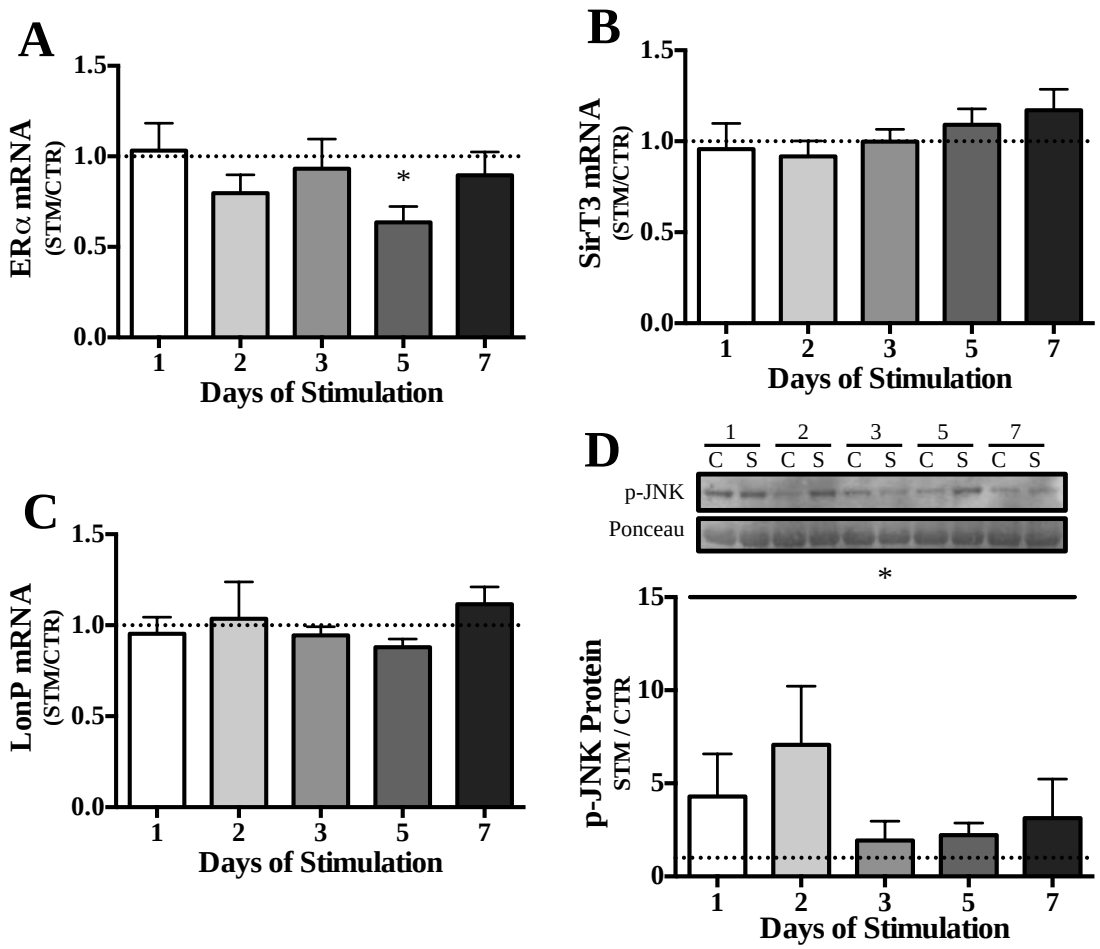

Figure S4. Fold-change in the mRNA expression of UPR^{mt} factors **(A)** ERα, **(B)** SirT3, **(C)** LonP, and **(D)** protein phosphorylation of activating kinase JNK throughout 1-7 days of muscle contractile activity (all graphs, n=6, per day). Bars represent fold-change in control TA muscle at a given time point.

Fig. S5

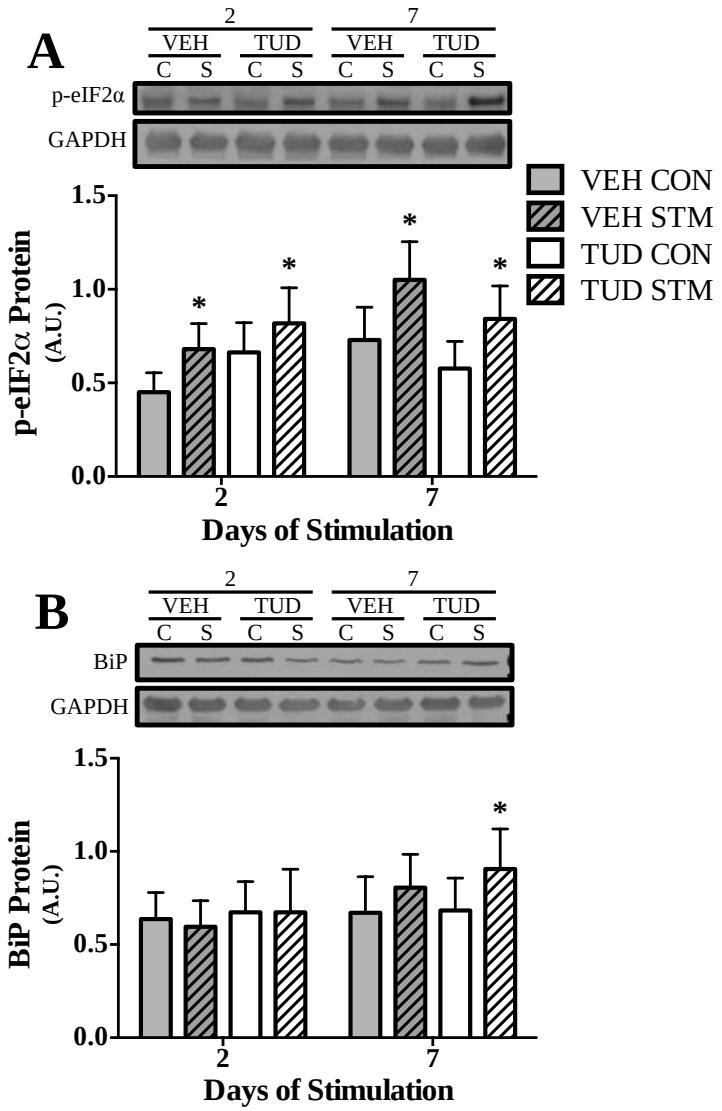

Figure S5. CCA-induced changes in protein expression of **(A)** phosphorylated eIF2α and **(B)** BiP thought repeated muscle contractile activity over 1-7 days (p-eIF2α, n=8; BiP, n=7, per day/treatment). Open grey, and open white bars represent control muscle in vehicle-, and TUDCA-treated animals, respectively; hatched grey, and hatched white bars represent stimulated muscle in vehicle-, and TUDCA-treated animals, respectively. Values represent means ± SEM. *$P<0.05$, stimulated vs. control TA muscle at a given time point and treatment.

Fig. S6

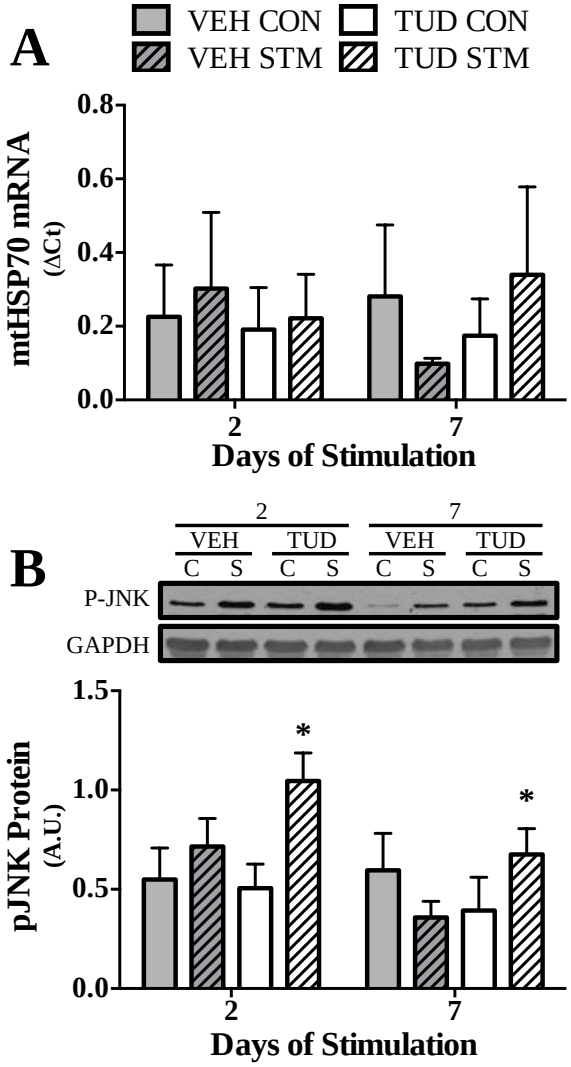

Figure S6. 1-7 days of CCA-induced changes in **(A)** mtHSP70 mRNA levels, and **(B)** phosphorylated JNK protein expression (mtHSP70, n=8; pJNK, n=7). Open grey, and open white bars represent control muscle in vehicle-, and TUDCA-treated animals, respectively; hatched grey, and hatched white bars represent stimulated muscle in vehicle-, and TUDCA-treated animals, respectively. Values represent means ± SEM. *$P<0.05$, stimulated vs. control TA muscle at a given time point and treatment.

APPENDIX C: LABORATORY METHODS AND PROTOCOLS

CHRONIC CONTRACTILE ACTIVITY SURGICAL PROCEDURE

Sterilize all surgical tools prior to commencing the surgical procedures outlined below and also keep lab bench as sterile as possible by wiping it down thoroughly with ethanol.

1. Shave the skin over the spinal column (between the apex of the scapulae) and over the left hindlimb just posterior of the knee joint. Wipe with iodine.

2. With animal lying on its stomach, carefully make a skin incision between scapular apexes along the center of the back (approximately 5-10mm in length).

3. Turn animal onto its right side so that the left hindlimb is upwards facing. In this position, make a small (10-15mm) skin incision from approximately 5mm posterior of the knee joint towards the top of the gastrocnemius muscle. Gently separate skin from superficial muscle.

4. Make a small horizontal cut into the underlying left hindlimb muscle (biceps femoris) and blunt through the muscle to expose the peroneal nerve.

5. Once the nerve has been exposed, affix the wire electrodes to the tunneler by folding over the end-piece (one with the slot) of the tunneler and carefully tunnel the electrodes from the left hindlimb to exit out the back being sure not to damage the electrodes.

6. Use 4 retractors gain a larger exposure of the nerve and underlying musculature.

7. Gently remove insulation to expose wire and make a coil of the wire ends. Tie a knot that attaches the suture silk to the last loop of the electrode.

8. Using forceps (with sharp teeth), pinch a small amount (between 0.5-1.0 mm) of muscle that is flanking the peroneal nerve. Place needle through the pinched muscle section and proceed to tie down the loop section of the electrode to the underlying muscle. Once the loop section has been tied down, tie down a proximal section of the electrode to another thin section of muscle that is 3-4mm away from the loop portion. Tie down a third section using the same method as the previous.

9. Repeat steps 7 and 8 for the other electrode lead this time suturing the electrode to the other side of the peroneal nerve.

10. Once both electrodes are sutured to the underlying muscle, the incision is closed with 3-5 independent sutures (5.0 silk). Leave a coil of excess wire under the skin in the hip region to allow for movement. At this point, the skin closure is stapled shut.

11. Once the hindlimb is complete, turn animal back on to their stomach to complete connection to the external stimulator. Cut folded wire that remains at the top of the back to give two wire ends and once again remove insulation to expose metal wire (approximately 5mm of exposed wire).

12. Place exposed wire into socket pin and solder into place using solder iron. Repeat for other lead wire.

13. Pass wires into simulator casing through the hole located on the underside (ensure gauze is played between casing and incision). Insert pins and add 2 CR2016 3V

Lithium Ion batteries into stimulation unit. Affix the stimulation unit to the casing using sticky-tack.

14. Using surgical tape, carefully fasten stimulation unit and casing around the torso of the rat. Provide approximately 2-3 layers of tape to the top of the casing to prevent ambient light from triggering the IR sensors. Finally, secure everything in place by wrapping a final strip of tape around the sides of the casing.

15. Test the stimulation unit by turning the unit on with the digital stroboscope (ON/OFF: 1-flash). Palpate the muscle to ensure adequate stimulation.

CYTOCHROME C OXIDASE (COX) ASSAY FOR MICROPLATE READER

Cell extract containing cytochrome c oxidase is added to the test solution containing fully reduced cytochrome c. The rate of cytochrome c oxidation is measured over time as a reduction in absorbance at 550 nm. The reaction is carried out at 30^{o} C.

Reagents

1. Horse Heart Cytochrome c (Sigma, C-2506)
2. Sodium Dithionite
3. 100 mM K-Phosphate Buffer (KPO_4; pH to 7.0)
   -make and mix equal proportions of 0.1 M KH_2PO_4 and 0.1 M $K_2HPO_4.3H_2O$
4. 10 mM K-Phosphate Buffer
   -dilute 100 mM K-Phosphate Buffer 1:10 with ddH_2O

Procedure

1. Add 50µl of muscle enzyme extraxtion buffer into labelled eppendorfs, weigh 5-7.5mg of powdered tissue into tubes and record values.
2. Volume up with appropriate amount of buffer to achieve a 20-fold dilution.
3. Stir on ice for 15 minutes. While tubes are stirring prepare test solution below;
   - weigh out 20 mg of horses heart cytochrome c
   - add 1 ml of 10 mM KPO_4 buffer and fully dissolve cytochrome c
   - make up a small volume of 10 mg/ ml sodium dithionite- 10 mM KPO_4 stock solution Note: make fresh each experiment and use within 20 minutes)
   - add 40 µl of dithionite stock solution to the Test Solution and observe the red to orange colour change
   - add 8 ml of ddH_2O
   - add 1 ml of 100 mM KPO_4 buffer (Note: the Test Solution becomes light sensitive at this step; make sure to the cover vial with aluminum foil and place in oven at 30°C).
4. Once samples have stirred for 15 minutes, sonicate samples 3x 30% power on ice.

5. Once samples are sonicated make 80-fold diluted samples in separate labelled eppendorfs (i.e. add 50µl of 20-fold sample extract with 150µl of muscle enzyme extraction buffer).
6. Add 300 µl of Test Solution into 4-8 wells of a 96-well microplate and incubate at 30°C for 10 minutes to stabilize the temperature and absorbance.
7. Open KC4 plate reader program. Select CONTROL icon, then PRE-HEATING tab, enter 30°C and select ON (Do not run assay until KC4 temperature has reached 30°C).
8. Set-up of COX activity protocol on computer.
9. Select WIZARD icon, then READING PARAMETERS icon.
    - Select Kinetic for Reading Type.
    - Select Absorbance for Reader and 550 nm for wavelength (drop-down).
    - Select Sweep for Read Mode.
    - Select 96 Well Plate (default) for Plate Type.
    - Enter first and last well to be read (eg. A1 and A4 if reading 4 samples simultaneously).
    - Select Yes and Pre-heating and enter 30 for Temperature Control.
    - For Shaking enter 0 for both intensity and duration (shaking is not necessary and it will delay the first reading).
    - Do not select either of the two options for Pre-reading.
    - Click on the KINETIC… rectangular tile to open the Kinetic window.
    - Enter run time (1 minute is recommended) and select MINIMUM for Interval time (under these conditions the minimum Interval time should be 3 seconds).
    - Select Allow Well Zoom During Read to see data in real time (optional).
    - Under Scales, checkmarks should appear for both Auto check boxes. Do not select Individual Well Auto Scaling.
    - Press OK to return to Reading Parameters window. Press OK to return to Wizard window. Press OK. Do not save the protocol.
10. Set the micropipette to 240 µl and secure 4-8 tips on the white projections (make sure they are on tight and all the same height).
11. In a second, clean 96 well plate, pipette 50µl of 80-fold samples into 4-8 empty wells (start with A1).
12. Remove microplate with Test Solution from the incubator (as long as it has been incubating for 10 minutes). Place this plate beside the plate with the sample extracts in it.
13. On KC4 program, select the READ icon and press the START READING icon, then press the READ PLATE button. A box will appear that says, “Insert plate and start reading”. Do not press OK yet, but move the mouse so that the cursor hovers over the OK button.

14. Using the micropipette (set to 240 µl) carefully draw up the Test Solution. Make sure the volume is equal in all the pipette tips, and that no significant air bubbles have entered any of the tips.
15. Pipette the Test Solution into the wells with the sample extracts (the second plate). As soon as all the Test Solution has been expelled from the tips (do not wait for the second push from the multipipette), place the plate onto the tray of the plate reader and with the other hand on the mouse, press the OK button. (Speed at this point is paramount, as there is an unavoidable latency period between the time of pressing the OK button and the time of the first reading.)
16. If desired, add 5 µl KCN to one of the wells to measure any absorbance changes in the presence of the CYTOX inhibitor.
17. Once reading is complete, hold the CTRL key on the keyboard, and use the mouse to click once on each of the squares corresponding to a well that had sample in it. Once all the desired wells have been highlighted by a black square (up to a maximum of 8 wells), let go of the CTRL key and a large graph will appear with lines on it representing each sample.
18. To obtain the rate of change of absorbance over different time periods, select Options and enter the amount of time for which you would like a rate of change of absorbance to be calculated. The graph, along with one rate (at whichever time interval is selected) for each sample can be printed on a single sheet of paper, and the results can be saved.
19. The delta absorbance will appear in units of mOD/min and the number given will be negative. Convert this to OD/min by dividing by 1000 and omit the negative sign in the calculation. (eg. if Mean V: -394.8 mOD/mn, then use 0.395 OD/min).

Calculation

$$\text{CYTOX activity} = \frac{\text{mean dealta absorbance/ minute x total volume (ml) x 1000}}{\text{18.5 (µmol/ml extinction coeff.) x sample volume (ml) x total µg/ well}}$$

Example Calculation:

55 µl of enzyme extraction
230 µl of Test Solution
Mean V: -584.30 mOD/mn
Protein concentration: 3.023 µg/ µl
Total µg/ well: 151.15

$$\text{COX activity} = \frac{(0.5843)(0.285)(1000)}{(18.5)(0.055)(3.023 \times 55)}$$

COX activity = 0.967 nmol/min/µg protein

GEL ELECTROPHORESIS (SDS-PAGE) – PROTEIN BIO-RAD SYSTEM

Reagents:

1. Acrylamide/Bis-Acrylamide, 30% Solution 37.5:1 (BioShop 10.502)
    a. Store at 4°C
2. Under Tris Buffer
    a. 1M Tris-HCl, pH 8.8 (60.5g/500ml)
    b. Store at 4°C
3. Over Tris Buffer
    a. 1M Tris-HCl, pH 6.8 (12.1g/100ml)
    b. Bromophenol Blue (for colour)
    c. Store at 4°C
4. Ammonium Persulfate (APS)
    a. 10% (w/v) APS in ddH_20 (1g/10ml)
    b. Stored at 4°C
5. Sodium Dodecyl Sulfate (SDS)
    a. 10% (w/v) in ddH_20 (1g/10ml)
    b. Store at room temperature
6. TEMED (Sigma T-9281)
7. Electrophoresis Buffer, pH 8.3 (10L)
    a. 25mM Tris 30.34g, 192mM Glycine 144g, 0.1% SDS 10g
    b. Volume to 10L with ddH_20
    c. Store at room temperature
8. 6X SDS
    a. Warm 100% glycerol in water bath at 65°C for 30 minutes
    b. Combine 1.2g SDS, 0.06g Bromophenol Blue, 3mls of 1M Tris, pH 6.8 and 1ml of ddH_20 and stir at 4°C for 5 minutes
    c. Add 3mls of 100% glycerol, stir and aliquot mixture.
    d. Store at -20°C
    e. Add 5% (v/v) ß-mercaptoethanol (Sigma M6250) to 6X SDS <u>just prior</u> to use
9. *tetra*-Amyl alcohol ReagentPlus, 99% (Sigma 152463)

Procedure:

1. **Prepare electrophoresis rack:**
    a. Clean glass plates thoroughly with soap followed by 95% ethanol then ddH_20.
    b. Dry carefully with a kimwipe.
    c. Assemble glass plates as shown below:
    d. Check the seal y adding a small volume of ddH_20 then pour off and let dry.

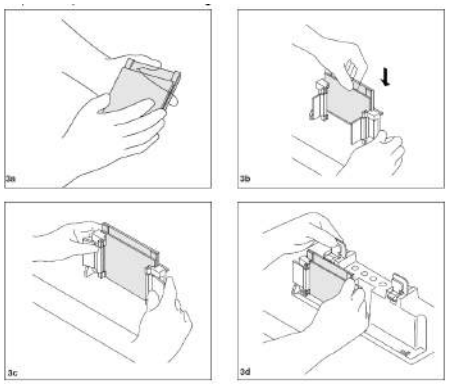

2. **Prepare separating gels:**

a. Mini Protean 3 Bio-Rad System volumes:

	8%	**10%**	**12%**	**15%**	**18%**
Acrylamide	2.7 ml	3.3 ml	4.0 ml	5.0 ml	6.0 ml
ddH_20	4.1 ml	3.5 ml	2.8 ml	1.8 ml	0.8 ml
Under Tris	3.0 ml	3.0 ml	3.0 ml	3.0 ml	3.0 ml
SDS	100µl	100µl	100µl	100µl	100µl
APS	100µl	100µl	100µl	100µl	100µl
TEMED	10µl	10µl	10µl	10µl	10µl

b. Mix the contents of the separating gel without adding APS or TEMED. Stir.
c. Add APS and TEMED. Stir.
d. Slowly pour the entire volume of the solution into the space between the two plates while keeping plates tilted to prevent bubble formation.
e. Add *tert*-Amyl alcohol to coat top surface of gel solution.
f. Allow 30 minutes for gel polymerization.
g. Remove *tert*-Amyl alcohol by pouring it off and remove any remainder with a kimwipe. Rinse with ddH_20.

3. Prepare stacking gel:

a. For a single mini gel use the following volumes:

Acrylamide	500 µl
Over Tris	625 µl
ddH_20	3.75 ml
SDS	50 µl
APS	50 µl
TEMED	7.5 µl

b. Mix the contents of the stacking gel without adding APS or TEMED. Stir.
c. Add APS and TEMED. Stir.
d. Using a Pasteur pipette slowly add the entire volume from the beaker in between the plates.
e. Add comb for desired number of wells.
f. Allow 30 minutes for gel polymerization.

4. Prepare samples:

a. Turn of the block heater to 95ºC.
b. Pipette required volume of sample into new eppendorf with 6X SDS (1 volume of sample to 1/6 sample volume of 6X SDS). Keep samples on ice until all samples are prepared.
c. Briefly spin each sample to bring volume to the bottom of the eppendorf.
d. Incubate each sample at 95 ºC for 5 minutes in the heating block to denature the proteins.
e. Briefly spin again to return volume to the bottom of the eppendorf.

5. **Assemble Mini-PROTEAN gel caster system:**
    a. See images below
    b. If you are only running one gel a plastic rectangular pseudo plate must be clamped on the other side of the caster.
    c. Fill with electrophoresis buffer between the plates and outside of the plates in the chamber.
    d. Slowly remove the comb using both hands (one on each side) by pulling the comb straight upwards.

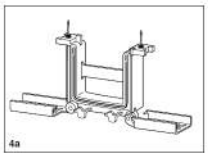
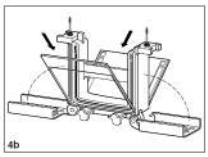
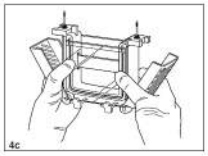
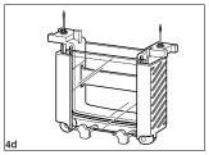
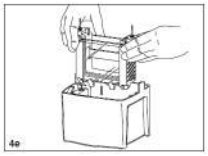

    e. Fix any wells that are deformed using a small spatula.
    f. Clean out the wells using a syringe filled with electrophoresis buffer.
    g. Withdraw the entire volume of the sample using a Hamilton syringe. Inject volume slowly into the bottom of the well.

6. **Gel electrophoresis**
    a. Immediately after all samples are loaded place the lid on the gel chamber.
    b. Place positive and negative plugs into the power supply and turn on power supply.
    c. Set power supply to 120V. Gel will run for ~2 hours depending on percent gel made.
    d. When the bromophenol blue has run off the bottom of the gel turn off the power supply. Remove plugs from power supply and remove lid.
    e. Prepare for electrotransfer of proteins from the gel to nitrocellulose membrane.

WESTERN BLOTTING AND IMMUNODETECTION

Reagents:

1. Transfer Buffer
    a. 0.025M Tris-HCl pH 8.3 12.14g
    b. 0.15M Glycine 45.05g
    c. 20% Methanol 800ml
    d. make up to 4L with ddH_20
    e. store at 4°C
2. Ponceau S stain
    a. 0.1% (w/v) Ponceau S
    b. 0.5% (v/v) Acetic Acid
    c. Store at room temperature

3. Wash Buffer
    a. Tris-HCl pH 7.5 12g
    b. NaCl 58.5g
    c. 0.1% Tween 10ml
    d. Store at room temperature
4. Blocking Solution
    a. 5% (w/v) skim milk power in wash buffer OR
    b. 5% (w/v) BSA in wash buffer
5. Enhanced Chemiluminescence Fluid (ECL; Santa Cruz sc-2048)
6. Film/Developer/Fixer

Procedure:

1. Transfer Procedure

a. Remove electrophoresis plates from chamber and separate the plates.
b. Cut away unnecessary parts of the gel using a spatula and measure remaining gel size.
c. Using a paper cutter cut 6 pieces of Whatman paper per gel to the same size as the gel. Wearing gloves cut nitrocellulose membrane (GE Healthcare RPN303D) to the dimensions of the gel.
d. Assemble Whatman paper, nitrocellulose memebrane and gel as shown below:

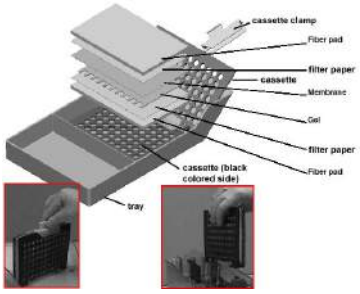

e. Close the cassette and place in the transfer chamber with the black side of the cassette facing the back side of the chamber.
f. Place ice pack in the chamber.
g. Place lid on the chamber and connect the leads to the power supply.
h. Turn on the power supply and run at 120V for 2 hours. This can vary depending on the size of the protein of interest.

2. Removal of transfer membrane:

a. Turn off the power supply and disconnect leads from the power supply then remove the lid from the chamber.
b. Remove the cassette from the chamber.
c. With gloves on, remove the Whatman paper and gel and place the nitrocellulose membrane in a plastic dish.
d. Add Ponceau S stain on the membrane and gently swirl.
e. Drain off the remaining Ponceau S and save for reuse.
f. Rinse the membrane with ddH_20 to reduce the red background. Wrap membrane in saran wrap and scan image.
g. Cut the membrane while protein bands are still visible at the desired molecular weight.

h. Rotate membrane at room temperature in wash buffer until remaining Ponceau S has been removed.
i. Incubate membrane for 1 hour with rotation in blocking solution.
j. Incubate membrane with desired antibody diluted in blocking solution overnight at 4ºC. Membrane is placed face down into the solution on a glass plate covered in parafilm. To maintain a moist environment overnight, wet a small kimwipe and form it into a ball and place in each corner of the dish. Cover the dish with saran wrap.

3. Immunodetection

a. Wash the blots in wash buffer with gentle rotation for 5 minutes 3X.
b. Incubate the blots for 1-2 hours with the appropriate secondary antibody diluted in blocking solution.
c. Membrane is placed face down in solution on a glass plate covered with parafilm. Place moist kimwipes in each corner of the dish and cover the dish with saran wrap.
d. Following the incubation, wash the membrane 3X for 5 minutes with wash buffer.

4. Enhanced Chemiluminescence Detection

a. Mix ECl fluids "A" and "B" in a 1:1 ratio in a disposable Rohr tube.
b. Place blots on saran wrap face up and apply ECL solution for 2 minutes.
c. Dab off excess ECL on a kimwipe and place blots face down on a fresh piece of saran wrap and wrap tightly.
d. Expose blot to film (time will vary depending on protein and antibody).
e. Place film into developer (time will vary).
f. Once image appears place film into fixer for 2 minutes. Wash with fresh water when complete.

RNA ISOLATION

Procedure:

1) Homogenize (approximately 30 sec. @ 30-40% power) tissues (100 mg) at 30% in 1 ml Trizol in a 13 ml Sarstedt tube;

OR

Homogenize (approximately 30 sec. @ 30-40% power) tissues (200 mg) at 30% in 1.25 ml solution D + 1.25 ml phenol + 0.125 ml 2M sodium acetate (pH 4.0) in a 13 ml Sarstedt tube

**Note: The homogenizer must be sterilized in 0.1M NaOH and rinsed in sterile water prior to use. Rinse in sterile water between samples.

2) Let stand for 5 min at room temperature;
3) Add 0.4 ml chloroform and shake vigorously for 15 sec, let stand for 2-3 min at room temperature;

4) Spin at 12,000 *g* for 15 min at 4°C;
5) Transfer aqueous phase to 13 ml Sarstedt tube;
6) Add 1 ml isopropanol, gently shake, and allow precipitation of RNA for 5-10 min at room temperature;
7) Spin at 12,000 *g* for 10 min at 4°C;
8) Remove supernatant and add 0.7 ml 75% ethanol;
9) Transfer RNA to eppendorf tube;
10) Rinse 13 ml Sarstedt tube with 0.3 ml 70% ethanol, add to eppendorf tube and mix by vortexing;
11) Spin 5 min in eppendorf centrifuge at 4°C;
12) Discard supernatant;
13) Dry pellet under a vacuum in dessicator (DO NOT DRY PELLET WITH CENTRIFUGATION UNDER A VACUUM);
14) Dissolve pellet in 50-200 µl sterile distilled DEPC water and measure absorbance at 260 nm and 280 nm.

Reagents:

1. *Solution D (Denaturing solution)*

4 M Guanidinium Thiocyanate	125 g
25 mM of 1 M stock NaCitrate (pH 7.0)	6.6 ml
N-Lauroyl Sarcosine;Sigma L-5125 (0.5% Sarcosyl)	1.32 g
ddH_2O	160 ml

**Note: make up solution D and store at RT for up to 3 months. On the day of the experiment, mix 50 ml of Solution D with 0.36 ml of beta-Mercaptoethanol (0.1 M b-MEtOH)

2. *Phenol (Nucleic acid grade)*
   a) Melt solid phenol at 68 °C (cap loose) in H_2O;
   b) Add 0.25 g 8-hydroxyquinoline to 250 ml of phenol, mix;
   c) Add 250 ml 1.0 M Tris HCl (pH 8.0) and stir overnight at 4 °C covered in foil
   d) Remove supernatant;
   e) Add 250 ml 0.1 M Tris-HCl containing 0.2 % b-MEtOH (0.178 ml/100 ml for S.G. = 1.12) and mix thoroughly;
   f) Allow solution to settle and remove supernatant;
   g) Repeat 2 more times as above or until pH of phenol is > 7.6 (test with pH paper).
   h) Store in 25-50 ml aliquots at -20 °C.

3. *2.0 M Na Acetate* (pH 4.0)
   10.88 g/100 ml sterile H_2O

4. *75% ethanol in sterile H_2O*
   (75 ml ethanol + 25 ml dH_2O)

RNA FORMALDEHYDE GEL

Reagents:

- 0.1% SDS (sodium dodecyl sulphate)
- 10x MOPS (morpholinepropanesulfonic acid)
  - 41.86g MOPS powder
  - 3.72g EDTA (ethylenediaminetetraacetic acid) powder
  - 900ml ddH_2O, pH solution to 7.4
  - Volume up to 1L, aliquot into smaller containers and autoclave
- Agarose powder
- sterile ddH_2O
- 0.5mg/ml ethidium bromide
- RNA sample buffer
  - 100% deionized formamide
  - 37% formaldehyde
  - 1M MOPS (pH 7.4)
  - 0.5M EDTA
  - 100% glycerol
  - 1% dyes (10mg bromphenol blue, 10mg xylene cyanol)
  - 10% SDS
- Sanitized pipettes and sterilized pipette tips/Eppendorfs to be used at all times

Procedure:

1. Prepare the gel and electrophoresis chamber after overnight or 1 hr sterilization with 0.1% SDS;
2. Rinse the gel plates, electrophoresis chamber, and comb with sterile ddH_2O, and wipe dry;

Running Buffer:

Small Chamber	**Large Chamber**
30ml 10x MOPS	200ml 10x MOPS
270ml Sterile ddH_2O	1800ml Sterile ddH_2O

Agarose Gel:

Small Gel	**Large Gel**
0.4g agarose	1.7g agarose
4ml 10x MOPS	17ml 10x MOPS
34ml sterile ddH_2O	144ml sterile ddH_2O
Weigh solution and record weight. Melt in microwave until all solute has been dissolved. Re-weigh and make up volume with sterile ddH_2O. Under the **fume hood**, add formaldehyde.	
2ml 37% formaldehyde	8.5ml 37% formaldehyde

3. Allow gel to coll for 15 minutes, pour, and let gel set for 30 minutes. Transfer the plate with the gel to an electrophoresis chamber, and place the end with the wells at the negative electrode;
4. Calculate the volume of RNA and sample buffer required for desired amount of RNA. Combine in a sterile eppendorf tube:
    i. RNA x µl
    ii. EtBr 4 µl
    iii. Sample buffer x µl

    NOTE: use at least a 1:1 ratio of buffer to RNA volume (max. volume of 30 µl).
5. Mix the samples by tapping;
6. Denature the samples at 65°C for 10 min, quick cool;
7. Spin down volume briefly in microfuge;
8. Pipette the entire volume into each well of the gel;
9. Run the gel at ~80V until second dye band, Xylene Cyanol, is 2/3 from the end;
10. Visualize and photograph the gel under UV light.

REVERSE TRANSCRIPTION, FIRST STRAND cDNA SYNTHESIS

First-strand cDNA synthesis is performed following the manufacturer's recommendations that are outlined below:

Reagents:

1. total RNA (isolated as described)
2. Oligo$(dT)_{12-18}$
3. 10 mM dNTPs (dATP, dTTP, dCTP, dGTP; 10 mM each)
4. Sterile ddH_20
5. RNAse OUT (40 units/ µl)
6. 0.1 M DTT
7. 5X First-strand Buffer
8. SuperScript II RT

*Note: All reagents except RNA are supplied with the SSII kit from Invitrogen.

Procedure:

1. Add following components to a nuclease/ RNA-free 500 µl eppendorf:

Oligo$(dT)_{12-18}$	1 µl
1 µg of RNA	x µl
dNTP mix	1 µl
Sterile ddH_20	to 20 µl

2. Heat mixture to 65°C for 5 minutes and quick chill on ice. Collect the contents with a quick spin in a tabletop microcentrifuge and then add:

5X First-strand buffer	4 µl
0.1 M DTT	2 µl
RNAse OUT	1 µl

3. Mix contents of tube gently and incubate at 42°C for 2 minutes.
4. Add 1 µl (200 units) of Superscript II RT and mix by pipetting gently up and down.
5. Incubate at 42°C for 50 minutes.
6. Inactivate the reaction by heating at 70°C for 15 minutes.
7. cDNA is ready for use in PCR amplification.

OLIGONUCTEOTIDE PRIMER DESIGN

Websites required:

- Pubmed Nucleotide Search
- Primer3 Primer Design Program – http://bioinfo.ut.ee/primer3/
- BLAST – http://www.ncbi.nlm.nih.gov/tools/primer-blast/
- IDT website – http://www.idtdna.com/calc/analyzer

1. Know the gene of interest.
2. Use the Pubmed.com nucleotide search and choose the most complete cDNA or mRNA version of the gene.
3. Copy the sequence and insert it into the Primer3 program.
4. Remove numbers from the copied sequence because the program will treat them as nucleotides.
5. In the text box for **Product Size Ranges,** input 100-150.
6. In the text box for **Number to Return,** input 10 (or whatever you want).
7. Under the heading **General Primer Picking Conditions** go to **Primer Size** and enter 10-20-22 from min to max.
8. For **Primer Tm** enter 58-60-62 from min to max.
9. For **Max Tm Difference** enter 2.
10. For **Primer GC%** enter 40-50-60 from min to max.
11. For **Max Self Complementary** enter 6.
12. For **Max Ploy-X** enter 3.
13. Under the heading **Objective Function Penalty Weights for Primer** go to **End Stability** and enter 9.
14. Click on the "Pick Primers" button.
15. Examine the primers on the list. 3' end of primer must not end with a G or C. No more than three G or C in last five nucleotides at 3' end.
16. Check specificity using BLAST.
17. Calculate the ΔG to estimate secondary structures that can form. Go to the IDT website.
18. Enter each oligo one at a time and press "Analyze". ΔG must be greater than or equal to -9 to continue.
19. Continue down the list selecting **Hairpin, Self-Dimer, Hetero-Dimer, Tm Mismatch.** Check ΔG for each one.

REAL-TIME POLYMERASE CHAIN REACTION (qPCR)

1) 2 ug of RNA is converted to 2 ug of cDNA (STOCK cDNA).
2) We dilute STOCK cDNA to 1:30 (2 uL STOCK cDNA added to 58 uL nuclease-free ddH_2O).
3) We add 2 µL of diluted cDNA, per well.
4) For SYBR Green analyses, primers were optimized, diluted and mixed with PerfeCTa SYBR® Green SuperMix, ROX Master Mix and nuclease-free ddH_2O.
5) Total reaction volumes were always 25 µL.
6) Samples must be duplicated to ensure accuracy.
7) Use negative wells to monitor contamination, using nuclease-free ddH_2O in place of cDNA.
8) Check for nonspecific amplification and primer dimers by analyzing melt curves.

APPENDIX D: OTHER CONTRIBUTIONS TO LITERATURE

PEER-REVIEWED PUBLICATIONS

1. Erlich AT, Tryon LD, Crilly, MJ, **Memme JM**, Moosavi, ZM, Oliveira AN, Beyfuss K, Hood DA. Function of specialized regulatory proteins and signaling pathways in exercise-induced muscle mitochondrial biogenesis. *Integrative Medicine Research.* [in progress].
2. Tryon LD, Vainshtein A, **Memme JM**, Crilly MJ, Hood DA. (2014). Recent advances in mitochondrial turnover during chronic muscle disuse. *Integrative Medicine Research*, 3(4), 161-171.
3. Hood DA, Tryon LD, Vainshtein A, **Memme JM**, Chen CW, Pauly M, Crilly MJ, Carter HN. (2015). Exercise and the regulation of mitochondrial turnover. In: *Molecular and Cellular Regulation of Adaptation to Exercise* 135: 99–127. Edited by Bouchard C.

PUBLISHED ABSTRACTS AND CONFERENCE PROCEEDINGS

1. Oliveira AN, **Memme JM**, Hood DA. Inhibition of the UPR^{ER} does not impair signaling to mitochondrial biogenesis during chronic contractile activity. *Experimental Biology 2016.* San Diego, CA. April 2016 – Poster presentation. *Submitted.*
2. **Memme JM**, Hood DA. Chronology of UPR signaling associated with contractile activity-induced skeletal muscle adaptations. *Canadian Society for Exercise Physiology conference 2015.* Hamilton, ON. October 2015 – Poster presentation.
3. **Memme JM**, Hood DA. Time course of signaling events associated with skeletal muscle adaptations to exercise. *Proceedings of the 6th Annual Muscle Health Awareness Day*. Toronto, ON. May 2015 – Poster presentation.
4. **Memme JM**, Hood DA. The Unfolded Protein Response in Skeletal Muscle Adaptations to Exercise. *Experimental Biology 2015.* Boston, MA. March 2015 – Poster presentation.
5. **Memme JM**, Hood DA. The role of the unfolded protein response in muscle contractile activity-induced adaptations. *Canadian Society for Exercise Physiology conference 2014.* St. John's, NL. October 2014 – Poster presentation.
6. **Memme JM**, Crilly MJ, Tryon L, Iqbal S, Hood DA. Denervation-induced adaptions in autophagy and mitochondrial morphology proteins. *Proceedings of the 4th Annual Muscle Health Awareness Day*. Toronto, ON. May 2013 – Poster presentation.
7. Crilly MJ, **Memme JM**, Pastore SP, Hood DA. Circadian regulation of mitochondrial content in skeletal muscle. *Proceedings of the 4th Annual Muscle Health Awareness Day.* Toronto, ON. May 2013 – Poster presentation.

ORAL PRESENTATIONS

1. **Memme JM**, Hood DA. The Unfolded Protein Response in Exercise. *KAHS Graduate Seminar 2015*. York University, Toronto, ON. March 2015 – Oral presentation.
2. **Memme JM**, Hood DA. Unfolded protein response-mediated adaptations to exercise in skeletal muscle. *Ontario Exercise Physiology conference 2014*. Barrie, ON. February 2014 – Oral presentation.